MOLECULAR COMPOSITION AND REGULATION OF THE FUSION PORE OF CALCIUM TRIGGERED EXOCYTOSIS

by

Xue Han

A dissertation submitted in partial fulfillment of

the requirements for the degree of

Doctor of Philosophy

(Physiology)

at the

UNIVERSITY OF WISCONSIN-MADISON

2004

ACKNOWLEDGEMENTS

This work could not have been completed without the participation of many people.

I am deeply indebted to my thesis advisor, Dr. Meyer Jackson. No words can express my gratitude for his guidance, inspiration and patience throughout these years. He taught me many theories, technical details and most importantly his critical, rigorous approach to science. When I joined his lab at the tender age of 22, I was naïve about the true nature of science in practice. In his laboratory, my interest in science was fostered and has become a true passion. I have Dr. Jackson's attitude to thank for this.

I would also like to thank other members in my thesis committee, Dr. Edwin Chapman, Dr. Thomas Martin, Dr. Cynthia Czajkowski, and Dr. James Ervasti. Special thanks go to Dr. Edwin Chapman for his inspirational discussions and generous assistance.

My former lab mate Dr. Chih-Tien Wang taught me amperometry, patch-clamp recording, and cell culture. Dr. Vitaly Klyachko helped me to conduct the cell-attached capacitance measurement. I want to thank them for their help, support, interest, and valuable hints.

I would like to thank all Jackson's lab members as well. Payne Chang wrote the analysis software for amperometry, and constantly supported me over the years. Also other people: Yukiko Muroi, Ebru Aydar, Nathan Philippi, Zhejie Zhang, Brandon Sonderegger, Jeff Rose, Camin Dean, and Sara Grosz.

I would like to express my gratitude to people in the physiology department. Dr. Xiaojie Cao and Dr. Jinling Wang, and Dr. Drew Boileau showed me valuable technical

details, also constantly supported and encouraged me. My classmates Karen Reece, Leah Carbonneau, Beth Olbinski, and Lauren Hanft have shared my joy and sadness over last 4 years. I would also like to thank Dr. Min Dong, Weiyun Chen, Dr. Dipanka Bhattacharya, Dr. Ward Tucker, and Elon Roti Roti for their help with molecular biology, also Sue Krey for her help on administrative assistance.

Especially, I am deeply indebted to my parents Bo Han and Shuyan Liang, also my brother Han Han for their constant support, understanding and encouragement. Without them these accomplishments could never be possible.

TABLE OF CONTENTS

FIGURES AND TABLES

ABSTRACT

Ca^{2+}-triggered neurotransmitter release is critical for synaptic transmission. It starts with an intermediate structure, known as the fusion pore. In this present study, amperometry and capacitance measurements were used to examine the fusion pore of large dense core vesicles in neuroendocrine PC12 cells. Genetic manipulation of the fusion machinery in PC12 cells was carried out by overexpressing the proteins of interest separately from a green fluorescent protein reporter. Regulation of the fusion pore was interpreted by applying single channel kinetic analysis.

In this work, the fusion pore flux was shown to be sensitive to manipulations of the side chain size or charge of certain residues in the syntaxin (syx) membrane anchor. These residues fell on the same face of the syx membrane α-helix, and thus were predicted to line the fusion pore. Based on the fusion pore conductance, 5-8 copies of the syx membrane α-helix in a circular arrangement were estimated to form the fusion pore in the plasma membrane.

Fusion pores open and soon dilate with a mean life time of ~2 msec. Manipulations of the syx membrane anchor altered the life time of an open fusion pore. Based on a simple kinetic scheme that an open fusion pore can either dilate or close, one can estimate changes in the kinetic parameters of a fusion pore. Syx pore lining residues appear to regulate the fusion pore dilation rate. This result is consistent with the notion that these residues would experience a transition during dilation, from a hydrophilic environment to a hydrophobic environment.

The SNARE (soluble *N*-ethylmaleimide-sensitive factor attachment protein receptor) complex has been proposed to serve an essential role in exocytosis. In the present study, mutations that reduced the SNARE complex thermostability were shown to slow the rate of secretion and the rate of fusion pore dilation. A fully formed SNARE complex was demonstrated to be important to complete exocytosis. However, only part of the SNARE complex experiences a conformational transition to dilate an open fusion pore.

CHAPTER 1. BACKGROUND AND SIGNIFICANCE

Synaptic transmission serves as the primary form of communication between neurons in the central nervous system. Changes in the strength of synaptic transmission, generally referred to as synaptic plasticity, have been implicated in learning and memory. Synaptic plasticity can take place on either side of the synapse.

On the postsynaptic side, modification could be related to the number and/or activity of receptors. The underlying mechanism has been broadly explored with a focus on the receptors. On the presynaptic side, synaptic plasticity may occur through changes in neurotransmitter release probability, quantal size, and the number of vesicles. Modification can occur at many steps: vesicle biogenesis, targeting, docking, priming, and fusion. These steps depend on the coordination of a series of molecules whose functions are poorly understood. It is often difficult to access the tiny presynaptic nerve terminals compared to the large postsynaptic neurons. Thus, little is known about the underlying mechanism of synaptic plasticity on the presynaptic side.

Over the last decade, extraordinary progress has been made toward the understanding of exocytosis. With the identification of a series of molecules involved in vesicular transport, the molecular mechanism of neurotransmitter release is starting to be explored. This thesis will explore the molecular mechanisms of Ca^{2+}-triggered exocytosis, with a strong focus on the fusion pore. The long-term goal of this work is to advance our understanding of synaptic transmission.

1. Features of Ca^{2+} triggered exocytosis

Exocytosis refers to the process in which an intracellular vesicle fuses with the plasma membrane and releases its content. It achieves two functions, insertion of the vesicular membrane and membrane constituents into the plasma membrane and releasing the vesicular content into the extracellular space. Exocytosis operates through two pathways, the constitutive pathway and the regulated pathway (Burgess and Kelly 1987). The constitutive pathway occurs universally in all eukaryotic cells to maintain the plasma membrane identity. It employs by small vesicles derived from the Golgi and occurs continually in the absence of secretagogue. By contrast, regulated exocytosis is limited to specialized secretory cells including neurons, endocrine and exocrine cells, mast cells and eggs. It requires stimulation, generally entailing a transient elevation of intracellular Ca^{2+} or other second messenger.

1.1. Quantal release

Studies on chemical transmission between nerve endings and the effector organs can be traced back to the early 1900s. Early on, chemical transmission was proposed by a few people including Howell, Bayliss, Elliott, and Dixon. Not until 1921 did Loewi first demonstrate the existence of chemical messengers (Loewi 1921). Then, in 1952 Katz and colleagues (Fatt and Katz 1952) introduced the "quantal release" hypothesis, which led the concept of packaging transmitter in vesicles (Whittaker 1965; Whittaker and others 1972). Exocytosis of these vesicles was first captured by electron microscopy in 1979 (Heuser and others 1979). Now the quantal release hypothesis has been widely accepted.

1.2. Different Secretary Vesicles: LDCV vs. SSV

It has been well established that neurons can secrete multiple neurotransmitters via at least two types of secretary organelles, small synaptic vesicles (SSVs) and large-dense-core vesicles (LDCVs) (De Camilli and Jahn 1990; Hokfelt and others 1986). Endocrine cells also possess two equivalent vesicle types, synaptic-like microvesicles corresponding to SSVs and secretary granules essentially identical to LDCVs. SSVs and LDCVs differ in their morphology, biogenesis, translocation, and exocytosis.

The most distinct feature of these two types of vesicles is their sizes. SSVs have a diameter of 30-60 nm, whereas LDCVs are more heterogeneous with an estimated range of 60-500 nm in diameter (Langley and Grant 1997). Vesicle sizes can be modulated by many factors, such as physiological activity (Maler and Mathieson 1985), genetic manipulation of the vesicular transporters (Karunanithi and others 2002; Pothos and others 2000), and pharmacological factors like L-DOPA and reserpine (Colliver and others 2000b).

Altered vesicle size was suggested to correlate with changes in quantal size (Colliver and others 2000b; Karunanithi and others 2002; Pothos and others 2000). One study estimated that the concentration of neurotransmitter serotonin in SSVs was similar to that in LDCVs (Bruns and others 2000). Another study reported that in chromaffin cells the concentration of neurotransmitter catecholamine stayed the same while the size of the LDCVs was altered (Gong and others 2003). If the neurotransmitter concentration also stays constant in SSVs, one would also expect the size of SSVs to be related to their quantal size. Modulation of the vesicle size thus might influence synaptic plasticity.

SSVs can actively take up or concentrate “fast” or “classical” transmitters including amino acids (GABA, glutamate, aspartate, and glycine), amines (serotonin and acetylcholine), and catecholamines (dopamine, noradrenaline and adrenaline) (De Camilli and Jahn 1990; Langley and Grant 1997). Because SSVs do not contain concentrated secretory proteins, they have a clear core under electron microscopy. But with certain staining methods, some small vesicles appear to have an electron-opaque core due to the content of noradrenaline. These were called small dense core vesicles (SDVs). The origin of SDVs is unclear, one hypothesis is that these vesicles might be recycled from LDCVs, since their membrane composition seemed different from SSVs (Winkler 1997). LDCVs have an electron-dense core, which is mainly due to the condensed proteins but may also due to small nonpeptide molecules (De Camilli and Jahn 1990). LDCVs usually contain peptide neurotransmitters or neuromodulators (Cox and others 1994). Some may also contain other proteins like matrix protein chromogranin-A and various antigens (Winkler and others 1991).

SSVs and LDCVs coexist in broad types of nerve terminals and neuroendocrine cells (Morris and others 1978). Segregation of different neurotransmitters is achieved by selective packaging into different vesicles, as well as into different nerve terminals. For example, the vesicles in the dorsal horn of the glutamatergic terminals contain no GABA (Merighi and others 1991). SSVs are frequently clustered at specialized synaptic membrane regions called "active zones". Active zones are believed to be in register with the post-synaptic receptors (Langley and Grant 1997). Neurotransmitter released from SSVs thus can reach the post-synaptic receptor rapidly to achieve fast signal transduction.

However, LDCVs usually spread out in cells, not only in the axon terminals but also in the cell body and dendrites. They are usually excluded from active zones.

The membrane contents of these two types of vesicles have been controversial due to the difficulty of separating SSVs from LDCVs. There is growing recognition that proteins directly associated with exocytosis like synaptotagmins and synaptobrevins are present in both SSVs and LDCVs (Winkler 1997). Proteins that appear to be preferentially localized to SSVs are the acetylcholine transporter (Usdin and others 1995) and synaptophysin/synaptin (Rindi and others 2004). LDCVs from adrenal medulla can be purified in high yield, and their membranes contain cytochrome b-561 (an electron transporter to provide electrons for the dehydroascorbate/ascorbic cycle) (Perin and others 1988; Srivastava 1995), Vo-ATPase (the vacuolar proton pump) (Nelson 1992; Supekova and others 1996), PAM (peptidylglycine α-amidating monooxygenase) (Eipper and others 1992), and VMAT (vesicular membrane amine transporter) (Erickson and Eiden 1993; Liu and others 1992).

1.3. Distinct functional vesicle pools

Vesicles undergo a few mobilization steps before exocytosis including targeting, docking and priming (Lin and Scheller 2000) (Figure 1-1). After fusion is completed, at least two endocytosis pathways have been postulated, kiss-and-run rapid local recycling and clathrin-mediated endocytosis through endosomal compartments.

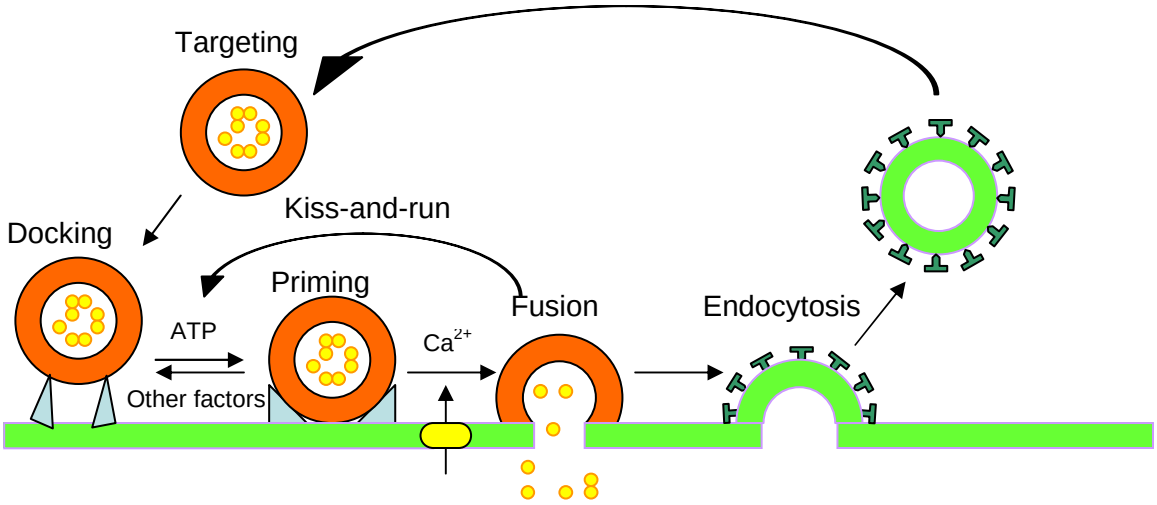

Figure 1-1. The synaptic vesicle cycle: Vesicles filled with neurotransmitter first target to active zones and become docked. The docked vesicles then undergo an ATP-dependent priming step. Ca^{2+} influx through Ca^{2+} channels triggers neurotransmitter release. After exocytosis, vesicles either undergo kiss-and-run recycling or clathrin-mediated endocytosis.

The mobilization steps in the vesicle cycle imply the presence of the functionally distinct vesicle pools. One categorization of these different pools is based on the release kinetics, which is thought to be heterogeneous for both SSVs and LDCVs (Dobrunz and others 1997; Hessler and others 1993; Murthy and others 1997; Rosenmund and others 1993). Much evidence has been drawn from studies of the LDCVs in chromaffin cells. At least two kinetic components of exocytosis have been observed, one is fast and the other is slow (Heinemann and others 1994; Parsons and others 1995). The fast component reflects the release of the "readily releasable pool" (RRP), since vesicles in this pool can fuse within a few hundred milliseconds of membrane depolarization. In contrast, the slow component corresponds to the "reserve pool", and these vesicles have to undergo further

mobilization steps before fusion (Neher and Zucker 1993). Later studies with neurotoxins revealed three kinetic components, but only two of these were related to catecholamine release (Xu and others 1998). These results were obtained from neuroendocrine cells, which raises a question of how much do neuroendocrine cells have in common with neurons. If the underlying mechanisms were similar, one would hope to learn a great deal about synapses from neuroendocrine cells.

The distribution of vesicles in different pools is dynamic and varied among different preparations. In a single hippocampal bouton the RRP size was estimated as 5-10 vesicles out of a total of 195-270 morphologically docked vesicles (Schikorski and Stevens 1997). Interestingly, one recent electron microscopy study suggested that synaptic vesicles in the RRP pool was not clustered close to the membrane, but rather distributed randomly throughout the nerve terminals (Rizzoli and Betz 2004). Segregation of LDCVs in different pools was proposed to change with vesicle age (Duncan and others 2003). These authors labeled vesicles with a fluorescent timer protein (Terskikh and others 2000), which changes color from green to red over time. With this protein marker, vesicle age can be recognized. Newly assembled vesicles were immobile and morphologically docked at the plasma membrane, presumably forming the RRP. By contrast, the older vesicles were mobile and located deeper inside a cell, likely forming the reserve pool.

1.4. Speed of exocytosis

The speed of exocytosis varies dramatically between different cell types. Exocytosis in neurons has been estimated to be at least 10 times faster than that in neuroendocrine cells, and 100,000 times faster than that in other types of cells. In synapses neurotransmitter

release is on a sub-millisecond to millisecond time scale (Augustine and others 1985; Katz and Miledi 1965; Llinas and others 1981). In neuroendocrine cells secretion starts tens of milliseconds after Ca^{2+} entry (Chow and others 1992). The slow rate of exocytosis in neuroendocrine cells is consistent with the modulatory function of their vesicle content, but the underlying mechanism is controversial. A few possibilities will be discussed here.

The longer distance between Ca^{2+} channels and vesicles is thought to contribute significantly to the delay in neuroendocrine cells. The spatial distribution of the Ca^{2+} concentration upon membrane depolarization is not homogeneous. Instead, there are high Ca^{2+} concentration microdomains that could be >100 μM (Augustine and Neher 1992; Llinas and others 1992; Melamed-Book and others 1999). Combining imaging techniques (Omann and Axelrod 1996) and membrane-bound Ca^{2+} indicator dyes (Etter and others 1994), single vesicle exocytosis within a single Ca^{2+} microdomain was observed (Becherer and others 2003). In chromaffin cells homogeneous elevation of the intracellular Ca^{2+} concentration by photolysis of caged-Ca^{2+} elicited secretion within a few milliseconds (Heinemann and others 1994). The time course of secretion depends on the level of the intracellular Ca^{2+} concentration (Heinemann and others 1994), and could be influenced by immobile and mobile Ca^{2+} buffers (Chow and others 1996).

There are also a few other possibilities: first, vesicular content expulsion after fusion is prolonged due to the vesicular matrix in LDCVs (Chow and others 1996); second, the kinetics of Ca^{2+} action at the Ca^{2+} sensing machinery could be slow; and third, SSVs and LDCVs could have different mobilization states. The delay between membrane fusion and content release is very short, as demonstrated by combined capacitance-amperometry

measurements in neuroendocrine cells (Chow and others 1992). The capacitance recording can resolve secretion instantaneously, and transmitter release was detected by amperometry with a comparable speed. Thus, the delay in content release after fusion is too short to explain the millisecond delay. Since the putative Ca^{2+} sensor synaptotagmin-I is present in both SSVs and LDCVs (Winkler 1997), different speeds of Ca^{2+} sensing may arise from the action of other modulatory components. Alternatively, LDCVs may need some other Ca^{2+} dependent mobilization steps before fusion.

2. The molecular mechanism of Ca^{2+}-triggered exocytosis

Ca^{2+}-triggered exocytosis is one of many membrane trafficking steps in eukaryotic cells. Membrane trafficking along with exocytosis and endocytosis is mediated by a series of intermediates and involves a number of proteins. In the late 1980s, identification of the molecules involved in vesicular transport between intracellular compartments started a revolution in understanding the molecular mechanism of membrane fusion. A large number of molecules have been identified since then (Fernandez-Chacon and Sudhof 1999; Lin and Scheller 2000). Our current understanding of the function of these molecules is far from complete. There are controversies surrounding almost every aspect of the signaling cascade mediated by these molecules. The following is a brief discussion of recent progress on the molecular mechanism of Ca^{2+}-triggered exocytosis.

2.1. Identification of SNAREs

In 1984 Rothman's group reconstituted a cell-free protein transport system between successive compartments of the Golgi stack (Balch and others 1984a; Balch and others 1984b). Using this reconstituted vesicular transport system, the first fusion related protein, NSF (N-ethylmaleimide (NEM)-sensitive protein), was identified (Block and others 1988; Wilson and others 1989). NSF was not only required for the vesicular transport within the Golgi stacks but also from the endoplasmic reticulum (ER) to Golgi (Beckers and others 1989). The action of NSF requires another soluble protein and an integral membrane receptor (Weidman and others 1989). They were later characterized as SNAP (the soluble NSF attachment protein) (Clary and others 1990; Whiteheart and others 1993) and SNARE (the SNAP receptor) (Sollner and others 1993b).

The SNARE proteins have many homologues, which are conserved from yeast to human (Bennett and Scheller 1993; Bock and others 2001; Ferro-Novick and Jahn 1994). Since different SNARE isoforms have their preferential subcellular locations, it was hypothesized that the SNARE proteins may dictate the specificity in vesicle trafficking among different intracellular compartments (Sollner and others 1993b). The neuronal SNAREs include three proteins (Sollner and others 1993b), syntaxin (Bennett and others 1992; Inoue and others 1992), synaptobrevin/VAMP (vesicle-associate membrane protein) (Trimble and others 1988) and SNAP-25 (synaptosomal-associated protein of 25-KD) (Oyler and others 1989).

2.2. The SNARE complex

The SNARE proteins can assemble into a highly stable, SDS resistant complex, called the SNARE complex (Hayashi and others 1994; Sollner and others 1993b). Structural studies indicated that the SNARE complex contains four parallel oriented α-helixes, one from syntaxin, two from SNAP-25 and one from synaptobrevin (Figure 1-2) (Sutton and others 1998). The four-α-helical bundle is about 12 nm long with each α-helix containing about 60-70 amino acids. Synaptobrevin is anchored to the vesicle membrane and syntaxin and SNAP-25 are attached to the plasma membrane. Formation of the SNARE complex was predicted to be essential for membrane fusion.

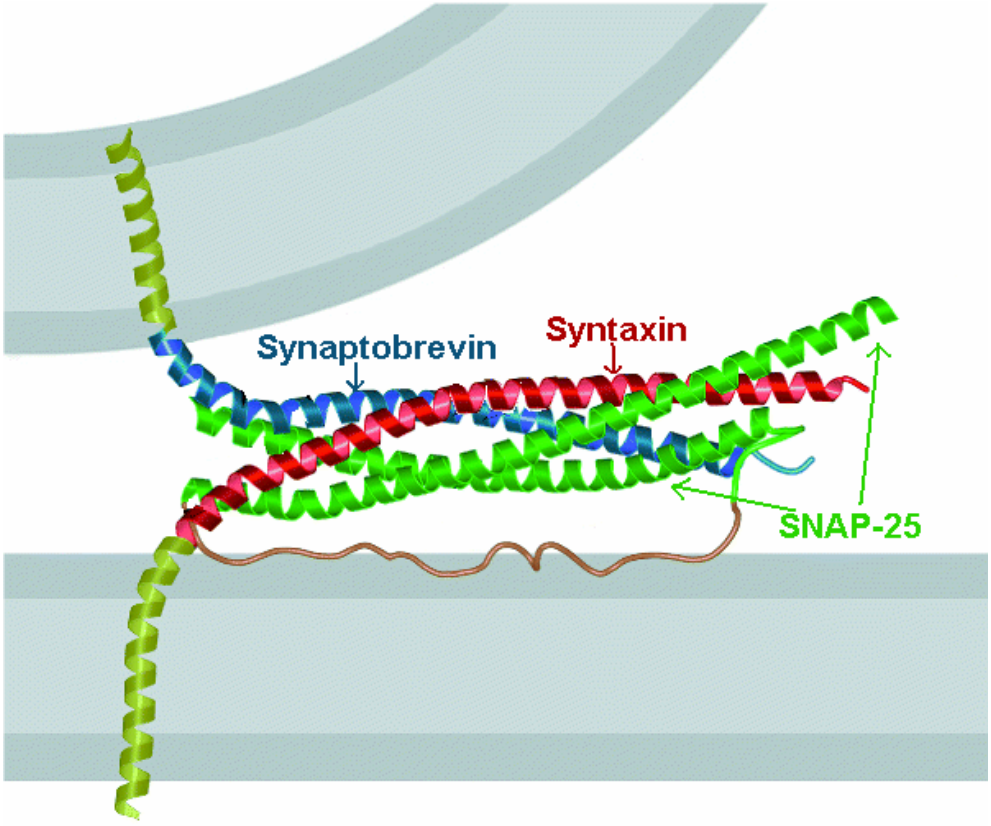

Figure 1-2. The SNARE complex contains four α-helixes. One α-helix is from syntaxin, one from synaptobrevin and two from SNAP-25 (adapted from (Sutton and others 1998)). Synaptobrevin resides in the vesicular membrane, whereas syntaxin and SNAP-25 are anchored in the plasma membrane. Formation of the SNARE complex was thus proposed to pull the vesicle membrane and the plasma membrane into close proximity.

The SNARE complex structure: Each α-helix in the SNARE complex is named the "SNARE motif". The most distinctive feature of the SNARE motif is the heptad-pattern repeats of hydrophobic residues (Fasshauer and others 1998b). When mapped on an α-helical structure, all these residues would be on the same face. The crystal structure of the SNARE complex (Sutton and others 1998) revealed 15 layers (-7 to -1 on the N-terminal

side and +1 to +8 on the C-terminal side) of mostly hydrophobic amino acid residues interacting in the central interface of the four-helix bundle (Figure 1-3). However, one layer at the center (layer 0) is ionic. The interacting amino acids on these 16 layers are highly conserved (Fasshauer and others 1998b).

SNARE complex structure-function relations: The ionic central layer contains three glutamines (Q) and one arginine (R), which are the most conserved in all SNARE proteins (Figure 1-3) (Bock and others 2001; Weimbs and others 1998). Three glutamines are provided by syntaxin and SNAP-25, so they are also called Q-SNAREs. The arginine is from synaptobrevin, thus it is called an R-SNARE (Fasshauer and others 1998b).

The ionic layer drew attention because of its unique location in the SNARE complex, but its exact function is obscure. One suggestion is that a charge layer in the middle of 15 hydrophobic layers could help the formation of the "right" SNARE complex, as mismatching will be strongly disfavored (Katz and Brennwald 2000; Ossig and others 2000). Disruption of the ionic interaction at the central layer by substitutions with hydrophobic residues like glycine led a total lost of function (Ossig and others 1991). A 3Q:1R is not required, since a 4Q complex supported normal fusion in yeast (Katz and Brennwald 2000). However, a 2R complex should be less stable due to the charge repulsion. This may explain why physiological complexes normally include only one R-SNARE (Jahn and others 2003). Another suggestion for the function of glutamine in the syntaxin central layer is that it facilitates binding of the SNARE complex to α-SNAP and NSF, which is essential for the SNARE complex disassembly (Scales and others 2001).

The 15 hydrophobic layers of the SNARE complex were predicted to be important for membrane fusion, but the underlying mechanism is still enigmatic. A rough correlation between complex formation and fusion has been observed in *drosophila*, *C-elegans*, yeast and PC12 cells. For example, some correlation between SNARE complex formation and membrane fusion was seen in permeabalized PC12 cells (Chen and others 1999). Chen *et al*. used a rescue assay by a peptide corresponding to the C-terminal SNARE motif of SNAP-25. The SNAP-25 peptides with point mutations at adjacent hydrophobic layers reduced the SNARE complex thermostability and failed to restore secretion to levels obtained with the wild-type SNAP-25 peptide.

Studies on different SNARE proteins with mutations at the hydrophobic layers also support an essential role for these hydrophobic interactions in secretion. A single point mutation at layer +7 (syx-T254I in *drosophila*) disrupted the SNARE complex formation and abolished synaptic transmission in the temperature sensitive flies (Littleton and others 1998). The double point mutations at layers +4/+5 (syx-A243V/V247A in *drosophila*) impaired neuronal secretion, but left non-neuronal secretion unaltered (Fergestad and others 2001). The mutation at layer +1 of SNAP-25 (Sec9-L627H in yeast (Brennwald and others 1994)) is temperature sensitive with a dominant negative effect at higher temperature (Rossi and others 1997). Mutations at layer -3 of SNAP-25 (Sec9-G458D in yeast) or synaptobrevin disrupted complex formation and resulted in a secretion defect (Grote and others 1995; Hao and others 1997; Rossi and others 1997). The same position in a leech SNAP-25 homologue showed reduced binding to syntaxin (Fasshauer and others 1997a). In contrast, a point mutation at layer -2 of synaptobrevin enhanced binary

binding to syntaxin/SNAP-25 complex, but reduced the SNARE complex thermostability (Grote and others 1995; Hao and others 1997).

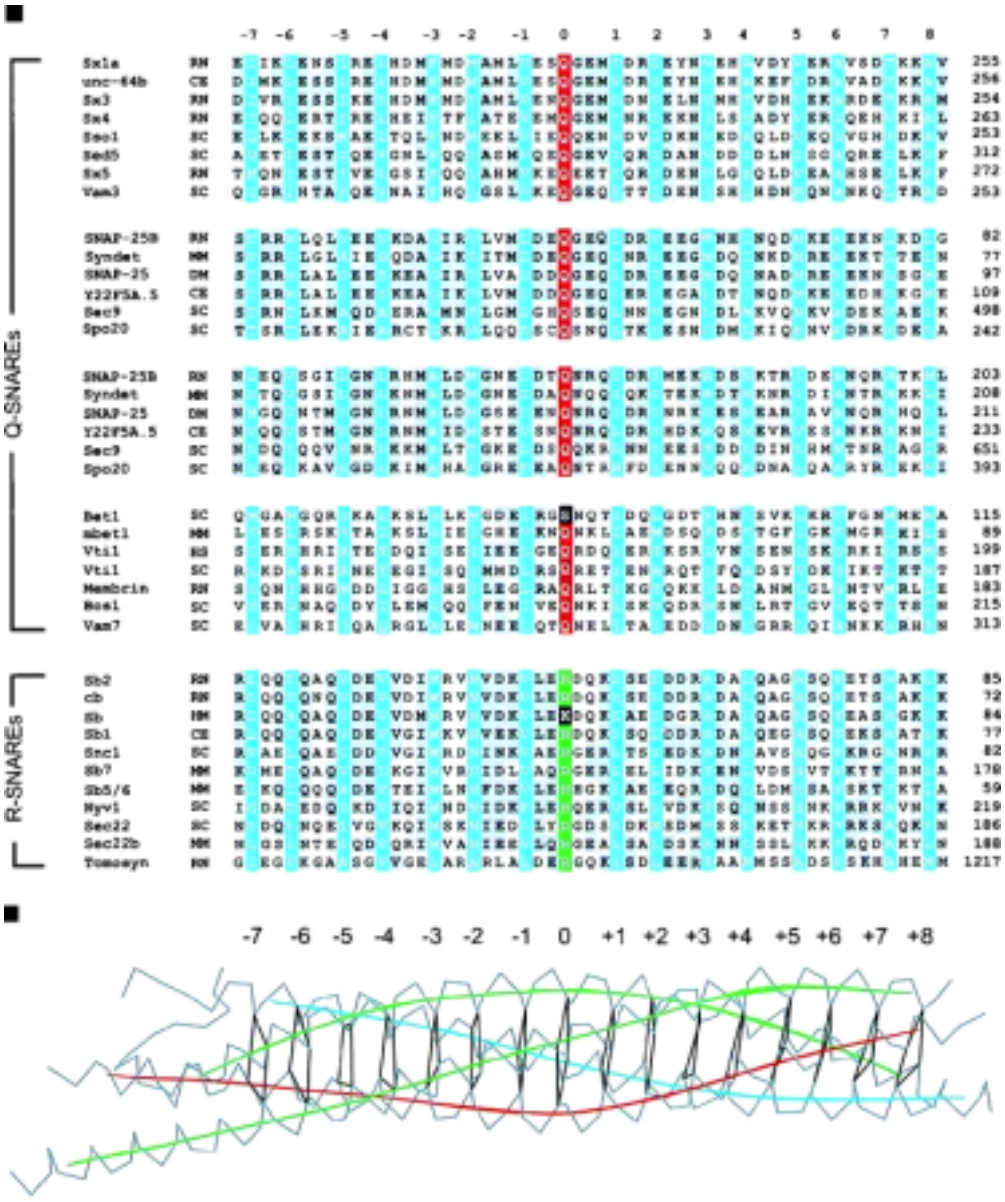

Figure 1-3. Sequence alignment of the SNARE motifs. The hydrophobic layers are in blue, whereas the central layer is in red for glutamine (Q) and in green for arginine (R). Variation in the central layer is highlighted in black. The lower graph is a backbone-stick representation of these layers

(modified from Fasshauer, Sutton et al. 1998). The abbreviations for species are indicated by two-letters as follows: HS, *Homo sapiens*; MM, *Mus musculus*; RN, *Rattus norvegicus*; SC, *Saccharomyces cerevisiae*; DM, *Drosophila melanogaster*; TM, *Torpedo marmorata*; CE, *Caenorhabditis elegans*; and HM, *Hirudo medicinalis*. The syntaxin family shown includes (with genebank number indicated): sx1a, RN, P32851; unc-64b, CE, AF047885; sx3, RN, Q08849; sx4, RN, Q08850; Sso1, SC, P32867; sed5, SC, Q01590; sx5, RN, Q08851; vam3, SC, Q12241. The SNAP-25 family proteins shown are SNAP-25B, HS, P13795; syndet, MM, U73143; SNAP-25, DM, U81153; Y22F5A.5, CE, AL021479; sec9, SC, L34336; and spo20, SC, Z49211. The bos-group includes bet1, SC, P22804; mbet1, MM, AF007552; vti1, HS, AF035824; vti1, SC, AF006074; membrin, RN, U91539; bos1, SC, P25385; and vam7, SC, P32912. The synaptobrevin/vamp family includes sb2, RN, M24105; cb/cellubrevin, RN, S63830; sb1 CE AF003281; sb, HM, U85805; Snc1, SC, M91157; sb5/6, HS, AA222692; sb7, MM, X96737; sec22 (Sly2), SC, L8479; sec22b, MM, U91538; nyv1, SC, Z73265; and tomosyn, RN, U92072.

The SNARE complex in exocytosis: It is clear that vesicles have to undergo a few preliminary steps, targeting, docking, and priming, before they are ready to fuse with millisecond kinetics (Lin and Scheller 2000). But in which steps the SNARE complex are involved is controversial. A late role for the SNARE complex was favored in Ca^{2+}-triggered exocytosis for the following reasons: first, the SNARE complex forms in a very late step, likely triggered by Ca^{2+}-binding (Chen and others 1999); second, disruption of the SNARE complex did not reduce the number of morphologically docked vesicles, but inhibited synaptic transmission (Augustine and others 1999). How the SNARE complex functions in the final fusion step is unknown. One hypothesis is the "zipper model", which predicts that the SNAREs complex formation is from the membrane distal end to the membrane proximal end (Fasshauer 2003; Fiebig and others 1999; Lin and Scheller 1997).

This sequential zipping can pull the opposite membranes close together to drive fusion with the energy released during the zipping process. However, the zipper model was challenged by a recent report that four different locations in the SNARE complex assembled simultaneously (Zhang and others 2004).

A docking role for the SNARE complex is also possible. This is primarily supported by studies on homotypic vacuolar fusion in yeast (Wickner 2002). In yeast the SNARE complex formation is essential for docking (Laage and Ungermann 2001; Ungermann and others 1998). Disassembly of the SNARE complex after docking did not block fusion (Ungermann and others 1998). One study in chromaffin cells also indicated a possible role in docking, where different botulinum neurotoxins selectively eliminated different kinetic components of exocytosis (Voets and others 1999; Xu and others 1998). This evidence suggests that the SNARE complex formation influenced some vesicle mobilization steps, thus pointing to an early role, presumably in docking.

2.3. Functions of individual SNARE proteins

Syntaxin: Syntaxin was first identified and cloned based on its interaction with synaptotagmin and N-type Ca^{2+} channels (Bennett and others 1992). The same protein was also observed and cloned as a neuronal membrane antigen (Barnstable and others 1985; Inoue and others 1992). Since then, 17 syntaxin isoforms have been identified and characterized (Jahn and Sudhof 1999).

Syntaxins form a family of proteins involved in vesicle transport with a broad tissue distribution and with different subcellular locations (Bennett and others 1993). Among characterized syntaxin isoforms, syntaxin 1, 2, 3 and 4 are localized to the plasma

membrane (Bennett and others 1992; Bennett and others 1993; Bock and others 2001; Bock and Scheller 1997; Jahn and Sudhof 1999).

Syntaxin1 (syx) is the neuronal isoform. Syx is anchored to the plasma membrane by a single membrane spanning segment of 23 amino acids (Bennett and others 1992) (Figure 1-2). Its cytoplasmic domain has four α-helixes, named Ha,b,c and H3. The Ha,b,c domains form a three-helix bundle (Fernandez and others 1998), and the H3 domain is the SNARE motif (Kee and others 1995; Rizo and Sudhof 2002).

Syx was proposed to function as a central coordinator in exocytosis (Bennett and Scheller 1993; Ferro-Novick and Jahn 1994; Rizo and Sudhof 2002; Rothman 1996; Wu and others 1999). Microinjection with soluble syx fragments or syx antibodies disrupted Ca^{2+}-triggered exocytosis in PC12 cells (Bennett and others 1993). Syx loss-of-function *drosophila* mutants lacked both evoked and spontaneous neurotransmission, also failed to secrete epidermal cuticles (Schulze and others 1995).

Syx has more binding partners than any other known presynaptic proteins. In addition to forming the SNARE complex with SNAP-25 and synaptobrevin (Sollner and others 1993b; Sutton and others 1998), syx can bind to Ca^{2+} channels (Bezprozvanny and others 1995; Bezprozvanny and others 2000; Sheng and others 1994), synaptotagmin (Bennett and others 1992; Chapman and others 1995), complexin (McMahon and others 1995), α/γ-SNAP (Hanson and others 1995; Sollner and others 1993b), rsec6/rsec8 (Hsu and others 1996), munc-18/n-Sec1 (Hata and others 1993), tomosyn (Fujita and others 1998), munc-13 (Betz and others 1997), cysteine string protein (Wu and others 1999), and amisyn (Scales and others 2002).

Syx can also modulate the function of other presynaptic proteins. For example, syx affected the gating and permeation of various channel proteins, including Ca^{2+} channels (Bezprozvanny and others 1995; Bezprozvanny and others 2000; Sheng and others 1994), CIRL/latrophilin Cl^--channel (Krasnoperov and others 1997), K^+-channels (Fili and others 2001; Pasyk and others 2004), and Na^+-channels (Berdiev and others 2004; Condliffe and others 2004). The syx-channel interactions may regulate the excitability of presynaptic nerve terminals. Moreover, syx may influence vesicle size through interactions with various transporters like the transporters for GABA (Deken and others 2000), glycine (Geerlings and others 2000), norepinephrine (Sung and others 2003), and serotonin (Quick 2003). Thus, syx may contribute to synaptic plasticity through its interactions with channels to change release probability, or through its interactions with transporters to alter quantal size.

The cytoplasmic domain of syx has been of interest due to its interactions with various proteins. Studies also indicated that the transmembrane domain affected the ability of the cytoplasmic domain to engage other proteins in a length-dependent and sequence-specific manor (Chapman and others 1995; Lewis and others 2001; Trus and others 2001).

SNAP-25: SNAP-25 was first detected as a protein specifically expressed in neuronal tissues (Oyler and others 1989). SNAP-25 contains two α-helixes, and is anchored to the plasma membrane through four palmitoylmoieties linked to the cysteine residues residing in the region connecting the two α-helixes (Hess and others 1992; Veit and others 1996; Vogel and Roche 1999).

SNAP-25 is essential for Ca^{2+}-triggered exocytosis. In SNAP-25 knockout mice evoked secretion at the neuromuscular junction (NMJ) was totally abolished, whereas spontaneous release remained (Washbourne and others 2002). This evidence along with botulinum neurotoxin blockade of secretion (Jahn and Niemann 1994) supports an essential role of SNAP-25 in evoked secretion. The residual spontaneous release at the NMJ agrees with the residual secretion from SNAP-25 null chromaffin cells (Sorensen and others 2003). The residual release could be due to other SNAP-25 isoforms. Alternatively, Ca^{2+}-independent fusion may not require SNAP-25.

Another possible function of SNAP-25 proposed by Sorensen *et al.* is to stabilize vesicles in the primed state (Sorensen and others 2003). This is supported by experiments showing that different SNAP-25 isoforms, SNAP-23, SNAP-25a and SNAP-25b (alternative splice variants) rescued secretion to different levels in SNAP-25 null chromaffin cells. The secretion rescue level was correlated with changes in the vesicle pool size.

Synaptobrevin: Synaptobrevin resides in the vesicle membrane in neurons and endocrine cells (endocrine pancreas, adrenal medulla, PC12 cells, and insulinoma cells) (Baumert and others 1989). It consists a short NH_2-terminal segment, a SNARE motif, and a COOH-terminal transmembrane region (Sudhof and others 1989). Synaptobrevin plays an essential role in Ca^{2+}-triggered exocytosis. In synaptobrevin knockout mice evoked synaptic secretion was almost totally abolished, but spontaneous lease remained but with reduced frequency (Schoch and others 2001).

There are a total of six synaptobrevin isoforms in human genome (Bock and others 2001), including synaptobrevin-1, 2, 3, 5 (Baumert and others 1989; Bernstein and Whiteheart 1999; Trimble and others 1988; Zeng and others 1998), cellubrevin (McMahon and others 1993), and endobrevin (Wong and others 1998). Synaptobrevin-1 and synaptobrevin-2 are isoforms expressed in the nervous system, but synaptobrevin-1 showed higher expression levels in the spinal cord compared with synaptobrevin-2 in the brain (Elferink and others 1989; Trimble and others 1988; Trimble and others 1990). Cellubrevin is ubiquitous and is thought to contribute to constitutive membrane trafficking (McMahon and others 1993). It has been proposed that cellubrevin can interchange with synaptobrevin-2 to execute the function in Ca^{2+}-triggered neurotransmitter release (Bhattacharya and others 2002). Endobrevin is located primarily with the perinuclear vesicular membrane. Synaptobrevin-5 is present both on the plasma membrane and the intracellular perinuclear vesicular myotubes (Zeng and others 1998). Synaptobrevin-3 is the isoform in blood cells (Bernstein and Whiteheart 1999).

2.4. Possible Ca^{2+} sensor: Synaptotagmin

Since the discovery that Ca^{2+} is the trigger for exocytosis, people have been searching for the Ca^{2+} sensor. The first strong candidate appeared in 1990, when Perin *et al.* cloned a protein that interacts with both Ca^{2+} and phospholipid bilayers (Perin and others 1990). This protein was first observed in 1981 as a 65-kDa antigen localized to the synaptic vesicle membrane (Matthew and others 1981). Only later was it named synaptotagmin (Perin and others 1991). So far, 15 isoforms have been identified (Chapman 2002;

Rickman and others 2004) and genomic analysis targets a total of 19 human isoforms (Craxton 2001).

Synaptotagmin has several distinct features making it the most likely Ca^{2+} sensor. First, synaptotagmin specifically localizes to the presynaptic vesicle membrane and is the most abundant vesicular protein (about 7% of the total vesicle proteins) (Chapman and Jahn 1994). Second, synaptotagmin can bind to Ca^{2+} and Ca^{2+} binding promoted synaptotagmin interactions with lipids and other secretory proteins. Third, Ca^{2+}-regulated liposome fusion can be reconstituted by addition of synaptotagmin to the minimal fusion machine (Tucker and others 2004).

Synaptotagmin structure: Synaptotagmins are usually anchored to the plasma membrane with a single transmembrane domain (Chapman 2002; Perin and others 1990). The N-terminal intravesicullar domain is short, and the C-terminal cytoplasmic domain is large. The short N-terminal domain was proposed to bind to botulinum neurotoxin B (Nishiki and others 1994; Nishiki and others 1996a; Nishiki and others 1996b), and mediate toxin entry (Dong and others 2003).

The cytoplasmic domain contains tandem internal repeats of a region homologous to the C_2-regulatory domain (C_2 domain) of protein kinase C. The two C_2 domains are connected by a short linker region. The one close to the amino-terminus is called C_2A, and the other one is called C_2B. The C_2A domain of synaptotagmin was the first characterized C_2 structure (Sutton and others 1995). It contains eight β-strands arranged in a barrel-like structure with a total length of approximately 130 amino acids. This β-strand structure is common to most of the C_2 domains characterized (Nalefski and Falke 1996).

C_2 domains are Ca^{2+} binding motifs identified in a number of eukaryotic signaling proteins. The presence of C_2 domains in synaptotagmin provided the first clue for its possible function of Ca^{2+} sensing (Perin and others 1990). Synaptotagmin binds a total of five Ca^{2+} ions, three to the C_2A domain (Ubach and others 1998) and two to the C_2B domain (Fernandez and others 2001). Binding of Ca^{2+} ions is mediated by a cup-shaped structure formed by five conserved amino acid residues residing in the two flexible loops connecting the β-strands (Sutton and others 1995).

Synaptotagmin interactions: Synaptotagmin was shown to bind membranes in response to Ca^{2+} (Brose and others 1992). The specific sites for lipid binding on the C_2A domain were mapped to the binding pocket for Ca^{2+} (Chapman and Davis 1998). Ca^{2+} binding induces membrane penetration of certain residues in the binding pocket. The C_2B domain can bind to the membrane when it was linked to the C_2A domain, but the isolated C_2B domain alone seems not to bind lipid (Bai and others 2002). The C_2B domain can also bind to PtdIns(4,5)P_2 (PIP_2) residing in the plasma membrane (Whipps and others 1987) in a Ca^{2+}-dependent manner (Hu and others 2002; Schiavo and others 1996). Ca^{2+}-dependent binding to PIP_2 increased the speed of Ca^{2+}-dependent penetration (Bai and others 2004a).

Synaptotagmin can bind to syntaxin (Sollner and others 1993a) and SNAP-25 (Schiavo and others 1997; Zhang and others 2002b). These interactions are enhanced by Ca^{2+} (Chapman and others 1995; Earles and others 2001; Gerona and others 2000; Li and others 1995; Zhang and others 2002b). Disruption of synaptotagmin binding to SNAP-25 diminished exocytosis (Earles and others 2001; Gerona and others 2000; Zhang and others

2002b). However, what steps of exocytosis these interactions come into play remains controversial.

Synaptotagmin in exocytosis: Synaptotagmin-I is essential for Ca^{2+}-triggered exocytosis. Genetic ablation of synaptotagmin-I in mice abolished the rapid component of exocytosis without affecting the release triggered by the hypertonic sucrose in both hippocampal neurons (Geppert and others 1994) and chromaffin cells (Voets and others 2001a). Ca^{2+}-independent asynchronous release was increased in the hippocampal neurons of the knockout animal, which led to a comparable amount of secretion upon a presynaptic stimulus (Nishiki and Augustine 2004a). Introducing synaptotagmin-I back into the synaptotagmin-I null hippocampal neurons rescued synchronous release and suppressed asynchronous release (Nishiki and Augustine 2004b). These experiments demonstrated that synaptotagmin-I synchronizes rapid release and suppresses asynchronous release.

Another line of experiments relating synaptotagmins with the fusion pore also support the function in the final fusion step. Overexpression of synaptotagmin-I in PC12 cells altered the fusion pore stability, which indicates a role in the final fusion step (Wang and others 2001a). In addition, overexpression of synaptotagmin-IV increased the fraction of vesicles undergoing kiss-and-run exocytosis (Wang and others 2003).

Synaptotagmin in endocytosis: Synaptotagmins may also function in endocytosis. The C_2B domain can bind to molecules involved in vesicle retrieval, such as clathrin-adaptor protein complex AP-2 (Zhang and others 1994), PIP_2 (Schiavo and others 1996; Slepnev and De Camilli 2000), stoned-A and stoned-B (Haucke and De Camilli 1999; Walther and others 2001). A current model for the action of synaptotagmin in endocytosis

(Haucke and De Camilli 1999; Walther and others 2001) is that it may help to increase the PIP_2 concentration around the membrane targeted for endocytosis. Synaptotagmin together with PIP_2 could help to recruit the adaptor protein AP-2 to form clathrin coats. This coat then deforms the plasma membrane to complete endocytosis. Later, synaptotagmin may facilitate the uncoating process by recruiting stoned-A and stoned-B.

Morphological studies in synaptotagmin-I null *drosophila* larvae showed fewer docked vesicles (Reist and others 1998). This could be due to defects in either vesicle docking or endocytosis. This phenotype was also observed in another fly mutant AD3 with a point mutation in the C_2B domain. The AD3 fly mutants had reduced Ca^{2+} sensitivity (Littleton and others 1998), but released the same amount of transmitter upon hypertonic sucrose stimulation (Yoshihara and Littleton 2002). The way hypertonic sucrose triggers exocytosis is unclear, nevertheless one widely held view is that it releases the docked and primed vesicles via a Ca^{2+}-independent pathway (Aravamudan and others 1999). Therefore, it is likely that the reduction in docked vesicles was due to defects in endocytosis.

Synaptotagmin Ca^{2+}-sensing mechanism: Synaptotagmin-I can bind to Ca^{2+}, lipid, the SNARE monomers, and the SNARE complex. However, the underlying mechanism of transduction of the Ca^{2+} signal to exocytosis initiation is unclear. One study showed that Ca^{2+} binding to the C_2B domain was required for synchronous release, but not for the suppression of asynchronous release (Nishiki and Augustine 2004b). Another hypothesis proposed that Ca^{2+} binding to both C_2A and C_2B domains initiates exocytosis. However, Ca^{2+} binding to the C_2B domain is responsible for the dilation of a fusion pore, as

disruption of this interaction increased the portion of kiss-and-run exocytosis (Wang, CT unpublished data).

2.5. Exocytosis modulators

The SNARE proteins have been considered as the essential fusion machine, and synaptotagmin-I is the best candidate for the Ca^{2+}-sensor. It is reasonable to consider the large number of other molecules that could influence exocytosis as modulators. Functions of most of these modulators are unclear. The following discussion will focus on a few that have been better studied over the last few years, including NSF, SNAP, and munc-18.

NSF and SNAP: NSF (N-Ethylmaleimide-sensitive fusion protein) is a 76-kDa homotetramer with two ATP binding sites (Morgan and others 1994; Wilson and others 1989). NSF can bind to the SNARE complex through SNAPs (soluble NSF attachment proteins) (Weidman and others 1989) and form a larger aggregate, known as the 20s complex (Sollner and others 1993b). In fact, only the SNARE complex, but not the SNARE monomers serve as the SNAP receptor.

The SNAP family includes three isoforms α-SNAP, β-SNAP, and γ-SNAP (35, 36, and 39 kDa respectively) (Whiteheart and others 1993). Among them, the α and γ isoforms are expressed in almost all tissues, whereas the β isoform is restricted to the brain. The universal expression pattern implies that NSF and SNAP might be general requirements for intracellular membrane fusion.

NSF and SNAP were suggested to disassemble the SNARE complex after fusion (Jahn and Sudhof 1999; Klenchin and Martin 2000; Sollner 2003). In *vitro* biochemical experiments showed that binding of α-SNAP and NSF catalyzed the SNARE complex

disassembly (Morgan and others 1994). The abundance of the SNARE complex is inversely correlated with NSF activity, and accumulation of the SNARE complex on one membrane (cis-SNARE complex) inhibited secretion (Babcock and others 2004; Littleton and others 1998; Tolar and Pallanck 1998). It thus seems that disassembly of the cis-SNARE complex plays an important role in reusing the SNARE proteins after fusion.

Munc-18: Munc-18 is a syx-binding protein that is highly conserved among species (Toonen and Verhage 2003). The crystal structure of the munc18–syx complex showed that munc-18 is arch-shaped and binds to syx in the central cavity of the arch (Misura and others 2000). In munc-18 null mice neurosecretion was totally abolished (Verhage and others 2000). Also the munc-18 null chromaffin cells have an over 10 folds of reduction on the secretion frequency, which correlated with a reduction on the number of morphologically docked vesicles. Correspondingly, overexpression of munc-18 in the wild type chromaffin cells enhanced exocytosis (Voets and others 2001b). Furthermore, *C. elegans* had fewer docked vesicles in the absence of munc-18 (Voets and others 2001b). Thus, munc-18 is likely to function in promoting vesicle docking. However, conflicting results were reported in PC12 cells, in which overexpression of munc-18 had no effect (Graham and others 1997).

2.6. A molecular model of Ca^{2+}-triggered exocytosis

Syx null *drosophila* had defects in both neuronal and non-neuronal secretion. However, genetic ablation of synaptobrevin, SNAP-25, and synaptotagmin-I only abolished synchronous release, not spontaneous release. This raises an interesting possibility that Ca^{2+}-triggered release and spontaneous release might employ divergent

pathways. However, syx is likely an essential component for both forms of secretion. Accordingly, a hypothetical model was proposed with syx as the central player.

This model predicts that syx undergoes a large conformational change from a "closed conformation" to an "open conformation" (Figure 1-4) (Carr and Novick 2000; Misura and others 2000). In the "closed conformation", the Ha,b,c domain of syx folds back onto the H3 domain. This closed syx is probably stabilized by munc-18 (Misura and others 2000). Disruption of the syx-munc18 complex opposes the syx H3 domain, to which other SNARE proteins can bind to and form the SNARE complex. Transitions from the syx-munc18 complex to the SNARE complex would prime vesicles to a fusion-competent state. Two candidate proteins that release the munc-18 inhibition are munc-13 (Augustin and others 1999) and RIM (Rab3-interacting molecule) (Castillo and others 2002; Koushika and others 2001). After fusion is complete, the cis-SNARE complex would be disassembled, possibly by α-SNAP and NSF. Then syx can return to the "closed" conformation with its Ha,b,c domain folding back to the H3 domain.

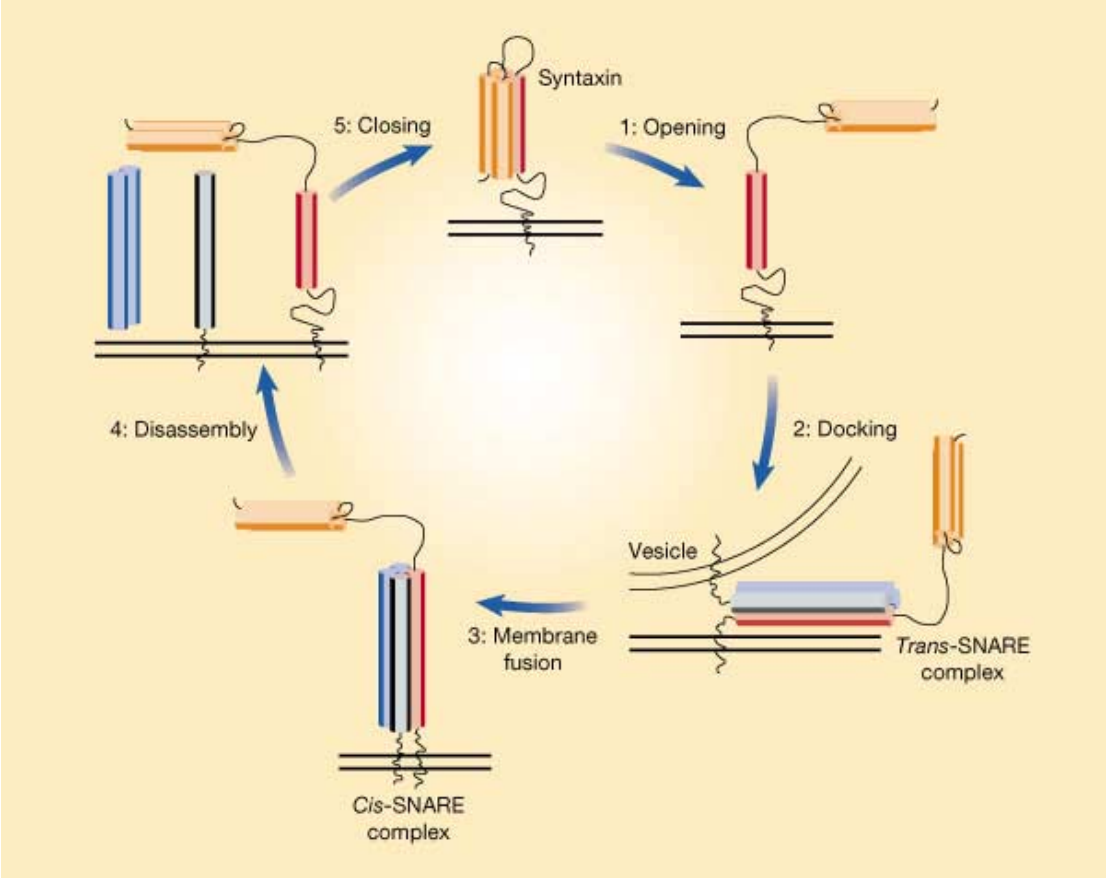

Figure 1-4. A hypothetical molecular model of syx mediated exocytosis. The syx H3 domain is the red bundle, and the Ha,b,c domain is the orange complex. Binding of the Ha,b,c domain to the H3 domain leads the closed form of syx. The blue bundle represents SNAP-25, whereas the black one signifies synaptobrevin. Open form syx can bind to SNAP-25 and synaptobrevin to facilitate fusion. See text for explanation (Carr and Novick 2000).

3. The Fusion Pore

Ca^{2+}-triggered exocytosis is thought to start with an intermediate channel-like structure, known as the fusion pore. The fusion pore starts small with a diameter on the order of a nanometer, but soon dilates into a large Ω-shaped structure of >20 nm in diameter. Thus the term "fusion pore" in the following discussion will be used to designate the initial opening state, whereas the later stage will be referred to as the dilated fusion pore.

3.1. Detection of the fusion pore

The existence of the fusion pore has been demonstrated by various experiments. Techniques applied to study the fusion pore include electrophysiological methods, electrochemical methods, electron microscopy (EM) and fluorescence microscopy. Electrophysiological methods can detect the very first moment upon fusion pore opening or monitor the fusion pore dynamics over a longer period of time; electrochemical methods measure the flux of certain neurotransmitter; whereas electron and fluorescent microscopy can detect a later stage, likely the dilated fusion pore.

Electron Microscopy: An exocytotic pore-like-structure was first morphologically identified in 1980 as a “narrow-necked Ω-shaped pore” in electron micrographs in mast cells (Chandler and Heuser 1980). This was followed by several similar descriptions in different cell types like amebocytes (Ornberg and Reese 1981), neutrophils (Chandler and others 1983) and chromaffin cells (Nakata and others 1990; Schmidt and others 1983).

The Ω-shaped pores captured in EM were large, with a diameter of ~20-100 nm (Chandler and Heuser 1980; Schmidt and others 1983). Since EM cannot report any dynamic activity of the fusion pore and fails to detect the morphology of any pore smaller than 20 nm, the large pore captured under EM is likely a later stage of fusion instead of the initial fusion pore. Based on the smoothness of the membrane lining the pore, these large Ω-shaped structures are likely composed of lipid (Chandler and Heuser 1980).

Electrophysiological Methods: Existence of the fusion pore was anticipated by the observation of reversal events in single-vesicle capacitance recording (Fernandez and others 1984; Neher and Marty 1982). Neher and Marty applied high frequency sine wave stimulation and a lock-in amplifier to measure the membrane capacitance. This was made possible by the development of the low-noise patch-clamp recording (Hamill and others 1981). Based on the equivalent electrical circuit model of a cell with a fusing vesicle, single vesicle fusion can be detected as stepwise capacitance increases. The capacitance steps were later identified as single vesicle fusion events because they were frequently accompanied by loss of the fluorescent dye loaded in vesicles (Breckenridge and Almers 1987b; Zimmerberg and others 1987).

The first direct demonstration of a fusion pore was made in 1987 by Breckenridge and Almers (Breckenridge and Almers 1987). They captured the fusion pore using combined current-capacitance measurement. Over the first millisecond of a fusion pore's existence, there is a transient current flow to charge the vesicle membrane to the holding potential applied to the plasma membrane. By recording and analyzing this current transient, the fusion pore conductance could be determined. In their remarkable study, Breckenridge

and Almers captured the initial fusion pore with a conductance of 200-300 pS. By modeling the fusion pore as a gap-junction channel across two lipid bilayers, this conductance gave a pore of 1 nm in radius. With the combined capacitance-current method, several similar studies were conducted on fusion pores in other cells (Breckenridge and Almers 1987; Hartmann and Lindau 1995; Spruce and others 1990).

Another electrophysiological method to study the fusion pore is combining the membrane capacitance measurement and admittance analysis (Alvarez de Toledo and Fernandez 1988; Alvarez de Toledo and others 1993; Lindau 1991; Lollike and others 1995). The combined capacitance-admittance measurement employs a lock-in amplifier to measure membrane capacitance and conductance simultaneously. Low noise capacitance-admittance measurement was made possible in the cell-attached patch configuration, which allows the detection of much smaller fusion pores (Lollike and others 1995). For example, ~20 pS pores were captured during fusion of the small-synaptic-vesicle-like granules in the posterior pituitary (Klyachko and Jackson 2002) and ~35 pS pores in neutrophils (Lollike and others 1995).

Studies in different preparations showed a wide variation in the size of the fusion pore (Hartmann and Lindau 1995; Klyachko and Jackson 2002; Lollike and others 1995). But overall the fusion pore has a conductance on the order of tens to hundreds of pico-Siemens, similar to that of large ion channels (Klyachko and Jackson 2002; Lindau and Almers 1995; Lollike and others 1995; Spruce and others 1990). The similarity in conductance raises the possibility that the fusion pore is an ion channel. Accordingly, the

fusion pore was envisioned as a proteinaceous structure across the closely adjacent vesicle and plasma membranes.

The combined capacitance-admittance measurement has a lower time resolution compared to the combined capacitance-current measurement. However, it can monitor the fusion pore conductance over a longer time period. If the fusion pore is a channel-like structure, the dynamics of the fusion pore would be analogues to ion channel gating. For this reason, the capacitance-admittance measurement may be especially valuable in the studying of fusion pores at the molecular level.

Electrochemical Methods: In 1992 the fusion pore was detected by an electrochemical method, amperometry (Chow and others 1992). Amperometry detects the release of catecholamines by electro-oxidization at the surface of a carbon fiber electrode. Exocytosis of a single vesicle can be detected as an amperometry spike (Wightman and others 1991). Chow *et al.* observed that a pedestal or foot signal often preceded unitary amperometry spikes, and proposed that the foot signal signifies neurotransmitter leaking through a narrow fusion pore. The amperometry foot signal was later confirmed as the neurotransmitter flux restricted by a fusion pore structure by simultaneous capacitance-amperometry measurement in a whole-cell mode (Alvarez de Toledo and others 1993).

Combined capacitance-amperometry measurement can also be made in cell-attached mode. This was achieved by inserting a carbon fiber electrode into a patch electrode. The amplitude of the amperometry foot signal was shown to correlate with the fusion pore size estimated from the capacitance measurement (Alvarez de Toledo and others 1993).

Applying the capacitance-amperometry measurement, the fusion pores smaller than 3-nm were observed in chromaffin cells (Albillos and others 1997).

Amperometry foot current signals the neurotransmitter flux through a fusion pore. Theoretically, the flux is subject to the influence of many factors, such as the neurotransmitter dissociation rate from the vesicular matrix, diffusion, and the concentration gradient between vesicle lumen and the extracellular solution. The dissociation rate was demonstrated to be very fast, as the rising phase of the amperometry signal was almost simultaneous with the capacitance step (Alvarez de Toledo and others 1993). If the amperometry electrode can be positioned within 1 μm of the releasing sites, diffusion will not affect the apparent kinetics of exocytosis (Chow 1995).

The duration of the foot signal indicates the time interval for the pore to maintain its initial structure. Thus, it represents the stability of an open fusion pore. Since amperometry has a time resolution slightly better than a millisecond, this technique could examine the kinetics of the initial fusion pore.

Fluorescent Microscopy: In 1992 Betz's group developed a styryl dye FM1-43 (Betz and Bewick 1992; Betz and others 1992). Styryl dyes, including FM1-43, FM2-10, and related compounds, are lipophilic fluorescent probes (Betz and others 1996). They spontaneously insert into the membrane but do not flip across the membrane, so they can be easily washed off. Once they are in the membrane, their fluorescence is enhanced.

Styryl dyes can be taken up into recycled vesicles in response to stimulation. Once in an endocytosed vesicle, styryl dyes are trapped and fluorescent (Betz and Bewick 1992; Betz and others 1992). Exocytosis of vesicles labeled with styryl dyes can be monitored

as dye departitioning from the vesicle membrane into the aqueous solution. In hippocampal neurons styryl dyes were retained for tens of milliseconds upon synaptic vesicle fusion (Pyle and others 2000). Another study recognized partial destaining of a single vesicle (Aravanis and others 2003). These results were interpreted as evidence for the presence of a barrier in the form of a fusion pore. Generally, the poor time resolution of the styryl dye destaining method cannot provide information about the initial fusion pore.

3.2. Fusion pore conductance and dynamics

Fusion Pore Conductance: The fusion pore conductance is highly variable, ranging from ~20 pS (Klyachko and Jackson 2002) to ~300 pS (Lindau and Almers 1995) (corresponding to a pore radius ranging from ~0.3 nm to ~2 nm). Even for the same type of vesicles in the same type of cells, the measured fusion pore conductance can vary in size over ten-fold. What causes this variation is unknown, but there are a few possibilities. First, the fusion pore structure is highly dynamic with many intermediates. Since the capacitance-admittance method has limited time resolution, the measured fusion pore conductance could be a mixture of different rapidly interconverting fusion states. Second, different proteins or different number of proteins may contribute to the variation in fusion pore conductance. Third, conformational changes during fusion pore opening could be regulated by other cytosolic factors, which may vary among cell types or different locations in a single cell.

Fusion pore dynamics: The capacitance-admittance measurements revealed that the fusion pore conductance stays small and constant for various time, often on an order of

hundreds of millisecond. (Alvarez de Toledo and Fernandez 1988; Alvarez de Toledo and others 1993; Klyachko and Jackson 2002; Lindau 1991; Lindau and others 1993; Lollike and others 1995). With whole-cell capacitance measurements, the fusion pore dilation rate was shown to be regulated by both intracellular Ca^{2+} concentration (Fernandez-Chacon and Alvarez de Toledo 1995; Hartmann and Lindau 1995) and phorbol ester (Scepek and others 1998). Amperometry estimated a mean fusion pore life time of ~2 msec, which was subject to the regulation of different synaptotagmin isoforms (Wang and others 2001a). Synaptotagmin-I prolonged the duration of an open fusion pore, whereas synaptotagmin-IV reduced it. However, the underlying mechanism for the observed effect on the fusion pore kinetics is unknown.

3.3. Fusion pores and kiss-and-run exocytosis

A fusion pore can progress through two pathways, dilation leading to full fusion and closure leading to kiss-and-run exocytosis. Kiss-and-run exocytosis gained its name in 1994 to describe a process where fusion pores close right after their opening without allowing the vesicle membrane to mix with the plasma membrane (Fesce and others 1994). During kiss-and-run exocytosis, neurotransmitter could also be released (Alvarez de Toledo and others 1993).

The notion of kiss-and-run exocytosis can be traced back to the mid 1980s. At that time, people observed that the fusion of secretary granules with the plasma membrane was not always all-or-none, as predicted by the quantal hypothesis, but sometimes transient and fluctuating (Breckenridge and Almers 1987; Breckenridge and Almers 1987b; Fernandez and others 1984; Neher and Marty 1982; Zimmerberg and others 1987). More

recently, optical studies with vesicles labeled with styryl dyes added new evidence for kiss-and-run exocytosis (Aravanis and others 2003; Klingauf and others 1998; Pyle and others 2000). Based on the destaining rate of different styryl dyes, FM1-43, FM2-10, and FM 1-84, synaptic vesicles in hippocampal neurons were shown to undergo rapid recycling (Klingauf and others 1998). Recycled vesicles can go through further rounds of exocytosis without leaving the RRP (Pyle and others 2000). Furthermore, on the single vesicle level, one vesicle can participate more than one round of exocytosis (Aravanis and others 2003).

By contrast, in the retinal bipolar cells styryl dyes can escape completely within a few milliseconds (Zenisek and others 2002). One possible explanation for these contradictory results is that retinal bipolar cells and hippocampal neurons are adapted to different physiological functions. Since goldfish retinal bipolar cells have nearly one million vesicles, it might not be necessary to recycle vesicles as rapidly as in hippocampal neurons. If this interpretation is correct that kiss-and-run exocytosis is restricted to specific neuron types, then the underlying mechanism of this divergence would be very interesting and would advance the understanding of exocytosis.

The molecular mechanism of kiss-and-run exocytosis is unknown and only a few factors have been studied. High extracellular Ca^{2+} concentration shifted the mechanism from full fusion to kiss-and-run exocytosis (Ales and others 1999). Also synaptotagmin isoforms influenced the fraction of vesicles that undergo kiss-and-run exocytosis (Wang and others 2003).

3.4. The molecular composition of the fusion pore

The molecular composition of the fusion pore has been controversial. Arguments were put forward for either a proteinaceous or a lipidic structure. There are two contrasting models: the channel model and the hemifusion stalk model (Figure 1-5) (Jahn and Sudhof 1999; Lindau and Almers 1995). Distinguishing between these two models has been difficult. Thus, inferences have been made based on the indirect evidence.

The channel model draws on the analogy with ion channels in which proteins or protein complexes line the wall. Open fusion pores subsequently dilate with lipid incorporated between proteins (Figure 1-5, A). The hemifusion model envisions the fusion pore as a pure lipidic structure sometimes referred to as a "stalk". The stalk is an intermediate state where the inner leaflets of two bilayers mix first (Figure 1-5, B).

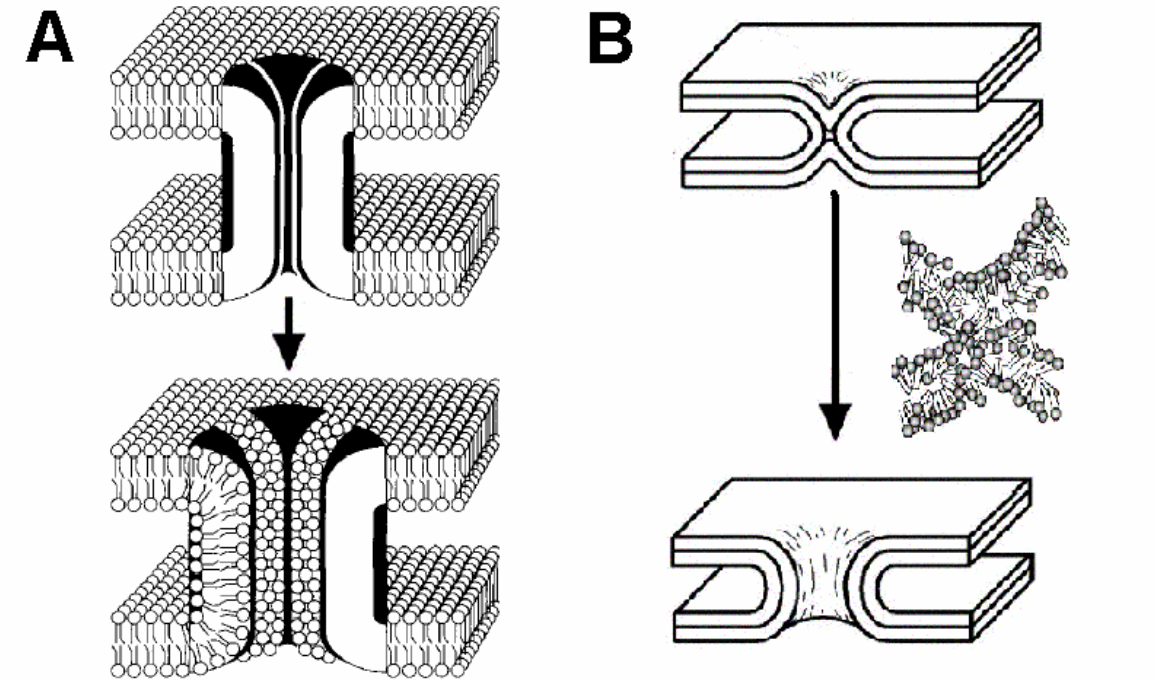

Figure 1-5. Two fusion pore models. (A) In the channel model, proteins line the initial fusion pore. Fusion pore dilation is through incorporating lipid between protein segments (adapted from Lindau and Almers 1995). (B) The hemifusion model contains a pure lipidic "stalk" intermediate structure (shown by the inset picture) (adapted from Jahn, Lang et al. 2003).

The channel model is supported by many parallels between fusion pores and ion channels (Lindau and Almers 1995; Lindau and Alvarez de Toledo 2003). Comparable conductance is considered as the main evidence. However, similar pore conductance was also observed when phospholipid vesicles fused with planar phospholipid bilayers under hypotonic stress (Chanturiya and others 1997). The fusion pore initiated by hypotonic stress may be completely different from that mediated by many proteins in the physiological conditions Thus, this observation of a fusion pore in a protein-free lipid fusion system does not argue strongly against a proteinaceous pore structure in exocytosis.

Kiss-and-run exocytosis also favors the channel model (Lindau and Alvarez de Toledo 2003). The channel model predicts that kiss-and-run exocytosis can arise from the closure of a fusion pore. Tight regulation of fusion pore could be explained as ion channel gating, through protein-protein interactions. In contrast, pure lipidic fusion pores would be more difficult to regulate.

Prior to the work presented here, there was no experimental evidence for the presence of any protein in the fusion pore structure. The transmembrane domains of the SNARE proteins have been proposed as the best candidate for the following reasons. The SNARE proteins are essential to membrane fusion. The transmembrane domains of syntaxin and synaptobrevin reside in the plasma membrane and the vesicle membrane respectively. Formation of the SNARE complex could bring these transmembrane domains together.

3.5. Fusion pores in synaptic transmission

Synaptic transmission is very fast, on the submillisecond to millisecond time scale (Augustine and others 1985; Katz and Miledi 1965; Llinas and others 1981). For example, in frog neuromuscular junction the synaptic delay was as short as ~400 μsec (Katz and Miledi 1965). In the squid giant synapse the latency between Ca^{2+} entry and the postsynaptic response can be less than 200 μsec (Llinas and others 1981). In goldfish retinal bipolar neurons the delay between elevated intracellular Ca^{2+} and exocytosis was ~1.5 msec (Heidelberger and others 1994). In cultured leech neurons SSVs discharged with a time constant of ~260 μsec and LDCVs with ~1.3 msec (Bruns and Jahn 1995). These examples demonstrated that the time course of neurotransmitter release is extremely fast at synapses.

The fusion pore can remain small for a few milliseconds (Hartmann and Lindau 1995; Lindau and Alvarez de Toledo 2003; Wang and others 2001a; Wang and others 2003). Expulsion of neurotransmitter may be complete within a few hundred microseconds for a large 300 pS pore (Almers and others 1991). But neurotransmitter release at synapses may employ much smaller fusion pores. So far, there is no direct measurement of the size of fusion pores in the hippocampal synapses, where synaptic plasticity is often studied. Based on a size of 19 pS for the fusion pores of micro-vesicles in the posterior pituitary, a few milliseconds was estimated for expulsion of the vesicle content (Klyachko and Jackson 2002). From this estimate, the initial conductance and the dilation rate of a small fusion pore might directly affect the post-synaptic response.

The degree to which fusion pores might influence synaptic transmission is unknown. Overexpression of synaptotagmin-IV in PC12 cells induced long lasting small fusion pores (Wang and others 2003). Since synaptotagmin-IV expression is upregulated during excessive synaptic activities (Vician and others 1995), the slow leakage of neurotransmitter was hypothesized to reduce synaptic strength by desensitizing the postsynaptic receptors.

3.6. Fusion pores in intracellular membrane trafficking

Membrane fusion is a universal event. It is reasonable to speculate the presence of fusion pores during intracellular membrane fusion. But due to lack of detection methods, there is no study of fusion pores during vesicular transport. Studies of the fusion pore of Ca^{2+}-triggered exocytosis may help to guide the related work on intracellular membrane trafficking.

3.7. The fusion pore in yeast vacuole fusion

Which molecule mediates the final fusion step in yeast is unclear (Wickner 2002). The SNARE complex was demonstrated to be essential in docking, but not in the final fusion step (Laage and Ungermann 2001; Ungermann and others 1998). One hypothesis suggests that fusion starts with a proteinaceous pore formed by the membrane-integral subunit of the vacuolar H^+-ATPase (V0) (Peters and others 2001).

V0 is a proteolipid, defined as a protein complex, but can be extracted into a non-polar medium like lipid (Stevens and Forgac 1997). V0 can form a hexameric ring structure that pumps protons by hydrolyzing ATP. By incorporating V0 into artificial lipid, a Ca^{2+} and calmodulin dependent liposome fusion was reconstituted (Peters and others 2001). In this reconstituted fusion system, V0 residing in opposing membranes can engage each other to form a trans-complex. Based on the finding that disrupting the trans-SNARE complex did not inhibit fusion, the V0 was put forward as the mediator of the final fusion step. From this study, it was anticipated that the yeast fusion pore resembles a proton channel. But there was no direct experimental evidence regarding the pore structure formed by V0.

3.8. The fusion pore in viral fusion

Viral fusion seems to be very different from Ca^{2+}-triggered exocytosis. Enveloped viruses fuse with their host through the action of a single protein showing no homology with the SNARE proteins. This single viral fusion protein binds to a receptor on the host cell and fuses the virus membrane with the host membrane (Skehel and Wiley 2000). One of the best characterized fusion proteins is hemaglutinin (HA), a glycoprotein of the influenza virus.

The fusion pore structure in viral fusion is controversial. Conflicting evidence supports both lipidic and proteinaceous structures. Several studies prefer the hemifusion stalk model (Jahn and others 2003). For example, in one study the transmembrane domain of HA was replaced with a lipid membrane anchor. This mutant HA induced the formation of a hemifusion stalk (Melikyan and others 1997; Melikyan and others 1995). In addition, lipid curvature seems to be a factor, as membrane lipid components affected the fusion pore opening through the shapes of their head groups (Chernomordik and others 1997). Moreover, lipid dye flux was observed but the aqueous content remained trapped (Melikyan and others 1997). This delayed expulsion of the aqueous day could be due to the existence of a lipidic stalk. Alternatively, it is also possible that a small proteinaceous fusion pore was formed which did not allow the passage of the large aqueous dyes (Zimmerberg and others 1994). Unfortunately, these authors did not distinguish these possibilities by checking the membrane capacitance during fusion.

Evidence also supports a proteinaceous pore in viral fusion. The fusion pore was observed as capacitance flickers in the HA mediated viral fusion, similar to that of Ca^{2+}-triggered exocytosis (Melikyan and others 1993a; Melikyan and others 1993b; Spruce and others 1991; Spruce and others 1989; Tse and others 1993; Zimmerberg and others 1994). 3-6 transmembrane segments of HA were predicted to mediate the formation of a fusion pore based on the fusion kinetics (Danieli and others 1996; Melikyan and others 1993a), as well as modeling (Blumenthal and others 1996; Clague and others 1991). During fusion, lipid movement cannot be detected before the dilation of the fusion pore (Blumenthal and others 1996; Tse and others 1993; Zimmerberg and others 1994).

Moreover, HA transmembrane domains can induce the fusion pore formation, which is different from the hemifusion stalk formed with mutant HA lacking a transmembrane domain (Chernomordik and others 1997; Melikyan and others 1995). But an alternative explanation for the fusion pore formed with the HA transmembrane domain is a lipidic pore influenced by lipid curvature (Melikyan and others 1997). This argument was supported by the observation that HA restricted lipid flux even before fusion pore opening (Chernomordik and others 1998). So far, there is no direct evidence for the molecular composition of the fusion pore in viral fusion.

CHAPTER 2. MATERIALS AND METHODS

1. Amperometry

1.1. Principles

Amperometry is an electrochemical method that uses oxidation/reduction to detect certain neurotransmitters. Electrochemical methods were initiated to measure the neurotransmitter concentration in brain over 30 years ago (Kissinger and others 1973). Then in 1990 amperometry was applied to detect single vesicle release (Leszczyszyn and others 1990; Leszczyszyn and others 1991; Wightman and others 1991), and has since been widely used to study exocytosis.

In order to oxidize/reduce a compound in solution, a voltage must be applied. Amperometry applies a constant potential to a carbon fiber electrode and records the oxidization current. An applied potential of several hundred millivolts is sufficient to oxidize a number of neurotransmitters, such as catecholamines (epinephrine, norepinephrine, and dopamine) and indoleamines (serotonin). Nitric oxide (Malinski and Taha 1992), ascorbic acid, and uric acid are also oxidizable. In theory, peptides and proteins containing tyrosine, tryptophan and cysteine could also be oxidized, but experiments on peptides have proven to be difficult due to the small amount being released and the slow diffusion rate (Chow 1995).

Cyclic voltammetry is another electrochemical method to study exocytosis, usually to identify a specific compound. Cyclic voltammetry uses a periodic voltage pattern, usually

a triangle wave. A voltammogram can be generated by plotting the applied voltage versus the recorded oxidation/reduction current. Because each compound has a specific redox potential and electron transfer rate, different compounds usually have distinct voltammograms. By comparing the pattern of a voltammogram, one can identify a specific compound.

Amperometry has a time resolution slightly faster than a millisecond. But cyclic voltammetry has a much lower time resolution as a result of employing a triangle voltage pattern. For a specific cell type under study, the molecules secreted are usually already identified. Thus, amperometry with its higher time resolution is preferred for the study of exocytosis kinetics. Furthermore, amperometry has several advantages over capacitance measurement: (1) exocytosis is not masked by endocytosis; (2) the released product is directly monitored; (3) there is no need to control the voltage of a cell.

1.2. Quantitative nature of amperometry

The amperometric oxidization current is proportional to the amount of molecules that reach the electrode. Based on Faraday's law, the relationship between the total charge transferred and the number of molecules oxidized can be written as:

$$Q = \int Idt = \frac{zFM}{N_A} = zeM$$

Q is the total charge detected by the electrode, which can be calculated by integrating the amperometry current over time. M is the number of molecules. z is the number of electrons transferred per molecule. In the case of norepinephrine (NE), z is 2 as oxidization leads to the loss of two electrons (Figure 2-1). F is Faraday's constant

(96,485coul/mole). N_A is Avogadro's number ($6.02x10^{23}$) and e is the elementary charge ($1.6x10^{-19}$ coul).

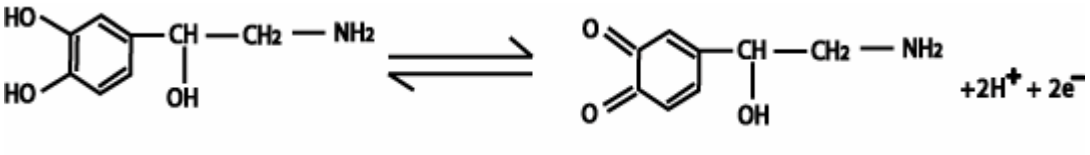

Figure 2-1. Oxidization of norepinephrine generates two electrons and two protons.

The quantitative nature of amperometry allows the estimation of the number of catecholamine molecules secreted from a single vesicle. A mean of ~3 million catecholamine molecules was estimated for the LDCVs in chromaffin cells (Chow and others 1992; Wightman and others 1991). By simultaneously measuring the number of catecholamine molecules released and the size of a vesicle, one can calculate the intravesicullar catecholamine concentration. It was estimated to be about 1 M for the LDCVs in chromaffin cells (Gong and others 2003).

1.3. Diffusion effect in amperometry

In amperometry the recorded current reflects the time course of transmitter release inferred from the oxidization rate and the diffusion rate. Since the oxidization rate is much faster than the diffusion rate, the oxidation kinetics has negligible effect. Diffusion follows the Einstein-Smolochowski equation as:

$$\left\langle X^2 \right\rangle = 2D\tau$$

$$\tau = \frac{\langle X^2 \rangle}{2D}$$

$\langle X^2 \rangle$ is the mean square of displacement. In amperometry recording X is the distance from the release site to the detection electrode. D is the diffusion constant and τ is the time needed to travel a distance of X. Since the effect of distance on diffusion time is nonlinear, diffusion affects amperometry dramatically when longer distances are traveled (Wightman and others 1995).

In most amperometry studies electrodes slightly touch the cell membrane. The distance for a catecholamine molecule to diffuse to the detection electrode can be estimated as less than 0.5 μm. For a distance this small, diffusion is very fast compared to the time course of neurotransmitter release (Chow 1995; Chow and others 1992). Under these conditions, amperometry can precisely follow the secretion time course.

1.4. Experimental setup

Amperometry recording was performed with a VA-10 amplifier (ALA Instruments) using carbon fiber electrodes polarized to 650 mV (ALA Instruments). Current was low-pass filtered at 1 kHz and digitized at 4 kHz by a PC-running pCLAMP-8 (Axon Instruments).

1.5. Solutions and KCl application

During experiments, cells were bathed in a solution containing (in mM) 150 NaCl, 4.2 KCl, 1 NaH_2PO_4, 0.7 $MgCl_2$, 2 $CaCl_2$, 10 glucose and 10 Hepes (pH 7.4) at ~22°C. Secretion was induced by depolarization using the bathing solution, but with KCl elevated

to 105 mM and NaCl reduced to 5 mM. The depolarization solution was ejected for 6 sec from a micropipette (1-2 μm tip) positioned about 10 μm away from the recorded cell. The ejection pressure was 10-30 PSI gated by a picospritzer (General Valve Corporation, Fairfield NJ). The precise timing of KCl application was achieved by computer through the data acquisition program. Cells were typically stimulated up to 6 times at about 2 min intervals.

1.6. Data analysis

Amperometry data were analyzed with a computer program to extract foot information according to the criteria of Chow and von Rüden (Chow 1995). Spikes were detected using a threshold of 2 pA (about 5-10*RMS of background noise). Feet were analyzed for spikes bigger than 20 pA. The onset of a prespike foot (PSF) was determined by departure of the signal from the baseline (5*RMS). The end of the prespike foot was the intercept of the spike rising phase and the line drawn through the spike rising from 35% to 60% of the peak.

The PSF duration was taken as the time from the onset to the end. The PSF area was the area bounded by the spike and the line through the rise from 35% to 60% of peak (Figure 2-2). The average foot current was calculated as the PSF area divided by the duration. PSF with durations briefer than 0.75 msec (three times the sampling rate) were rejected as too brief for reliable detection.

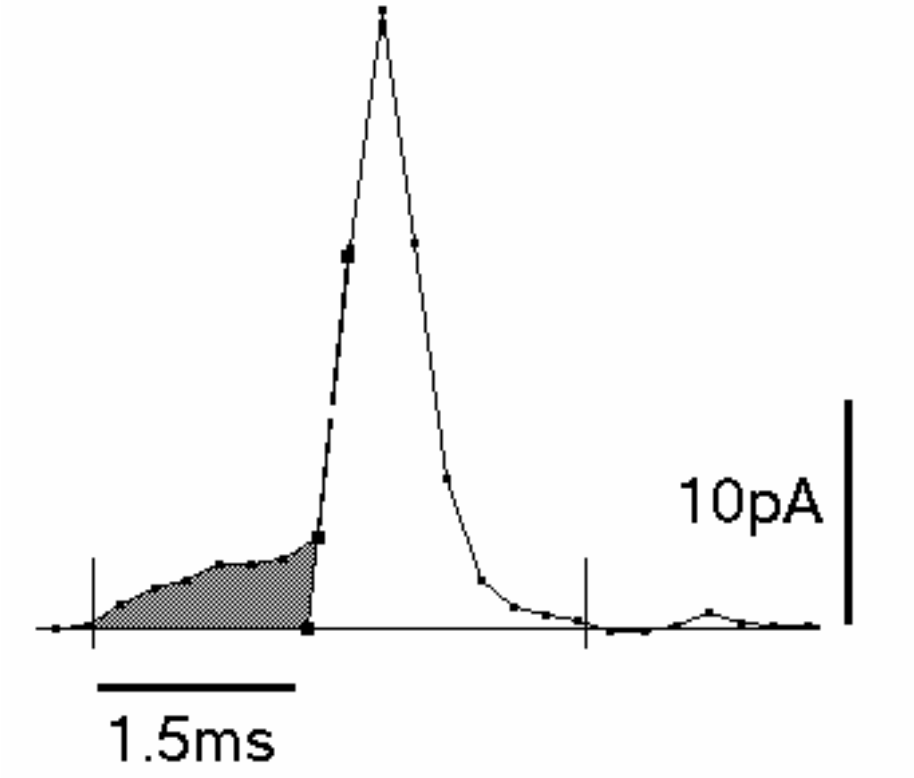

Figure 2-2. An amperometry spike with the prespike foot shaded.

2. Cell-attached capacitance measurement

2.1. Principles

The capacitance-admittance measurement combines the patch-clamp technique with admittance analysis (Lindau 1991; Neher and Marty 1982). This method can be used to estimate the fusion pore conductance based on the equivalent circuit of a cell and a fusing vesicle (Figure 2-3). In order to measure the fusion pore conductance continuously, a sine wave was applied to charge and discharge the vesicle capacitance repetitively.

There are two configurations for the capacitance measurement, the whole-cell configuration and the cell-attached configuration. The equivalent circuits for these two configurations are shown in Figure 2-3. In the whole-cell configuration (Figure 2-3, A), R_A is the access resistance including the resistance of the pipette and any obstacles at the pipette tip; Cm is the cell membrane capacitance; Gm is the cell membrane conductance. In the cell-attached configuration (Figure 2-3, B), Cpa is the patch capacitance and Gpa is the patch conductance.

Once a vesicle fuses with the plasma membrane, the fusion pore conductance (Gp) changes from Gp=0 to Gp (figure 2-4, C). And the vesicle capacitance (Cv) is in series with Gp. Assuming that Cpa, Gpa, R_A and Cm are constant, the admittance of the equivalent circuit changes by

$$\Delta Y = T^2(w) \times \left[\frac{(wCv)^2 / Gp}{1 + \left(wCv / Gp \right)^2} + i \frac{wCv}{1 + \left(wCv / Gp \right)^2} \right]$$

where

$$T^2(w) = 1 \Big/ (1 + R_A G_M + iwC_M R_A)^2 = |T(w)|^2 \cdot e^{i\Phi}$$

Besides the scaling factor and the phase shift in the factor of $T^2(w)$, the admittance change has a real part and an imaginary part:

$$\text{Re} = \frac{(wCv)^2 / Gp}{1 + \left(wCv / Gp\right)^2}$$

$$\text{Im} = \frac{wCv}{1 + \left(wCv / Gp\right)^2}$$

The Re and Im parts can be used to calculate the vesicle capacitance (Cv) and the fusion pore conductance (Gp):

$$wCv = \frac{\text{Re}^2 + \text{Im}^2}{\text{Im}}$$

$$Gp = \frac{\text{Re}^2 + \text{Im}^2}{\text{Re}}$$

In the whole-cell mode the intrinsic capacitance noise is mainly generated by Cm. Correspondingly, in the cell-attached mode the intrinsic noise arises from Cp. Because Cp is much smaller than Cm, the cell-attached configuration has much lower noise compared to the whole-cell configuration. With the cell-attached configuration, fusion pores as small as ~10 pS have been detected (Debus and Lindau 2000; Klyachko and Jackson 2002).

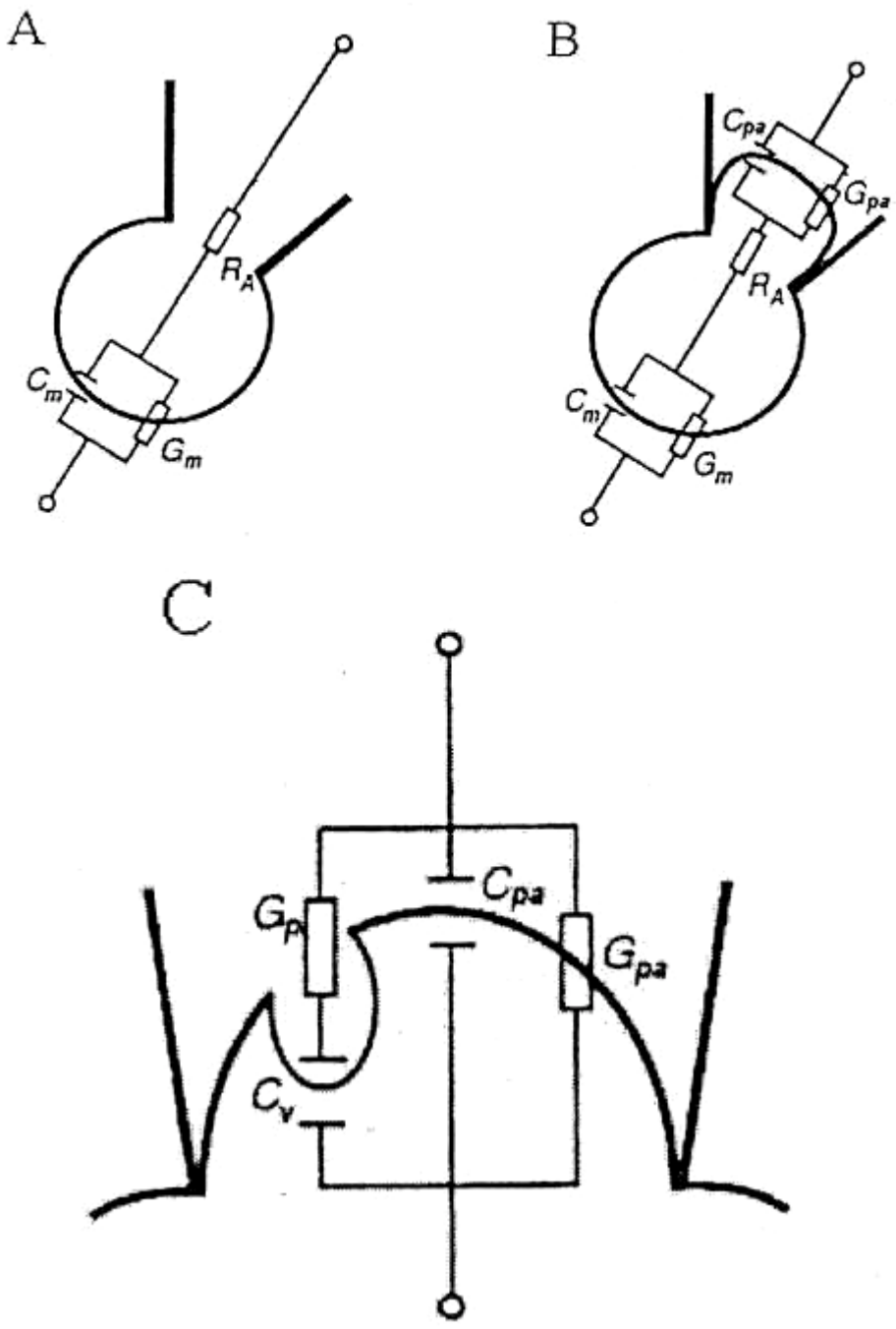

Figure 2-3. The equivalent circuit of a cell in the whole-cell configuration (A), and the cell-attached configuration (B). Once a vesicle fuses with the plasma membrane, the corresponding equivalent circuit under the cell-attached configuration can be visualized as in (C). (modified from (Lollike and Lindau 1999)).

2.2. Phase adjustment and calibration

Phase was adjusted by dithering a resistance in series with the C_{slow} potentiometer on the patch clamp amplifier. After this adjustment, a dithering pulse should produce no change in the in-phase component (real component, Re), but produce steps in the 90°-out-of-phase component (imaginary component, Im) of the lock-in amplifier output. A 100 fF equivalent dithering was performed with stimulus scaling set to 0.001 on the patch-clamp amplifier to prevent saturation. During an experiment the stimulus scaling was set at 0.1. Thus, the dithering produced a 1 fF change on the Im output of the lock-in amplifier.

Even though the phase was adjusted perfectly at the beginning of an experiment, it often changed during recording, especially after a few capacitance steps. A phase shift leads to a small projection of the Im trace onto the Re trace. To compensate for these small phase errors, the Re ($Gcorr$) and Im ($Ccorr$) traces can be recomputed from the original Re and Im traces by introducing a phase shift Φ according to the formula (Lindau 1991):

$$Gcorr = \mathrm{Re} * \cos(\Phi) + \mathrm{Im} * \sin(\Phi)$$
$$Ccorr = -\mathrm{Re} * \sin(\Phi) + \mathrm{Im} * \cos(\Phi)$$

With Φ correctly adjusted, a change on the Im trace would no longer project onto the Re trace.

2.3. Instrumentation

Recordings were made with an EPC-7 patch-clamp amplifier (List-Electronic, Germany) connected to a lock-in amplifier (model SR830, Stanford Research). The sinusoidal signal from the lock-in (100 mV, 10 kHz) was superimposed on a command

potential of 0 mV and fed into the patch amplifier. The high amplitude (100 mV) and high frequency (10 kHz) sinusoidal signal does not activate voltage-gated channels. The sinusoidal patch clamp current output was fed back to the lock-in amplifier for phase-sensitive detection (PSD). The current output of the PSD includes the in-phase (Re) and 90^{o}-out-of-phase (Im). The Re and Im outputs of the lock-in amplifier were then low-pass filtered at 3 msec or 10 msec and digitized at 2 kHz. Data acquisition was through the computer program Igor pro Pulser.

The patch-clamp amplifier was operated at a gain of 50 mV/pA. The C_{slow} potentiometer was set to the minimum value and G_{slow} was set to 0.2μS. The input stimulus was filtered with 2 μsec. The output signal of the patch-clamp amplifier was fed into the lock-in amplifier through a 5:1 voltage divider without filtering. Before each recording, the sinusoidal current was cancelled out with the C_{fast} and τ_{fast} potentiometers (Debus and Lindau 2000; Klyachko and Jackson 2002).

The noise level was reduced by using thick-wall borosilicate glass pipettes (1.1mm I.D., 1.7mm O.D.) well coated with sylgard (Dow Corning, midland, MI). Pipettes with resistance of 4-6 MΩ were used to form cell-attached patches. The solution level in the recording chamber was as low as possible and occasional surface application of mineral oil was used to reduce the noise level even further. Low noise capacitance recordings with a 10 aF RMS allowed the detection of fusion pores in PC12 cells.

Data analysis was performed with the programs Igor and Origin.

2.4. Solutions and drugs

For capacitance measurement cells were pretreated with 100 nM phorbol myristate acetate for 6 minutes to enhance secretion (Gillis and others 1996). Recordings were made with 30 mM K^+ in the bathing solution (in mM: 115 NaCl, 30 KCl, 5 $CaCl_2$, 1 $MgCl_2$, 20 glucose, 10 HEPES, pH 7.3) to increase the basal level of exocytosis. Patch pipettes contained (in mM): 50 NaCl, 100 TEA-Cl, 5 KCl, 5 $CaCl_2$, 1 $MgCl_2$, 10 HEPES, pH 7.3.

3. Whole-cell voltage clamp recording

Whole-cell patch clamp of the Ca^{2+} current (Bean 1992) was performed with an EPC-7 patch amplifier (List-Electronic, Germany). Current was low-pass filtered at 100 Hz and sampled at 4 kHz. Leak currents were subtracted by a P/4 procedure. Whole-cell capacitance of PC12 cells ranged from 5-15 pF. Uncompensated series resistances were <15 MΩ. Series resistance compensation was unnecessary in most cells, because the input resistance of PC12 cells was high (1-10GΩ) and the maximal Ca^{2+} current was low (<200 pA). Stimulus, data acquisition, and analysis were carried out with pClamp8.

The borosilicate glass patch pipettes of 3-8 MΩ were filled with a pipette solution containing (in mM): 90 *N*-methylglucamine, 20 TEA-Cl, 0.2 EGTA, 2 $MgCl_2$, 20 Na_2-creatine phosphate, 5 Mg-ATP, and 0.1 guanosine triphosphate, and 10 Hepes (pH 7.35). The bathing solution was (in mM): 105 NaCl, 20 $CaCl_2$, 1.5 $MgSO_4$, 15 glucose, 5 Hepes and 0.003 tetrodotoxin (added right before each experiment) (pH 7.35).

4. Molecular Biology

The pIRES2-EGFP vector (Clontech) was used for all mutants in this study (Figure 2-5). The pIRES2-EGFP vector allows the transcription of a bicistronic mRNA for separate expression of the protein of interest and the GFP reporter. cDNA encoding the protein of interest was inserted into the multiple cloning sites (MCS) after the Pcmv, whereas the GFP encoding sequence follows an internal ribosomal entry site (IRES). The GFP provided a convenient marker to identify cells successfully transfected.

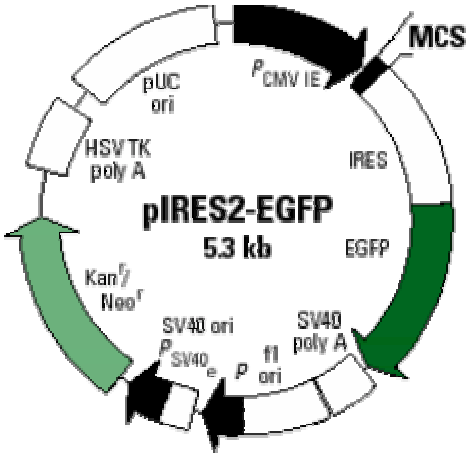

Figure 2-4. The pIRES-EGFP vector used in this study. Genes of interest inserted into the MCS can be transcripted to a bicistronic mRNA together with GFP. The IRES allows the separate expression of the protein of interest from the GFP reporter.

The wild type syx and SNAP-25 genes were from Chapman's laboratory. They were subcloned into the pIRES2-EGFP vector by a single PCR reaction with the restriction sites XhoI and EcoRI. The syx-linker mutants were obtained from Rothman's laboratory (McNew and others 1999) and were inserted between XhoI and EcoRI sites in the pIRES2-EGFP vector.

The syx transmembrane domain point substitutions at positions 276-281, 283, 285, 287, and the truncated form of syx were made with a single PCR reaction with the designated point mutation on one primer. The syx point mutations at positions 269-275 in the transmembrane domain, together with SNAP-25 and syx mutations in the SNARE motifs, were made by modified sequential PCR (Cormack 1994). Construction of these mutants required four oligonucleotides, two of which are complementary and encode the mutation site in the middle. The other two primers complement two selected restriction sites upstream (XhoI) and downstream (EcoRI) of the mutation site. Mutants were confirmed by DNA sequencing.

5. Cell culture and transient transfection

Cell culture: PC12 cells were cultured in 100 mm dishes in Dulbecco's modified eagle medium (DMEM) with glucose (4.5 mg/ml), $NaHCO_3$ (3.7 mg/ml) (Sigma), 5% horse serum and 5% iron-supplemented calf serum (HyClone) at 37°C in a humidified atmosphere of 10% CO_2-air (Hay and Martin 1992). Cells from passage number of 18-50 were used for experiments. Since PC12 cells tend to cluster, cells were passed through 22½ needles in order to separate them well.

For amperometry recording, cells were plated at $2.0x10^5$ cells per 35mm dish. Dishes were freshly coated with 2.5 μM poly-D-lysine and 2.5 μM collagen-I (BD Bioscience, Bedford MA). Cells were loaded with 1.5 mM NE and 0.5 mM ascorbic acid for 14-16 hours. For capacitance measurement, cells were transferred to glass cover slips coated with 2.5 μM poly-D-lysine and 2.5 μM collagen-I the day before recording.

Transient transfection: Transient transfection was performed with an ECM-830 electroporator (BTX, San Diego, CA) set at 210 V, 7 msec. Cells were transfected with 50 ug of DNA in a solution containing (in mM): 120 KCl, 0.15 $CaCl_2$, 10 KH_2PO_4, 2 EGTA, 5 $MgCl_2$, 2 Mg-adenosine triphosphate (ATP), 5 glutathione, and 2.5 Hepes (pH 7.6). Experiments were performed 48-96 hours after transfection. The fraction of the fluorescent cells indicated that the transfection was about 30% efficient. Control cells were transfected with the pIRES2-EGFP vector lacking a protein encoding at the MCS after the Pcmv.

6. Fluorescence microscopy

Cells were viewed with a Nikon inverted fluorescence microscope equipped with a 75 Watt Xenon arc lamp (Model 770U, Opti-Quip, Highland mills, NY). The GFP fluorescence was detected with an Endow EGFP filter cube (Chroma Technology Corp. Brattleboro, VT) with a 470±20nm excitation filter, a 495nm dichroic mirror, and a 525±25nm emission filter. Excessive exposure was prevented by an electric shutter (Model D122, Vincent Assoc., Rochester, NY).

7. Electron microscopy

Electron microscopy was performed with a Philips CM120 transmission electron microscope. Cells were fixed at room temperature in 2.0% paraformaldehyde and 2.5% glutaraldehyde for 2 hours, post-fixed with 2% osmium-tetroxide for 1 hour, dehydrated, embedded, and sectioned at 80 nm. (Samples were prepared by the EM facility personal at UW-Medical School.)

8. Biochemical analysis:

Immunoblot analysis: Immunoblot analysis was used to determine the expression level of the transfected proteins in PC12 cells. The PC12 cell membranes were prepared by incubating cells in a hypotonic buffer (10 mM Tris-HCl, pH 7.0, 2 mM EDTA, 1 mM phenylmethanesulfonyl fluoride, 1 μg/ml pepstatin A, 1 μg/ml leupeptin, and 1 μg/ml aprotinin) for 20 min (4°C) followed by homogenization (30 strokes, Dounce glass/glass). The post-nuclear supernatant was prepared by centrifugation (400 *g,* 2 min). Membranes were collected by centrifuging the post-nuclear supernatant (21,000 *g*, 15 min) and solubilized in 1% SDS. Protein concentrations were determined by BCA (Pierce Chemical Co). Recombinant standards (GST-Syx) and 1 μg of the total protein from the PC12 cell membranes were subjected to SDS-PAGE. Syntaxin, synaptotagmin, SNAP-25 and synaptobrevin were immunoblotted using monoclonal antibodies HPC-1, 41.1, 71.2 and 69.1 respectively and visualized with the enhanced chemiluminescent substrate (Pierce, Rockford IL).

GST pull-down assays: GST pull-down assays were used to examine syx-synaptotagmin-I interactions. GST-syx was immobilized on glutathione-sepharose beads. Fifteen micrograms of wild-type or mutant GST-syx was incubated with the cytoplasmic domain of synaptotagmin-I (2 μM) in 150 μl of HBS solution (containing 100 mM NaCl, 50 mM HEPES, pH 7.4) with 0.5% Triton X-100, and either 2 mM EGTA or 1 mM Ca^{2+}. Protein-protein interactions were allowed by incubating samples for 1.5 hours at 4^{o}C. Beads were then washed 3 times with the binding buffer. Fifteen percent of the bound

materials and 10% of the total were subjected to SDS-PAGE and visualized by immunoblotting for synaptotagmin-I with the monoclonal antibody 41.1.

CHAPTER 3. THE SYNTAXIN MEMBRANE ANCHOR LINES THE FUSION PORE OF CALCIUM TRIGGERED EXOCYTOSIS

1. Introduction

A proteinaceous fusion pore has been hypothesized by analogy with ion channels (Lindau and Almers 1995). Ion channel conductance is uniquely sensitive to the manipulation of the pore-lining residues of a channel-forming protein (Imoto and others 1988; Lester 1992). Mutations that alter the charge or size of the side chains exposed to the ion permeation pathway can markedly alter the channel conductance. Applying the same rational to the fusion pore, one would expect that the flux through a fusion pore should also be sensitive to changes in its pore-lining constituents. Thus, examining an effect on the fusion pore flux could identify proteins that line the fusion pore.

We selected the membrane anchor of syntaxin (syx) as the best candidate protein in the formation of the fusion pore for the following reasons: first, syx is essential for exocytosis, as demonstrated by genetic ablation (Schulze and others 1995) and by the action of clostridial neurotoxins (Blasi and others 1993); second, among the proteins essential for exocytosis, syx is the only plasma membrane protein with a membrane-spanning segment (Jahn and Sudhof 1999; Lin and Scheller 2000); and third, syx is the only neuronal t-SNARE with a membrane anchor that is necessary for the reconstitution of proteoliposome fusion (Weber and others 1998).

Rat neuroendocrine PC12 cells were used in the current study. PC12 cells have large dense core vesicles, which can undergo Ca^{2+}-triggered exocytosis (Figure3-1). Low release frequency of the LDCVs in PC12 cells allows the detection of a fusion pore without interference from the subsequent vesicle fusion events.

Here, the fusion pore flux during LDCV exocytosis in PC12 cells was shown to be sensitive to the size of certain residues in the syx membrane anchor. Residues that influenced the fusion pore flux lay along one face of the syx transmembrane α-helix. In addition, residues that influenced the fusion pore flux also electrostatically interacted with the charged neurotransmitter passing through the fusion pore. Thus, a fusion pore model formed by the syx membrane anchor was proposed. (Results were published in (Han and others 2004) and (Han and Jackson submitted))).

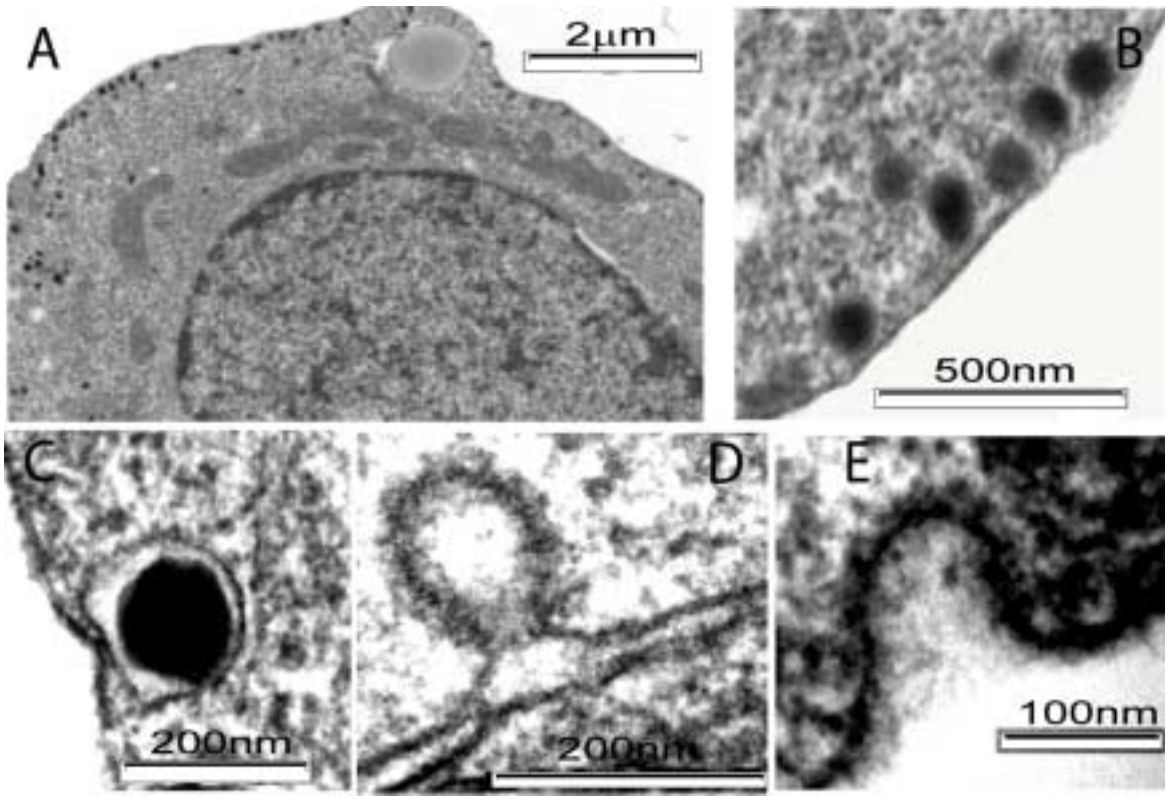

Figure 3-1. PC12 cell under electron microscopy. Large dense core vesicles can be easily distinguished (A). Vesicles in different states were captured, close/docked to the plasma membrane (B,C), Ω–shaped (D), and collapsed (E).

2. Results and Discussion

2.1. Amperometric investigation of fusion pore obstruction

To test the hypothesis that the membrane anchor of syx lines the fusion pore, we employed tryptophan scanning. By introducing a tryptophan to each position along the syx transmembrane domain, we hoped to identify potential pore lining residues. The rationale for using tryptophan is that its bulky side chain can serve as a physical blocker as it protrudes into the neurotransmitter pathway.

Obstruction of an open fusion pore was first examined with amperometry. LDCV exocytosis was elicited by elevating the extracellular KCl concentration, which depolarized the PC12 cell membrane and elevated the intracellular Ca^{2+}. Figure 3-2 shows amperometry traces from cells transfected with syx, blank vector (GFP), and two syx mutants. Single vesicle fusion events registered as spikes.

Expanding a single amperometry spike revealed a prespike foot (PSF), a rapid rising phase and a roughly exponential decay phase (Figure 3-3). The interpretations for the spike rising phase and decay phase have been controversial, but the PSF has been well demonstrated as corresponding to NE leaking through the fusion pore (Albillos and others 1997; Alvarez de Toledo and others 1993; Chow and others 1992; Schroeder and others 1996). The shapes of PSF were highly variable (Figure 3-4).

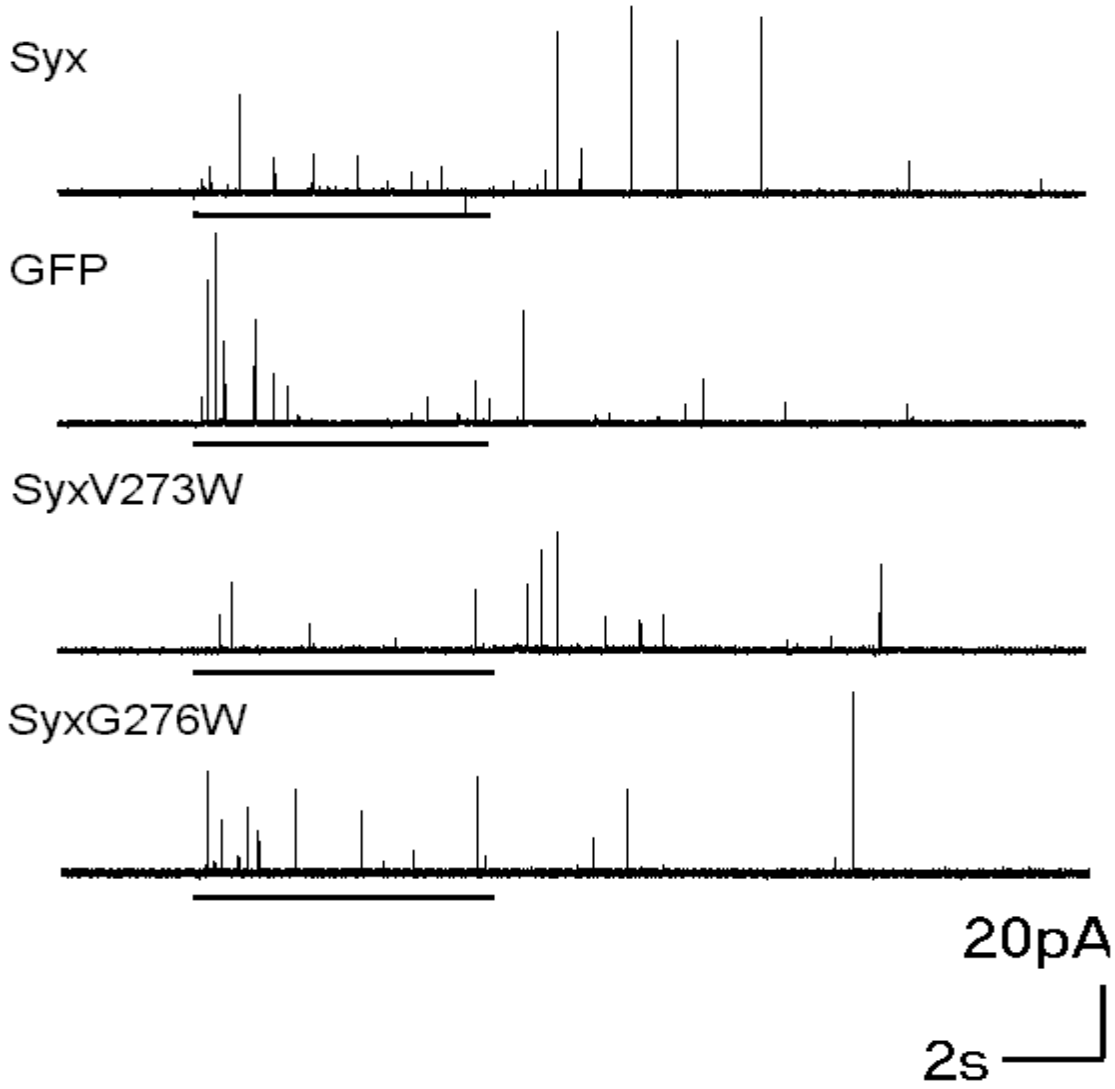

Figure 3-2. Amperometry recordings from PC12 cells. Six seconds of KCl depolarization (indicated by bars below each trace) elicited NE release. Single vesicle release events registered as spikes from cells transfected with wild-type syx, the control vector (GFP), and two syx mutants. (Figure from (Han and others 2004), work done by Han, X)

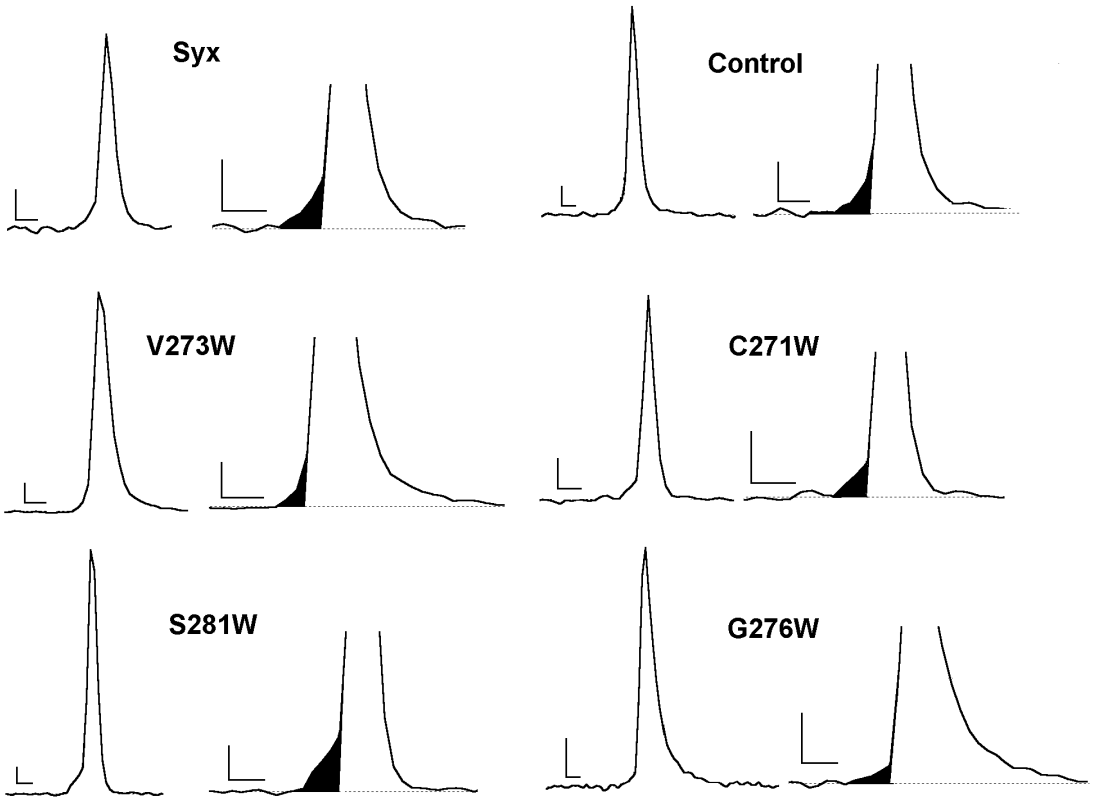

Figure 3-3. The prespike foot (PSF) in amperometry represents the fusion pore flux. Amperometry spikes (left of each panel) generally have a PSF, a rising phase and a decay phase. Expanded traces (right) show the PSF (shaded regions) recorded from cells overexpressing the indicated proteins. Scale bars are 5 pA and 1 msec. (Figure from (Han and others 2004), work done by Han, X).

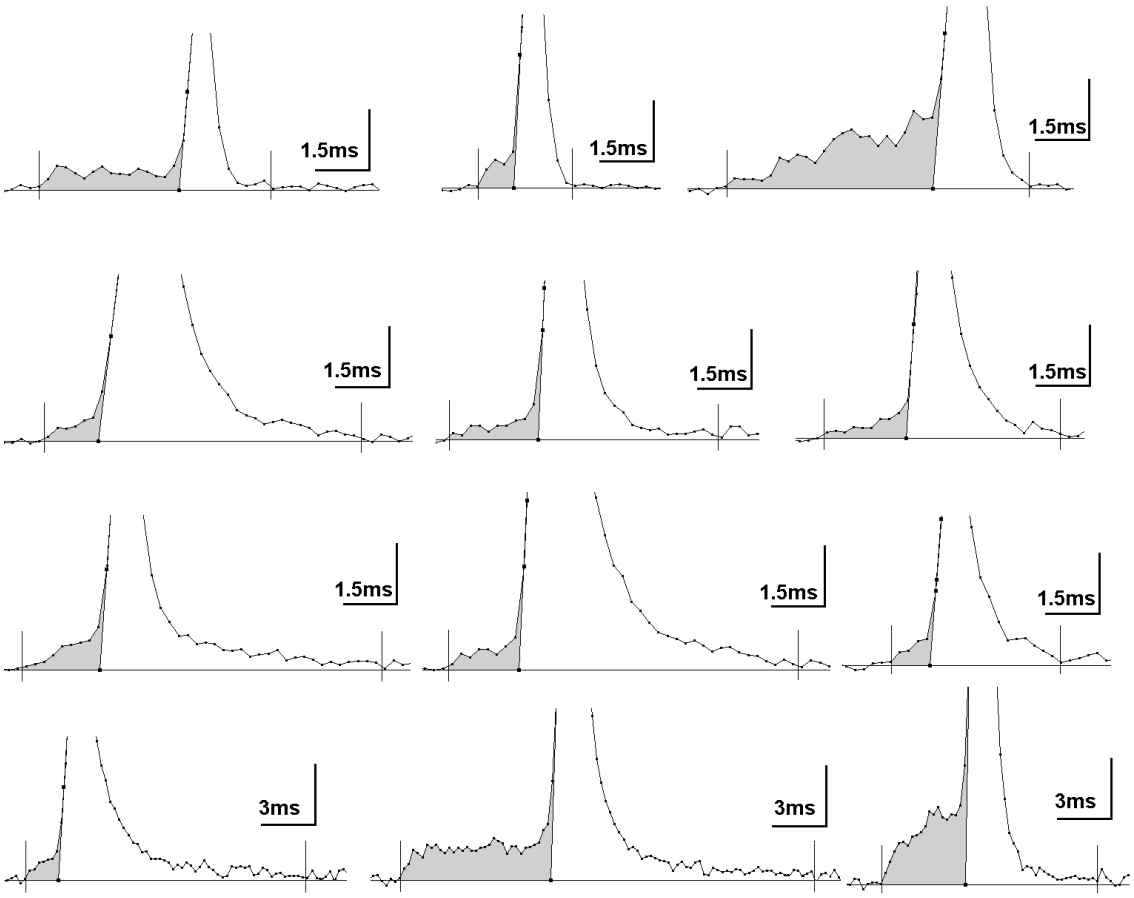

Figure 3-4. The prespike feet have highly variable shapes. All examples were from cells transfected with the control vector GFP. Foot area is shaded, and the vertical scale bar is 5 pA.

The syx membrane anchor contains 23 amino acids (positions 266-288) (Figure 3-5). We tested positions 269 to 281 and 283 by introducing single point substitutions with tryptophan. Overexpressing most of the mutants in PC12 cells, including those with wild-type syx and the control vector, produced PSF with average amplitudes in the range 2.3-2.6 pA. However, tryptophan substitutions at three positions isoleucine 269 [$I^{269} \rightarrow W^{269}$ (I269W)], glycine 276 (G276W), and isoleucine 283 (I283W) produced highly significant ($P < 0.001$) reductions in the PSF amplitude (Figure 3-6, A). V273W and I278W had smaller reductions that were also significant ($P < 0.05$).

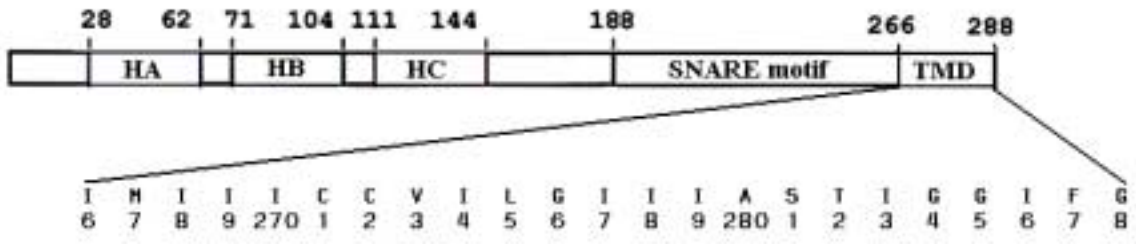

Figure 3-5. Syx contains three helical domains (Ha,b,c), a SNARE motif and a transmembrane domain (TMD). The amino acid sequence of the TMD is shown from position 266 to 288.

A reduction in the PSF amplitude indicates that the mutant tryptophan side chain interferes with the NE flux, presumably by protruding into the fusion pore lumen. These effects on the PSF current place these residues in the lining of the fusion pore. Three positions where tryptophan produced the largest effects (269, 276, and 283) reside on the same face of an α-helix (Figure 3-6, B). Residue 273 is near this face. Residue 278 falls on a very different face of the helix. But one or two false positives at the level of $P < 0.05$ are

acceptable for 14 measurements. From this tryptophan scanning experiment, the syx membrane anchor was predicted to form an α-helical structure. The fusion pore can then be hypothesized to form by a circular arrangement of several copies of syx membrane anchors.

Mutations that reduced the PSF amplitude had no effect on current through voltage-activated Ca^{2+} channels (Figure 3-7). This result rules out an effect of syx mutants on the fusion pore flux through an interaction with Ca^{2+} channels. Also, syx tryptophan mutants did not alter the Ca^{2+}-dependent association with synaptotagmin-I (Figure 3-8, A).

The expression level of syx was determined by immunobloting (Figure 3-8, B). With reference to the standards, the amount of wild-type syx and mutant G276W could be estimated as three times as great as the amount of endogenous syx expressed by the control cells. Because about 30% of the cells in the culture were transfected, the expression level in an individual transfected cell can be estimated to be increased by ~10 fold. Thus, the transfected protein was the predominant form of syx in cells from which recordings were made. Moreover, overexpressing syx did not alter the expression level of synaptobrevin or SNAP-25 (Figure 3-8, B).

To examine the effect of side-chain size further, possible pore lining positions were substituted with a series of mutants containing different side chain size, like glycine (G), valine (V), leucine (L), isoleucine (I) and phenylalanine (F). For positions 269, 276, and 283, increasing the side chain volume produced a graded reduction in the PSF amplitude (Figure 3-9, A, C, and E). An inverse correlation was expected for residues that protrude to the lumen of the fusion pore. This result thus provides further evidence that these three

positions line the wall of the fusion pore. In contrast, for positions 275 and 280, the plots were flat (Figure 3-9, B and D). This is consistent with the notion that these are not pore lining residues.

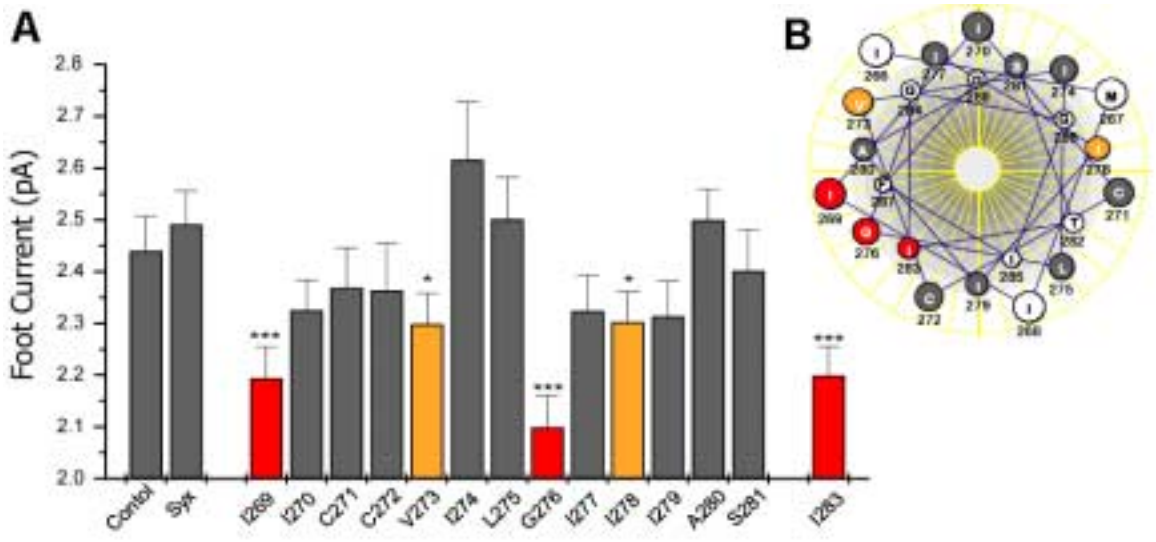

Figure 3-6. (A) The mean PSF amplitude was significantly reduced in 5 of 14 syx tryptophan mutants tested. *, *P* < 0.05; *, *P* < 0.001 for a Student's *t* test compared with the results of wild-type syx. Pooled values were used (195 to 432 PSF from 24 to 62 cells in 4 to 14 transfections). All values with *P*<0.001 by the *t* test on the pooled mean were also significantly different (*P*<0.05 for I269W and I283W; *P*<0.01 for G276W) on the basis of the *t* test on the double mean (Colliver and others 2000a). Error bars show the mean ± SEM. (B) A helical wheel model placed the three locations 269, 276, and 283 with the strongest effects on the same face of the α-helix. Color coding reflects the level of significance for the pooled means (A). Open circles were not tested. (Figure from (Han and others 2004), work done by Han, X).**

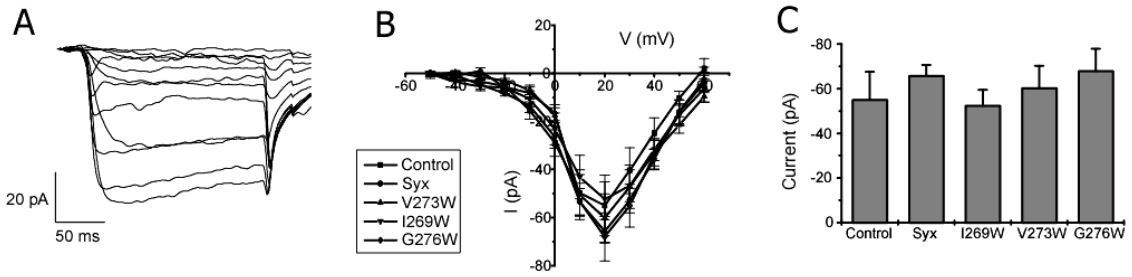

Figure 3-7. Ca2+ current in PC12 cells. (A) Voltage steps (from –80 mV to levels from –50 to 60 mV) open Ca2+ channels and elicit inward current. (B) Mean peak Ca2+ current plotted versus voltage for wild-type syx, control and mutants. Error bars show mean ± SEM. (C) The maximum peak Ca^{2+} current with pulses to 10 or 20 mV for syx, control-GFP, and three mutants (7 to 10 cells). (Figure from (Han and others 2004), work done by Han, X)

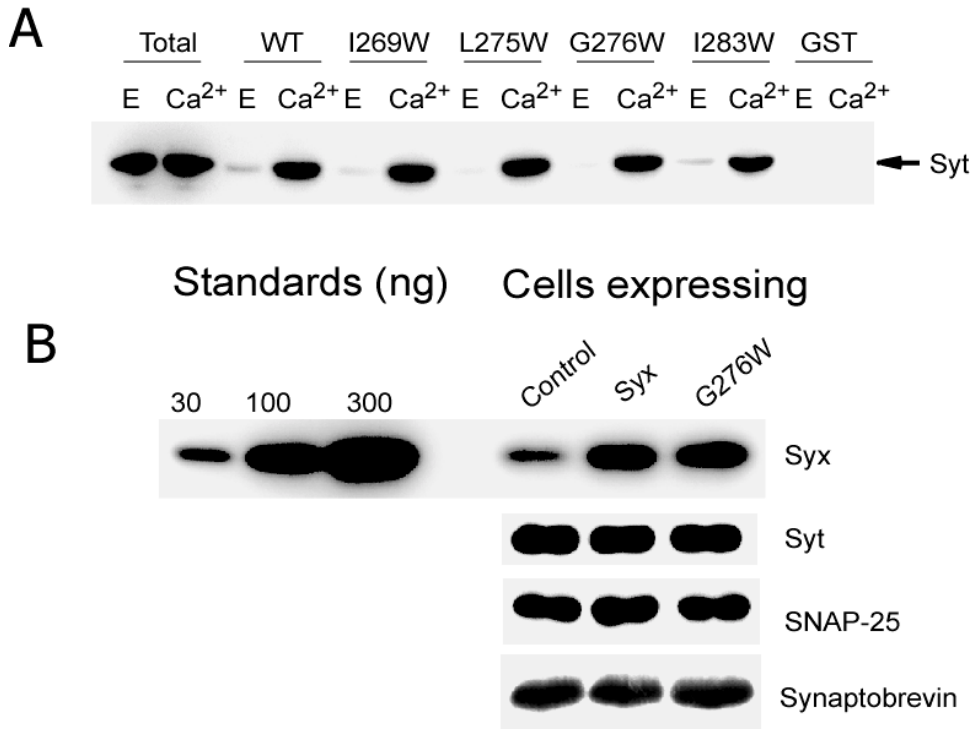

Figure 3-8. (A) Interactions between syx and the cytoplasmic domain of synaptotagmin-I (Syt) (containing the C2A and C2B domains) were unaffected by syx mutants. Syt binding to wild-type syx (WT) and syx mutants were detected in 2 mM EGTA (E) or 1 mM Ca^{2+} (Ca^{2+}). (B) Transfection of PC12 cells with wild-type syx and G276W increased the syx signals in the western blots of the PC12 cell membrane by 3 folds over the control cells. The expression level of syt, SNAP-25, and synaptobrevin was unchanged. (Figure from (Han and others 2004), work done by J. Bai and E. Chapman).

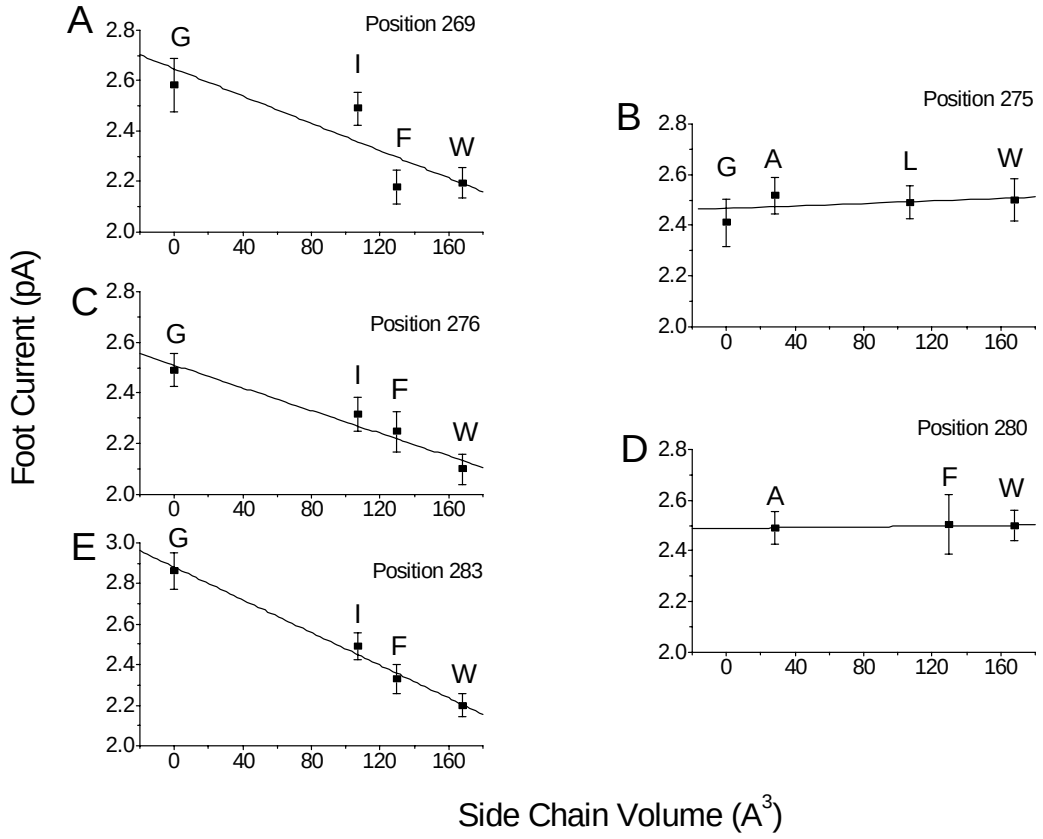

Figure 3-9. The relationship between the PSF amplitude and the side chain volume at various locations. These plots include tryptophan mutants of Figure 3-6. Substitutions at positions 269 (A), 276 (C), and 283 (E) produced graded reductions in the PSF amplitude with increase in the side chain volume. Substitutions at positions 275 (B) and 280 (D) showed no reduction with the side-chain volume. All points were means of 183 to 432 events. Error bars show means ± SEM. Best-fitting lines were drawn in each plot. Letters identify the amino acids present at the indicated position. *P* values for no correlation were 0.19 (A), 0.58 (B), 0.03 (C), 0.32 (D), and 0.007 (E). (Figure from (Han and others 2004), work done by Han, X)

2.2. Capacitance measurement of fusion pore obstruction

To evaluate fusion pore obstruction by a different method, we applied a lock-in amplifier to measure the complex impedance of the membrane patches in the cell-attached configuration. These measurements revealed single vesicle fusion events as stepwise changes in the 90º-out-of-phase (membrane capacitance trace, C trace in Figure 3-10), but with no change in the in-phase (membrane conductance trace, G trace in Figure 3-10) of the lock-in amplifier output. Sometimes, it is possible to resolve transient changes in the G trace during a capacitance step (Figure 3-11). An analysis of the equivalent circuit shows that the fusion pore conductance can be calculated as (Lollike and others 1995):

$$Gp = \frac{C^2 + G^2}{G}$$

Because it is more difficult to perform these experiments, we could not do all of the mutants tested with amperometry. Instead, we focused on two mutants that reduced the amperometric PSF amplitude (I269W and G276W) and one that did not (L275W). All the mutants together with the wild-type syx produced capacitance steps with a mean of ~0.2 fF ($0.2X10^{-15}$ F) (Figure 3-12, A). The average values for the mutants varied by <5% and were statistically indistinguishable. This indicates that none of the mutants altered the vesicle size. With a conversion factor of 0.9 μF cm^{-2} for a biological membrane (Gentet and others 2000), a 0.2 fF vesicle capacitance corresponds to a vesicle of 84 nm in diameter.

The two mutants I269W and G276W that reduced the amperometry PSF amplitude also reduced the fusion pore conductance from ~100 pS to ~50 pS. But the mutant L275W that did not alter the PSF amplitude had no effect on the fusion pore conductance (Figure

3-12, B). Thus, mutants that reduced the NE flux also reduced the ionic current through open fusion pores.

The larger reduction in conductance (a factor of ~2) compared with the amperometry PSF amplitude (~15%) may indicate that inorganic ion flow is more sensitive to tryptophan obstruction than the flow of the organic cation NE. Alternatively, the difference may reflect a difference in the population of fusion pores detected with the lock-in amplifier. The lock-in amplifier can only detect fusion pores open for longer times, usually tens to hundreds of milliseconds. However, the PSF seen with amperometry have a much shorter life time of a few milliseconds. It is also possible that fusion pores detected by these two different methods are from the same population but with different life times. Only ~5% of the capacitance steps have a recognizable fusion pore. In contrast, over 50% of the amperometry spikes have PSF (longer than 0.75 msec). If we consider fusion pore gating as a stochastic process with an exponential distribution, then the probability of being open after tens of milliseconds will be much smaller than that for a few milliseconds.

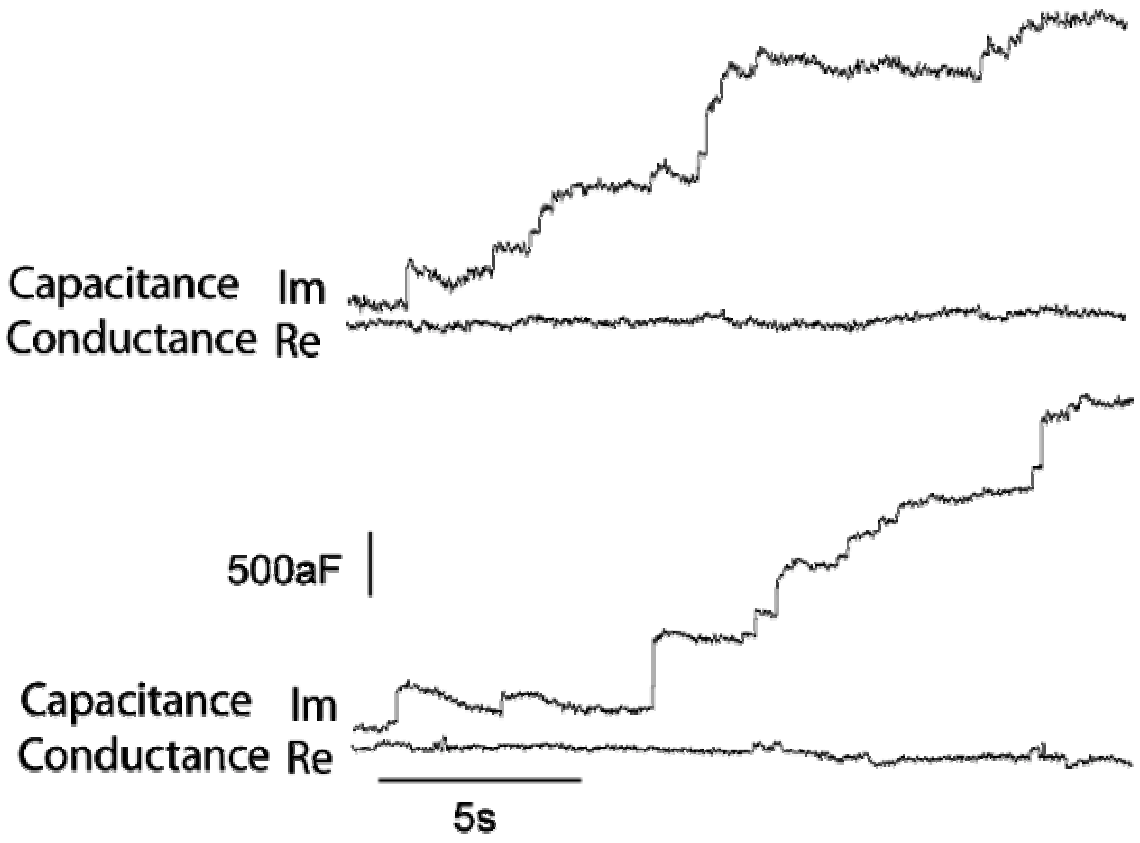

Figure 3-10. Capacitance steps in cell-attached patches of PC12 cells. Examples of recordings from two different patches show upward steps in capacitance (C) with no changes in conductance (G). Each capacitance step corresponds to a single vesicle fusion event. (Figure from (Han and others 2004), work done by Han, X)

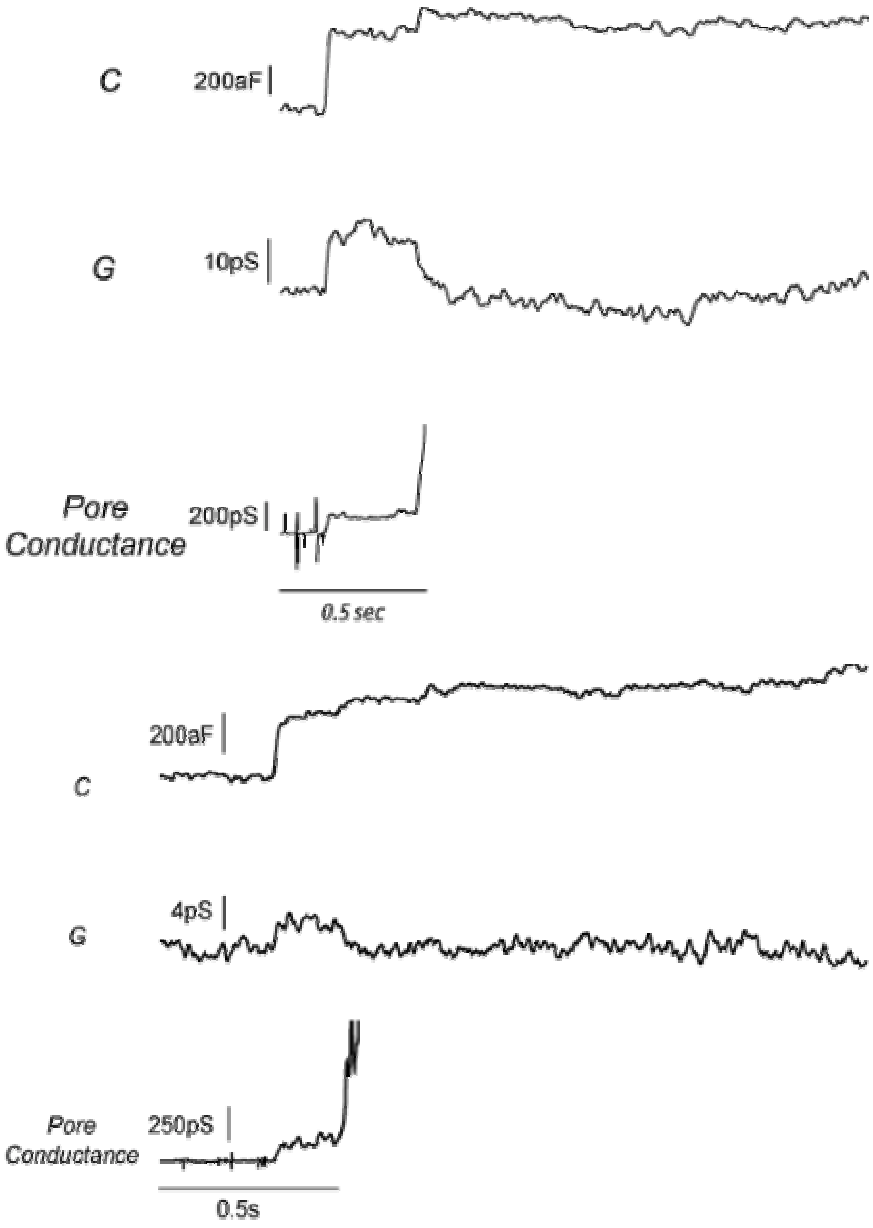

Figure 3-11. The fusion pore conductance is calculated in the cell-attached patches of PC12 cells. Expanding the time scale of the membrane conductance trace (G trace) such as those in figure 3-10 reveals small deflections, which can be used to compute the fusion-pore conductance by using the formula $Gp = \frac{C^2 + G^2}{G}$ **(Lollike and others 1995). Two examples are shown. (Figure from (Han and others 2004), work done by Han, X)**

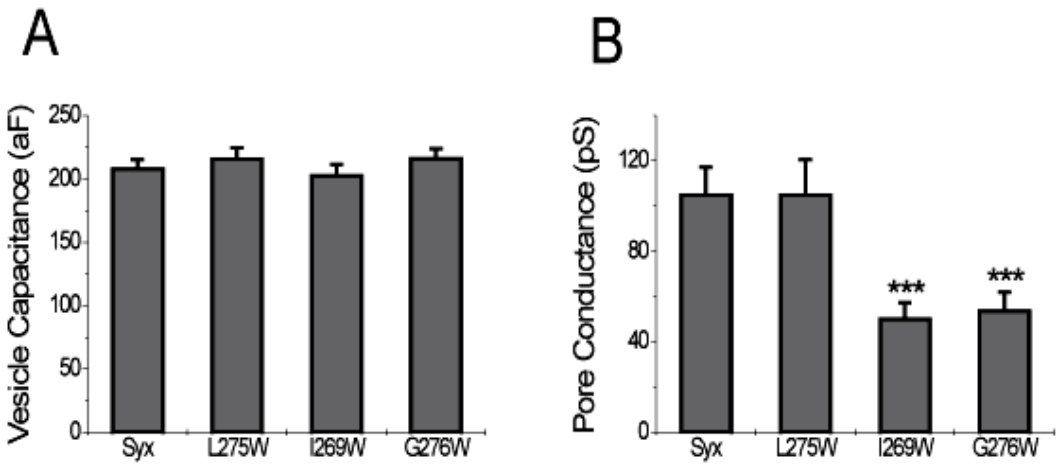

Figure 3-12. The mean vesicle capacitance (A) and the mean fusion pore conductance (B) in PC12 cells overexpressing the indicated proteins. (A) Mean capacitance step sizes for syx and the mutants (N = 503 to 696) were ~0.2 fF. (B) The mean fusion pore conductance for syx is about 100 pS. Fusion pore conductance was significantly reduced by the mutants I269W and G276W to about 50 pS. But L275W did not alter the fusion pore conductance (N = 38 to 60). ***, P < 0.001. Error bars show the mean ± SEM. (Figure from (Han and others 2004), work done by Han, X)

2.3. Electrostatic interaction between NE and pore forming residues

Previous results demonstrated that altering the side chain size of certain residues in the syx membrane anchor influenced the fusion pore flux. Here we altered the charge of these pore lining residues to examine the electrostatic interactions between these residues and neurotransmitter NE passing through the fusion pore.

NE carries a positive charge at the neutral pH of the extracellular fluid or the acidic pH inside a vesicle. When passing through a fusion pore formed by the syx membrane anchor, an electrostatic interaction is possible if the pore contains a charge. We therefore introduced amino acids with ionizable side chains into the syx membrane anchor.

Residues 276 and 283 were previously identified as pore lining residues. Substitutions at these positions with aspartate (D), which ionizes to form a negative charge, increased the fusion pore flux above that expected for the size of its side chain (Figure 3-13, A and B). Substitution with glutamate (E) also enhanced NE efflux, but not as much as aspartate. This indicates that glutamate may not ionize as readily as aspartate. Moreover, the larger side chain of glutamate compared to aspartate may bring the carboxyl groups into closer proximity making ionization more difficult.

Substituting positively charged arginine (R) at sites 276 and 283 reduced the fusion pore flux below that expected for the size of arginine side chain (Figure 3-13, A and B). But lysine (K) substitutions failed to alter the fusion pore flux, again suggesting different degrees of ionization. Substitution with histidine (H) at position 276 did not alter the fusion pore flux (Figure 3-13, A), which is consistent with the fact that histidine has a weaker tendency to ionize at the neutral pH. In contrast, substitutions of residues 275 and

280, with strongly ionizable residues (aspartate and arginine) did not alter the fusion pore flux (Figure 3-13, C and D), which agrees with the hypothesis that they are not exposed to the neurotransmitter expulsion pathway. Altered fusion pore flux by aspartate and arginine at positions 276 and 283 indicates an electrostatic interaction between the pore lining residues and NE escaping through the fusion pore.

Subtracting the experimentally recorded foot current from the current calculated based on the side chain sizes of nonpolar residues yields the "current offset", which represents the effect of electrostatic interactions. Interestingly, the current offset showed an inverse correlation with the side chain pK (Figure 3-14). The pK values used in this plot were based on the ionization of these side chains in an aqueous solution (Weast 1977-1978), which may deviate from the values when located in the fusion pore environment. Moreover, the conformational transition of these residues upon fusion pore opening may influence their ionization states in some way. But the observed inverse correlation indicates that there is an electrostatic interaction between these residues and positively charged NE. This finding strengthens the case that the syx membrane anchor is a structural component of the fusion pore.

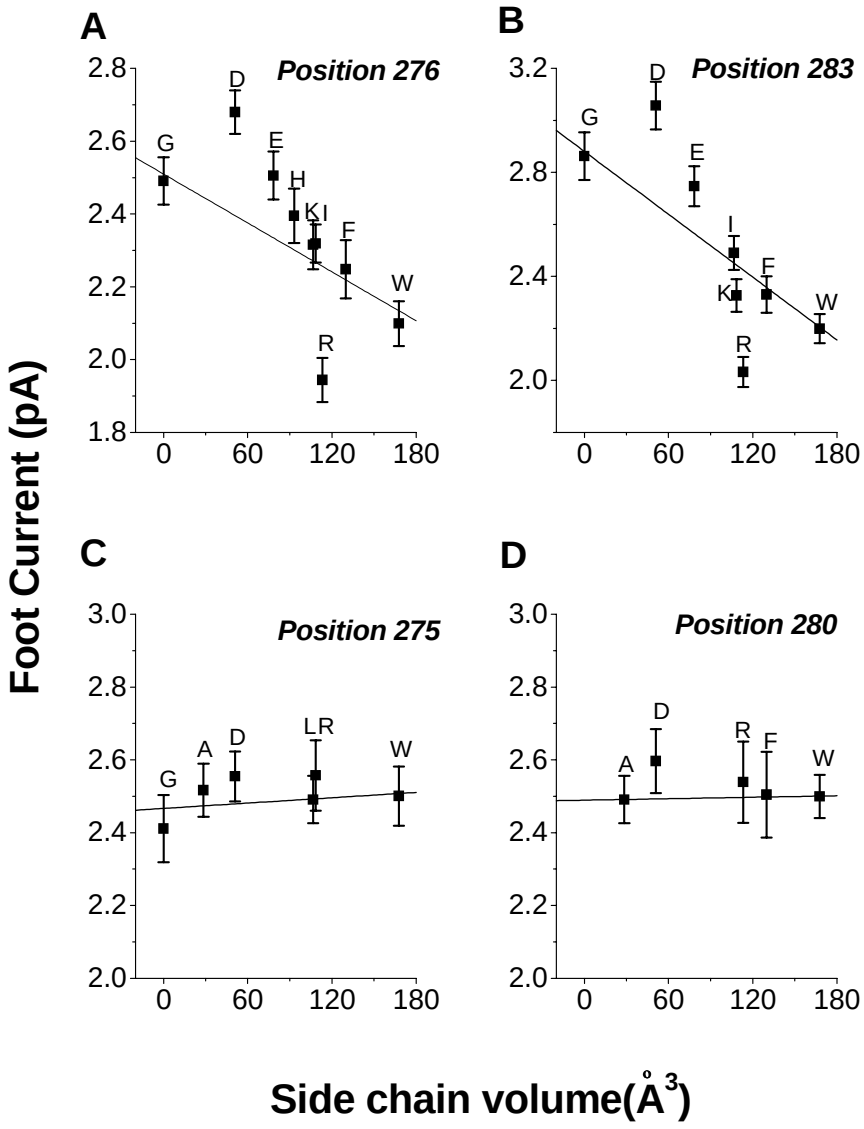

Figure 3-13. Positively charged NE electrostatically interacts with residues residing in the syx membrane anchor. The mean foot current is plotted against the side chain volume at residues 276 (A), 283 (B), 275 (C) and 280 (D). Data for non-polar residues in this plot are from (Figure 3-9). The line drawn in each plot is the linear fit of the data from the non-polar residues. (Figure from (Han and Jackson submitted))).

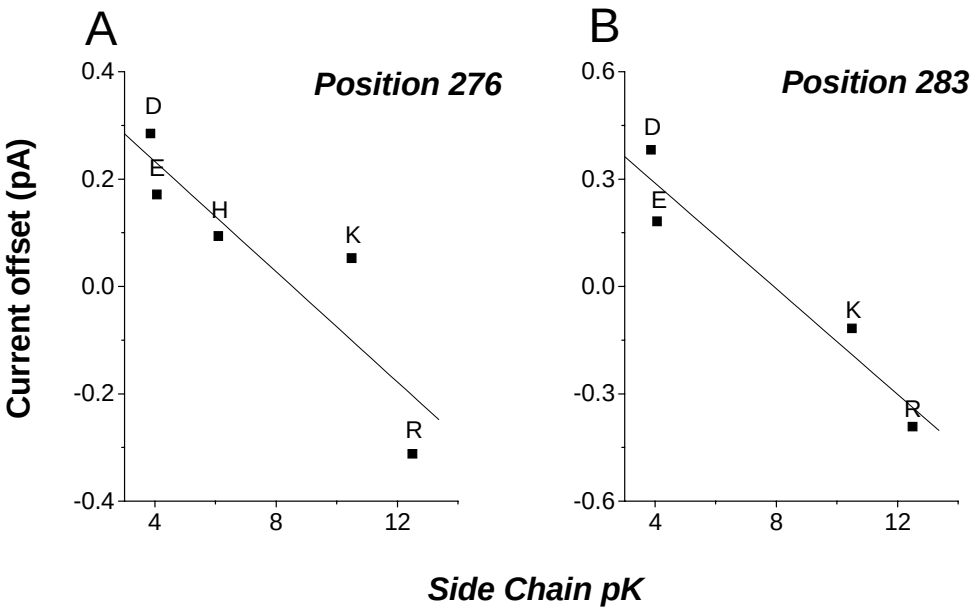

Figure 3-14. The current offset is plotted against the side chain pK for positions 276 (A) and 283 (B). The current offset was calculated as the measured foot current minus that computed from the relevant linear fit in figure 3-13. Linear fit gave p=0.04 for plots at both positions. (Figure from (Han and Jackson submitted)))

2.4. A fusion pore model formed by syx membrane anchors

In the present study at least three residues in the syx membrane anchor were placed in the lining of the fusion pore. Mutations that alter the size or charge of the side chains at these locations altered the fusion pore flux. In contrast, mutations at the other positions failed to influence the fusion pore flux. Moreover, the residues that influenced the fusion pore flux fell on the same face of an α-helix, whereas the residues that failed to alter the fusion pore flux faced away. From these findings, we envisioned the fusion pore in the plasma membrane as a barrel-like structure formed by a circular arrangement of several copies of the syx membrane anchor.

To estimate the size of the fusion pore we used a simple formula for ion channel conductance: $\gamma = A/\rho l$ (Hille 1992). The fusion pore conductance γ is taken as 100 pS as determined from our capacitance measurement (Figure 3-12, B). ρ is the resistivity of the pore lumen, taken as that of the physiological saline (100 ohm·cm). l is the length of the fusion pore, which is ~10 nm because it spans two lipid bilayers. A represents the open fusion pore area which can be solved as 1 nm^2. This gives a circle of 0.56 nm in radius.

To solve for the number of the syx membrane anchors needed to form a fusion pore with 0.56 nm in radius, we constructed a simple model using the α-helix with a radius of 0.35 nm as the basic building block (Figure 3-15, A). A parallel arrangement of 5.62 α-helices forms a circle with a 0.56 nm radius, in which the points of contact form the circle (Figure 3-15, B), or 7.92 α-helices, for which the innermost points can form the circle with a 0.56 nm radius (Figure 3-15, C). This estimation yields the copy number of the syx

membrane anchor as ranging from 5 to 8 depending on whether we used the contact points or the innermost points.

We cannot exclude the possibility that other molecules, either protein or lipid, intercalate between syx membrane anchors to complete the pore structure. Inclusion of other molecules in the pore structure would reduce the number of participating syx molecules. Also other molecules may be necessary to form the connection with the extracellular fluid, if the syx membrane anchor does not traverse the entire plasma membrane (Suga and others 2003), even after the fusion pore opens. However, syx together with SNAP-25 and synaptobrevin constitute the minimal fusion machinery (Weber and others 1998), which suggests that syx might be the only molecular component of the fusion pore in the plasma membrane. Our current results provide no direct evidence regarding the participation of other proteins. Variations in the size of the fusion pore (Klyachko and Jackson 2002; Lindau and Almers 1995) could reflect a difference in the molecular partners or the number of participating syx membrane anchors.

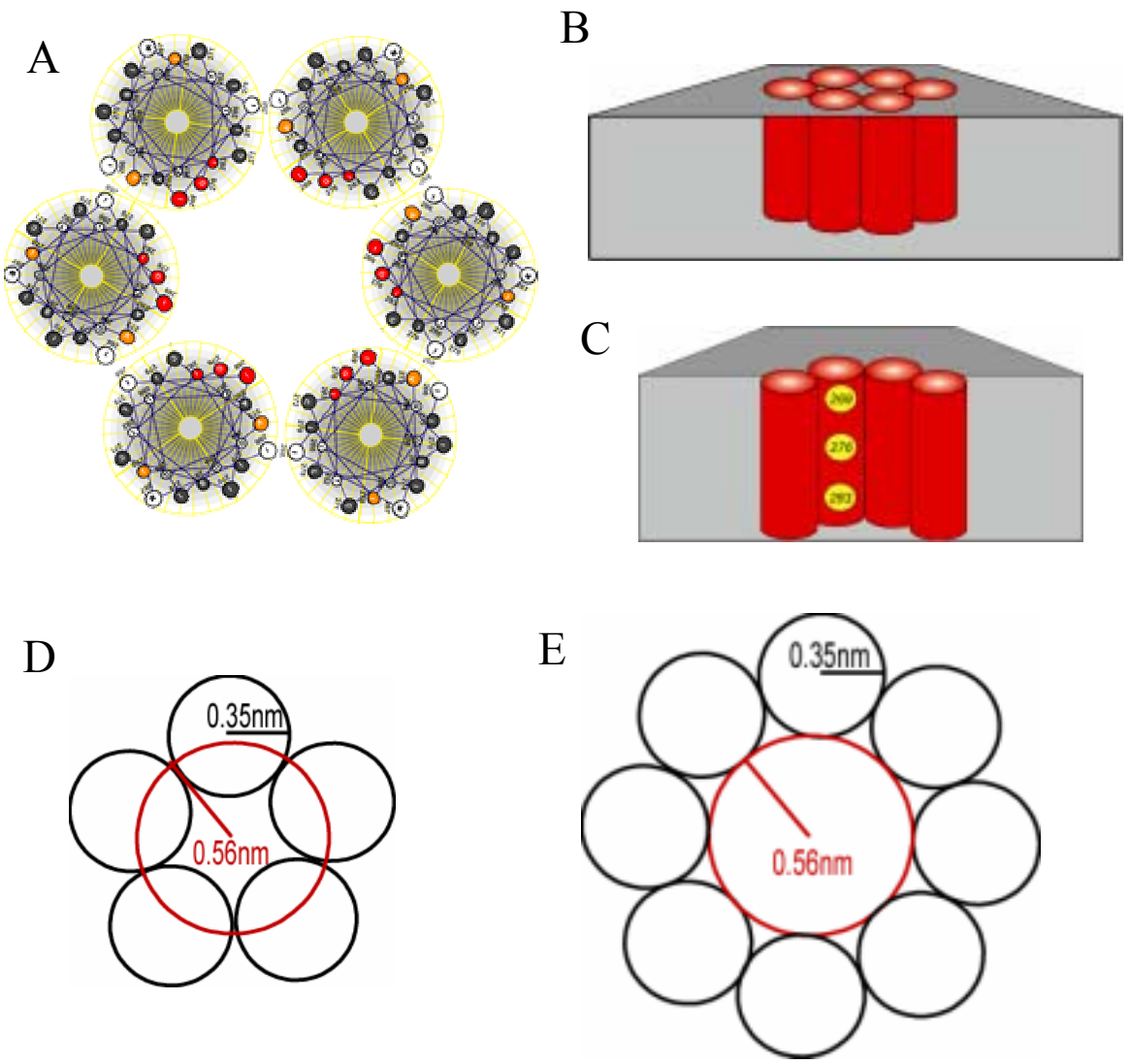

Figure 3-15. A fusion pore model formed by multiple copies of the syx membrane anchor. (A) A few copies of the syx transmembrane α-helix arranged in parallel to form the fusion pore. The pore lining residues are indicated in red. The color coding of the α-helix was based on the effect on the fusion pore flux (from figure 3-6, B). (B) the lateral view of the fusion pore model. (C) residues face into the lumen of the fusion pore are position 269, 276 and 283 from the intracellular face to the extracellular face of the plasma membrane. (D, E), the fusion pore formed by different copies of α-helixes. α-helixes are taken as circles with 0.35 nm in radius (solid circles). The fusion pore is simplified as a circle with 0.56nm in radius (dashed circles). Solving for the number of α-helix needed for a circle of radius 0.56-nm gave 5.62 and 7.96 as by the points of contact or the inner most points respectively. Thus, 5 α-

helixes can be arranged to form a fusion pore of 0.56-nm with the pore edge slightly outside the points of contact (D). Or 8 α-helixes can be arranged into a 0.56-nm fusion pore in radius with the pore edge slightly inside the innermost points (E).

2.5. Further discussion

Fusion pore opening and dilation constitute critical steps in exocytosis and synaptic transmission. Regulation of these steps by Ca^{2+} requires that a Ca^{2+} sensor targets the proteins that form the fusion pore. Synaptotagmin has been demonstrated as the best candidate for the neuronal Ca^{2+} sensor, which interacts with syx and the SNARE complex in a Ca^{2+}-dependent manner (Chapman 2002; Chapman and others 1995; Schiavo and others 1997; Zhang and others 2002b). Previous studies showed that synaptotagmins regulate fusion pore dynamics (Wang and others 2001a; Wang and others 2003). Moreover, the Ca^{2+}-promoted synaptotagmin-I binding to the SNARE complex could be very rapid with a time constant in the millisecond range (Bai and others 2004b). With a fusion pore formed by the syx membrane anchor, regulation of the fusion pore dynamics by synaptotagmin could be through interacting with syx or the SNARE complex.

Extrapolating the present results to the vesicle membrane suggests that the synaptobrevin membrane anchors form the complementary fusion pore in the vesicle membrane. SNARE complex formation could hold these two parts of the fusion pore together. However, synaptotagmin also contains a vesicular membrane anchor. It is also possible that the membrane anchor of synaptotagmin is a structural component of the vesicular membrane fusion pore. Membrane anchors of synaptobrevin and synaptotagmin would be able to engage syx to complete the fusion pore structure. But synaptobrevin has

been demonstrated as part of the minimal fusion machinery, whereas synaptotagmin is only essential for Ca^{2+}-triggered exocytosis. A universal underlying mechanism for intracellular membrane fusion favors a fusion pore formed by the membrane anchors of syx and synaptobrevin.

A fusion pore formed with syx and synaptobrevin predicts that the SNARE complex forms at some point before the fusion pore opening and neurotransmitter release. Our estimation of a fusion pore formed with 5-8 copies of syx supports the cooperative participation of the SNARE complexes in fusion (Hua and Scheller 2001; Stewart and others 2000). Moreover, the SNARE complex could mediate exocytosis by initiating a conformational change of the syx membrane anchor.

CHAPTER 4. REGULATION OF THE FUSION PORE BY THE SYNTAXIN MEMBRANE ANCHOR

1. Introduction

Fusion pore opening provides the first aqueous contact between the vesicle lumen and the extracellular fluid. An open fusion pore could subsequently dilate leading to full fusion or close resulting in kiss-and-run exocytosis (Fesce and others 1994). Regulation of exocytosis thus can be related to these the basic transitions of a fusion pore: opening, closing, and dilation. By analogy with ion channel gating, the kinetics of the fusion pore was predicted to be influenced by a diverse constellation of molecules.

Exocytosis is triggered by an elevation of the intracellular Ca^{2+} concentration. However, the underlying mechanism of the tight coupling between Ca^{2+} and fusion initiation is poorly understood. A few attempts have been made to associate the exocytosis kinetics with Ca^{2+} or some fusion related proteins. For example, an increase in the extracellular Ca^{2+} concentration shifted full fusion to kiss-and-run exocytosis (Ales and others 1999). Overexpressing Ca^{2+} channel proteins stabilized an open fusion pore (Wang and others 2001a). As the best candidate of the Ca^{2+} sensor, synaptotagmins were the first protein family demonstrated to influence the fusion pore (Wang and others 2001a; Wang and others 2003). Furthermore, Ca^{2+}-dependent synaptotagmin-I binding to SNAP-25 was described to be on a millisecond time scale, and disruption of this binding reduced the fusion pore stability (Bai and others 2004b). In addition, genetic ablation of SNAP-25 reduced the fusion pore stability (Sorensen and others 2003). The influence of fusion pore

kinetics by Ca^{2+}, synaptotagmin-I and SNAP-25 predicts that these molecules interact with the fusion pore components, but the underlying mechanism remains obscure. As demonstrated in CHARPTER 3, the syx membrane anchor is a structural component of the fusion pore. It is possible that the above mentioned molecules influenced fusion pore dynamics through interactions with syx.

In this chapter we tested the function of the syx membrane anchor in regulating fusion pore kinetics. Mutations in the syx membrane anchor were shown to affect the fusion pore opening and stability. In particular, the pore lining residues influenced the fusion pore dilation rate. The observed effect on fusion pore dilation is consistent with the notion that during dilation, the pore lining residues experience a change in surroundings, moving from the aqueous pore lumen to a hydrophobic environment. Thus, this result agrees with the fusion pore model formed by the syx membrane anchor.

2. Results and discussion

2.1. Fusion pore stability is altered by the syx membrane anchor mutations

In this study, the duration of the prespike foot (PSF) was used to evaluate the stability of an open fusion pore. The PSF duration measured in PC12 cells transfected with various proteins followed an exponential distribution (Figure 4-1, A, B, C). This indicates that fusion pore termination is a stochastic process, like ion channel gating. The best fitting single exponential have a time constant (t_f) of ~1.0 msec. Another way of evaluating the PSF duration is the arithmetic mean ($\bar{t}$), which is ~1.85 msec. The arithmetic mean ($\bar{t}$) and the fitted time constant (t_f) are related as (Colquhoun and Sigworth 1995):

$$t_f = \bar{t} - t_c$$

where t_c is the recording cut-off time. In our recordings t_c is 0.875 msec. Thus, the arithmetic mean was in good agreement with the fitted time constant. We used arithmetic means to evaluate the fusion pore duration (τ) in this study.

Most of the tryptophan substitutions in the syx membrane anchor failed to alter the mean PSF duration, leaving values near ~1.85 msec (Figure 4-2). Only two mutants C272W and I283W slightly altered the PSF duration. Overexpression of syx did not alter the fusion pore lifetime compared to the control cells overexpressing GFP vector. In addition, the tryptophan mutants I269Wand G276W that were shown to reduce the flux of the fusion pore (Figure 3-6) did not alter the PSF duration either.

For mutants with different side chain sizes or charge other than tryptophan, 5 out of 23 mutants altered the mean PSF lifetime (Figure 4-3). Aspartate substitutions L275D, G276D, A280D, and I283D significantly prolonged the foot duration. The consistent effect of aspartate substitutions indicates that this polar residue stabilized the fusion pore in some way. The charge residues of L276D and L283D were hypothesized to protrude into the lumen of the fusion pore, whereas L275D and L280 did not. Fusion pore dilation is a complicated process with many factors involved. Since little is known about these factors, the observed effects on the fusion pore lifetime are hard to interpret.

Dilation of the fusion pore was predicted to begin with a separation of the syx transmembrane segments, probably by intercalating lipid. Polar or charged groups tend to aggregate in a non-polar environment, especially when they are in close proximity. Separating the transmembrane segments with polar groups would be more difficult, which

could be detected as an increase in the fusion pore lifetime. Results with small acidic aspartate agreed with this interpretation, but results with arginine did not. Negative results from the large basic arginine could also be due to the longer distance between the polarized side chains.

Residue 283 is the pore lining residue closest to the extracellular surface. Substitution with residues containing bulky side chains like phenylalanine (I283F) (figure 4-3) and tryptophan (I283W) (figure 4-5) reduced the fusion pore life time. This result indicates that this outer most location of the fusion pore may be more sensitive or critical than other positions along the fusion pore.

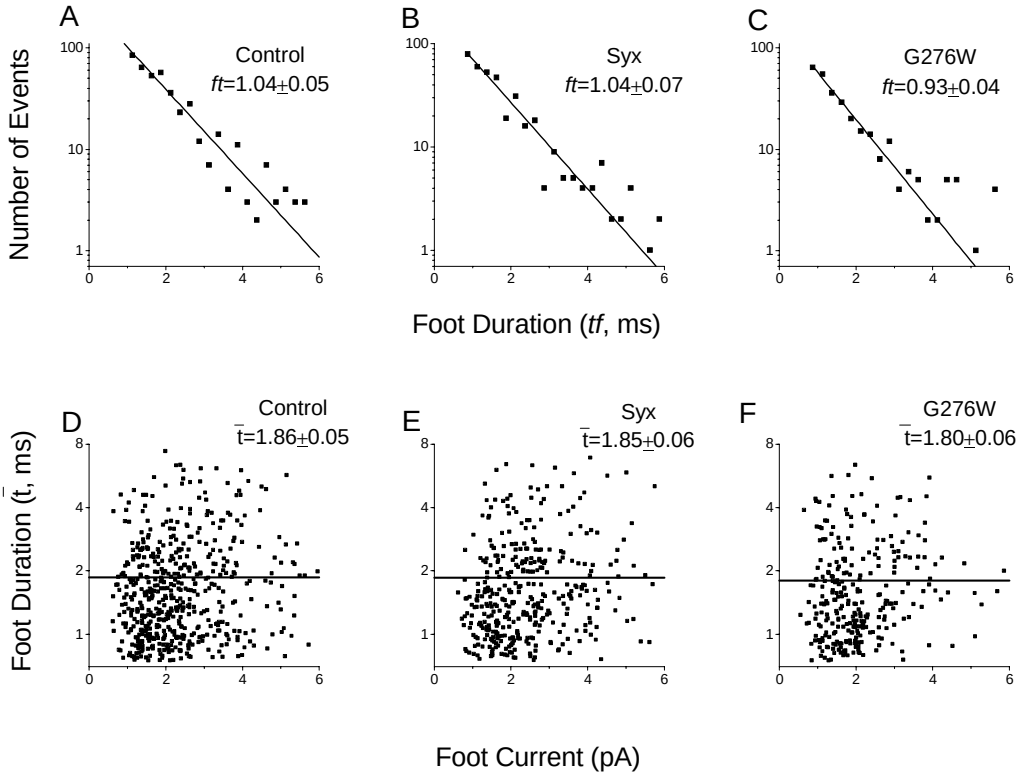

Figure 4-1. The duration of the fusion pore in PC12 cells overexpressing the indicated proteins. The fusion pore duration follows an exponential distribution (A, B, C). The best fitting exponential is drawn and the time constant (t_f) is indicated. Another way of calculating the fusion pore duration is the arithmetic mean ($\bar{t}$) (D, E, F). In plots D, E and F, the foot duration of any single event is plotted against the foot current. The line in each plot indicates the arithmetic mean of the foot duration.

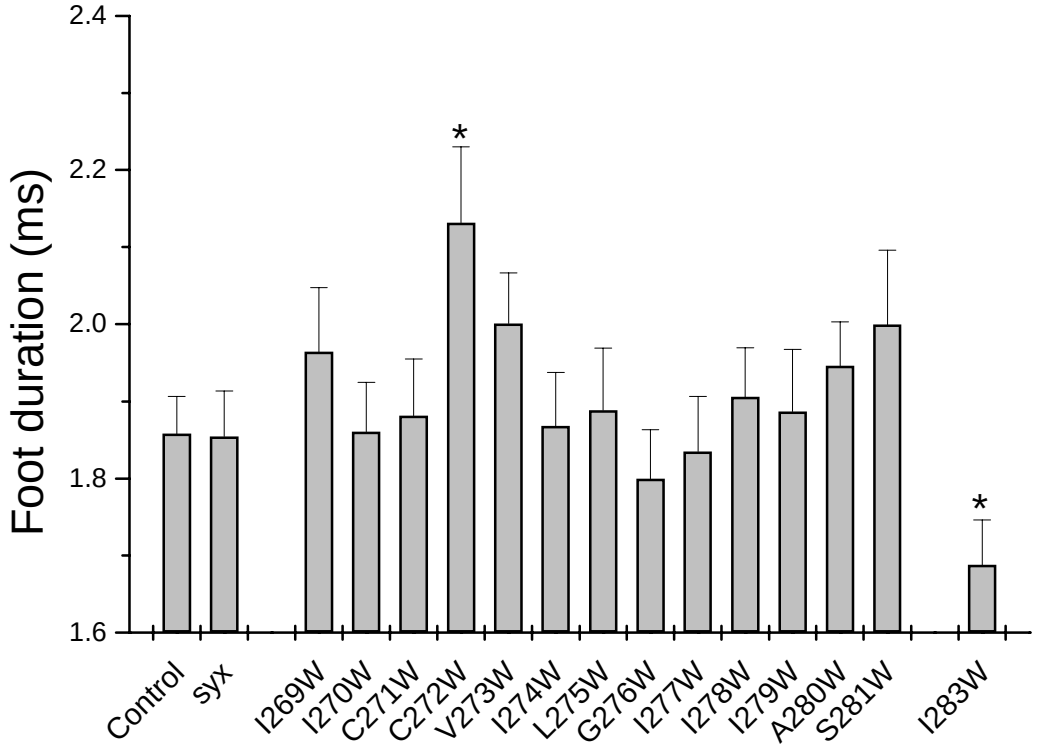

Figure 4-2. Most of the tryptophan substitutions in the syx membrane anchor did not alter the foot duration. The mean PSF duration for cells overexpressing the indicated syx mutant is compared to the wild-type syx. C272W slightly increased the foot duration (p=0.01 with the student's t-test), whereas I283W reduced the foot duration (p=0.05 with the student's t-test).

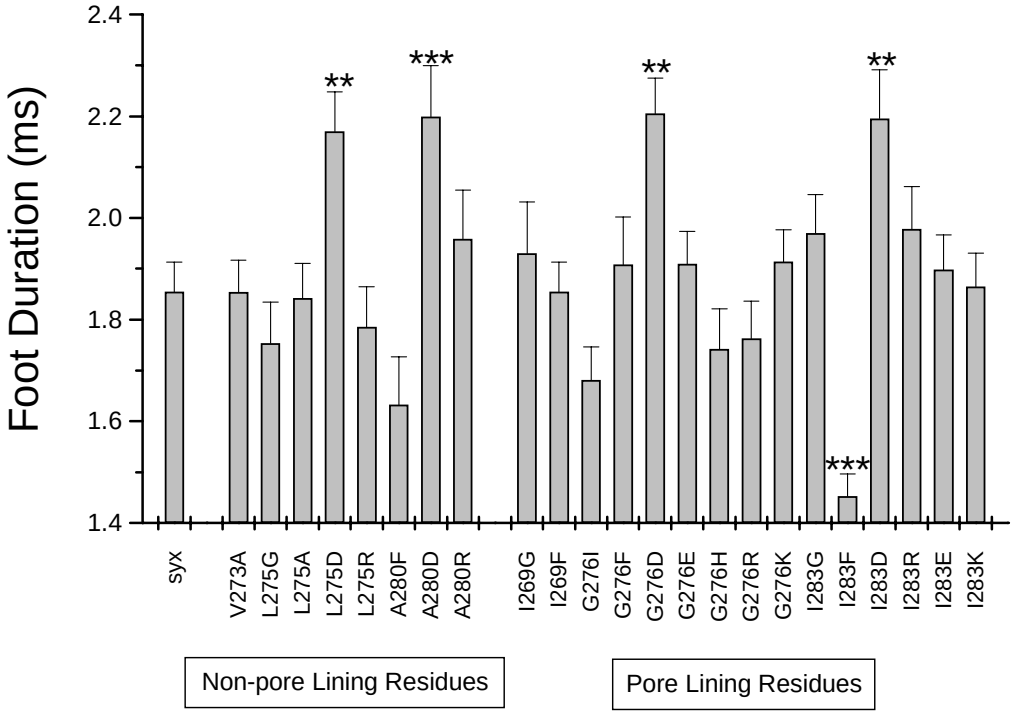

Figure 4-3. The mean foot duration for cells overexpressing the indicated mutant proteins at various positions. (, p<0.01 and *** p<0.001). Positions 273, 275 and 280 are the non-pore lining residues, whereas positions 269, 276 and 283 are the pore lining residues.**

2.2. Release kinetics is altered by the syx membrane anchor mutants

Plotting the number of spikes over time, named the cumulative plot, can provide some insight into release kinetics (Figure 4-4, A). A cumulative plot contained a delay of a few seconds, followed by a linear rising phase during KCl stimulation. A slow rising phase continued after KCl application was stopped. A linear fit to the rising phase of the plot gave the secretion rate (Figure 4-4, B).

Syx overexpression reduced the secretion rate to about 70% of that seen in the control GFP overexpressing cells. It is not obvious why overexpressing syx would inhibit secretion. Syx was shown to self-oligomerize (Fasshauer and others 1998a; Margittai and others 2001; Misura and others 2001b; Poirier and others 1998a), and form a ternary complex with SNAP-25 in a 2:1 stoichiometry (Fasshauer and others 1997b; Margittai and others 2001; Xiao and others 2001; Zhang and others 2002a) or 1:1 stoichiometry (An and Almers 2004; Misura and others 2001a). Overexpression of syx might favor these interactions, which could compete with the interactions that promote secretion. In addition, in wild-type PC12 cells the level of syx is about 7 times lower than that of SNAP-25 (Tucker and others 2003). The abundance of SNAP-25 in PC12 cells promotes exocytosis, since overexpressing SNAP-25 enhanced exocytosis (CHAPTER 5).

Most of the syx membrane anchor mutants altered the secretion rate (Figure 4-5 and Table 4-1). Among a total of 36 mutants tested, 12 mutants up-regulated the secretion rate, 16 down-regulated the secretion rate and 8 had no effect. The observed effect on the secretion rate (Table 4-1) is much more prominent than on the PSF duration (Figure 4-2

and 4-3). This indicates that the secretion rate is more sensitive to manipulations of the syx membrane anchor.

The secretion rate is subject to regulation by many factors involved in vesicle mobilization and fusion, whereas the stability of a fusion pore is more likely to be regulated by molecules coupled to a particular fusion step. As the syx membrane anchor can modulate the cytosolic domain in its interaction with other proteins (Chapman and others 1995; Lewis and others 2001; Trus and others 2001), it is possible that the observed effect of the syx membrane anchor on the secretion rate was through altered interactions with other proteins.

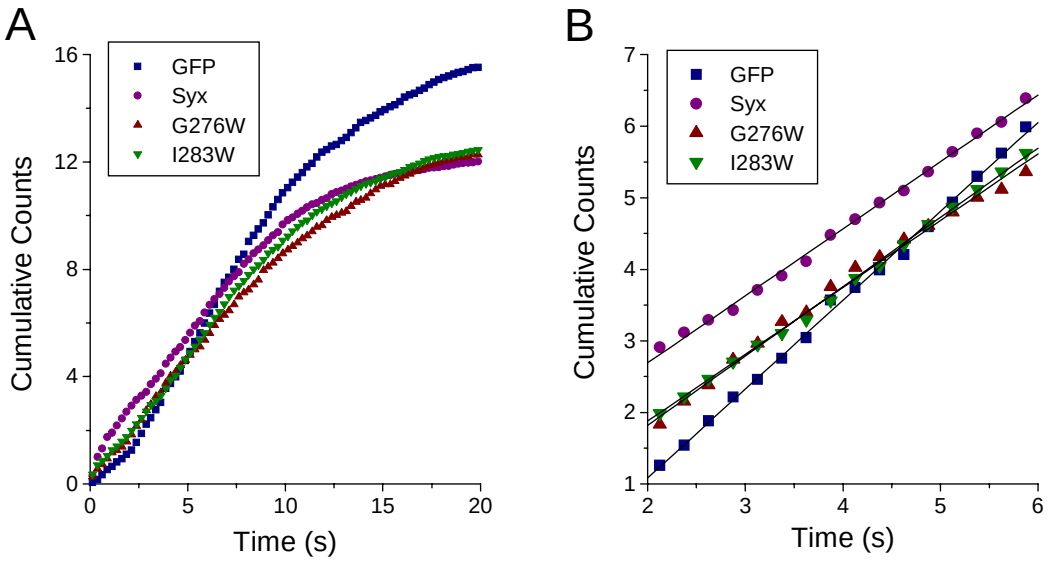

Figure 4-4. Release kinetics in PC12 cells. (A) Examples of cumulative spike plots for cells overexpressing control vector GFP, wild-type syx, and two syx mutants. (B) The secretion rate is estimated by a linear fit to the rising phase of the cumulative plot during KCl stimulation. Spikes with an amplitude of ≥2 pA (about 5-10*RMS of the baseline noise) were counted.

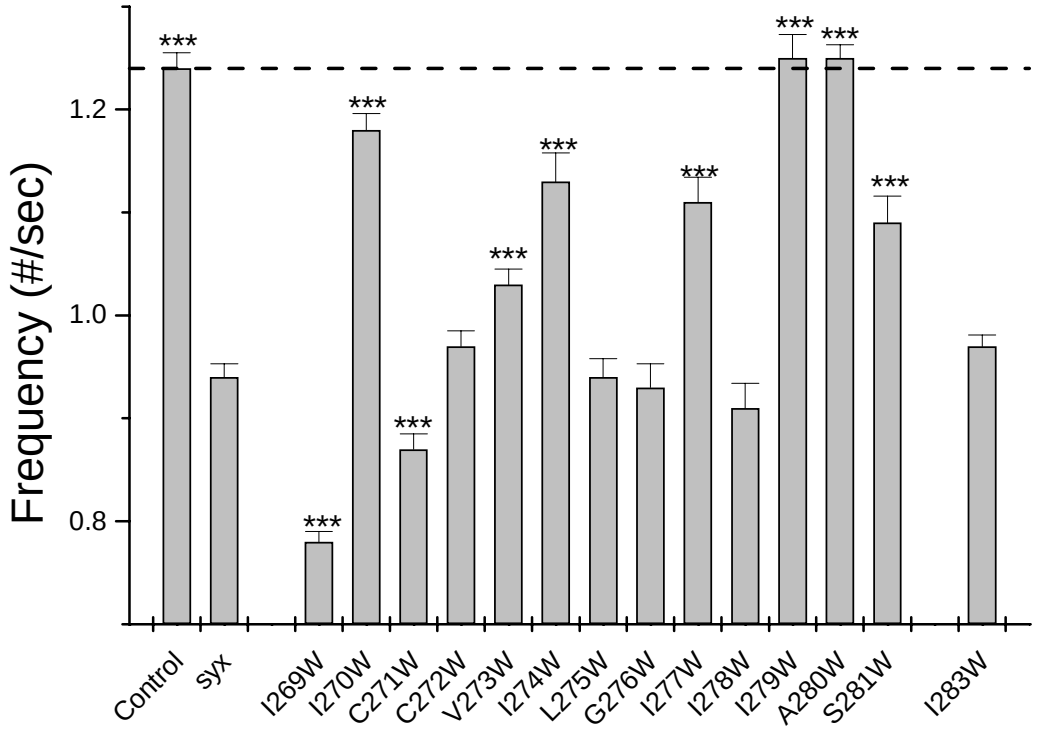

Figure 4-5. The secretion rate was altered by the syx membrane anchor tryptophan mutants (*, P<0.001 with a student's t-test versus wild-type syx). The dashed line indicates the secretion rate in the control cells that overexpressing GFP vector.**

Table 4-1. Secretion rates in cells overexpressing wild-type syx, control GFP vector and various mutant proteins. Most mutants altered the secretion rate significantly. (*, P<0.001; **, P<0.01 with a student's t-test).**

Proteins		Secretion Rate (#/sec) ± Standard Error	Cell Number	P value
Wild-type syx		0.94±0.013	100	-
Control GFP		1.24±0.015	74	***
Tryptophan mutants	I269W	0.78±0.010	167	***
	I270W	1.18±0.016	61	***
	C271W	0.87±0.015	69	***
	C272W	0.97±0.015	74	No
	V273W	1.03±0.015	50	***
	I274W	1.13±0.028	31	***
	L275W	0.94±0.018	32	No
	G276W	0.93±0.023	53	No
	I277W	1.11±0.024	48	***
	I278W	0.91±0.024	66	No
	I279W	1.25±0.023	41	***
	A280W	1.25±0.013	59	***
	I283W	0.97±0.011	138	No
Non-pore-lining Residues	V273A	0.90±0.013	132	No
	L275G	0.84±0.015	72	***
	L275A	1.25±0.031	35	***
	L275D	0.68±0.021	44	***
	L275R	0.64±0.024	26	***
	A280F	0.89±0.023	24	No
	A280D	0.30±0.010	26	***
	A280R	0.32±0.011	29	***
Pore-lining Residues	I269G	0.75±0.017	65	***
	I269F	1.01±0.020	82	**
	G276I	1.14±0.021	100	***
	G276F	0.76±0.008	127	***
	G276D	0.74±0.013	59	***
	G276E	0.92±0.013	56	No
	G276H	1.08±0.037	58	***
	G276R	0.86±0.019	39	***
	G276K	1.03±0.034	46	**
	I283G	0.73±0.013	47	***
	I283F	1.52±0.017	39	***
	I283D	0.54±0.024	33	***
	I283R	0.63±0.014	34	***
	I283E	0.58±0.024	36	***
	I283K	0.56±0.013	32	***

2.3. Syx pore lining residues affect the fusion pore dilation

Regulation of the fusion pore can be interpreted according to a simple kinetic scheme with the form:

$$C \underset{Kc}{\overset{fo}{\rightleftharpoons}} O \xrightarrow{Kd} D$$

In this scheme, a closed fusion pore (state C) can open (state O) with an estimated speed of *fo*. An open fusion pore subsequently dilates (state D) with a rate constant *Kd* or closes with a rate constant *Kc*. Dilation of a fusion pore is registered as a spike in amperometry. Closed fusion pores were likely missed in our recording, since they would be too small or too brief to be detected. The opening speed, *fo* covers all the steps before fusion pore opening, including targeting, docking, and priming.

Applying the single channel kinetic analysis (Jackson 1992), the fusion pore duration (τ) and the secretion rate (*Fd*) can be calculated as:

$$\tau = 1 / (Kc + Kd)$$

$$Fd \propto fo * Kd / (Kc + Kd)$$

To extract the physical meaning of these formulas, we could first start with a simplified situation by considering *fo* as a constant. By comparing the fusion pore duration (τ) and the secretion rate (*Fd*), one can estimate changes in the corresponding rate constants. For example, an increase in τ could be due to a reduction in either *Kc* or *Kd*. With *Kc* held constant, a reduction in *Kd* will predict an decrease in *Fd*. In this case, τ and *Fd* will be inversely correlated. In contrast, with *Kd* held constant, a reduction in *Kc* will correspond

to an increase in *Fd*, and τ and *Fd* will be positively correlated. Thus, the simplest explanation for an inverse correlation between τ and *Fd* will predict a change in *Kd*, whereas a direct correlation will predict a change in *Kc*.

When we consider the opening speed factor (*fo*) in this kinetic scheme, the relation between τ and *Fd* will be more complicated. However, if τ stays constant, it is more likely that *Kc* and *Kd* are unaltered. Then a change in *Fd* could be related to a corresponding change in *fo*. In our study most of the mutants altered the secretion rate *Fd* but not the foot duration τ. This result supports the view that *fo* is likely to be more sensitive than *Kc* and *Kd*, as *fo* can be regulated by many molecules that are involved in vesicle targeting, docking, and priming, whereas regulation of *Kc* and *Kd* is likely restricted to molecules associated with a certain final fusion step.

The influence on the fusion pore permeation by residues at different locations in the syx membrane anchor did not weigh the same, as demonstrated in CHAPTER 3. Here, we tested whether the fusion pore kinetics is equally sensitive to various locations in the syx transmembrane segment. We examined this hypothesis by plotting the secretion rate versus the foot duration for the tryptophan mutants that covered a great portion of the syx membrane anchor. Most of the tryptophan substitutions produced significant changes on the secretion rate (figure 4-2). But no correlation was observed between the secretion rate (*Fd*) and the foot duration (τ) (Figure 4-6, A). As most of the tryptophan mutants did not alter the fusion pore duration significantly, we further looked at the aspartate mutants. Aspartate substitutions at four positions tested (275, 276, 280 and 283) altered the mean fusion pore duration (Figure 4-3), as well as the secretion rate significantly (Table 4-1).

Also, no correlation was seen between *Fd* and τ for aspartate substitutions either. Thus, these data fail to reveal a clear role for the syx membrane anchor as a single unit in regulating the fusion pore dynamics.

We then examined specific locations in the syx membrane anchor. Inverse correlations between the fusion pore duration (τ) and the secretion rate (*Fd)* were significant for locations 276 and 283 (Figure 4-7, C and E). The simplest way to interpret this inverse correlation is an effect on the dilation rate *Kd*. For positions 275 and 280 (Figure 4-7, D and F), no correlation is observed between τ and *Fd.* A lack of correlation indicated that fusion pore kinetics were sensitive to a combination of various factors without a specific link to the dilation rate.

Positions 269 and 273 also failed to show a correlation between τ and *Fd* (Figure 4-7, A and B). Manipulations at residues 269 and 273 did not alter τ significantly, but altered *Fd* to a great extent. This result suggests that these mutations influenced the opening speed *fo*. Positions 269 and 273 are closer to the intracellular face of the plasma membrane, whereas positions 275, 276, 280 and 283 are closer to the extracellular face. Thus, it is likely that the intracellular part of the fusion pore is more tightly coupled to the fusion pore opening, whereas the more extracellular part is more related to the fusion pore dilation.

Opening of a fusion pore involves the formation of an aqueous channel, whereas dilation of a fusion pore expands the existing aqueous pore. For a fusion pore formed by the syx membrane anchor, prior to the opening, the pore lining residues reside in a hydrophobic environment, interacting with other proteins or lipid. Opening would expose

the pore lining residues to the pore lumen. In this manner, during the opening step, pore lining residues will experience a transition from a hydrophobic environment to an aqueous environment. After fusion is completed, pore lining residues should move back to a hydrophobic environment. Thus, during the dilation step, pore lining residues will experience a second transition step from an aqueous environment back to a hydrophobic environment.

Regulation of the fusion pore dilation rate by residues 276 and 283, but not 275 or 280 reflects the transition that the pore lining residues encountered upon dilation. Position 269 was also predicted to line the fusion pore. However, no special effect was distinguished for position 269. Fail to detect an effect on fusion pore dilation could be due to a greater interference by the altered secretion rate, which dominates over the dynamic behavior of the fusion pore. The effects of substitutions at positions 276 and 283 on dilation are consistent with a luminal location, and thence support the structural model proposed here.

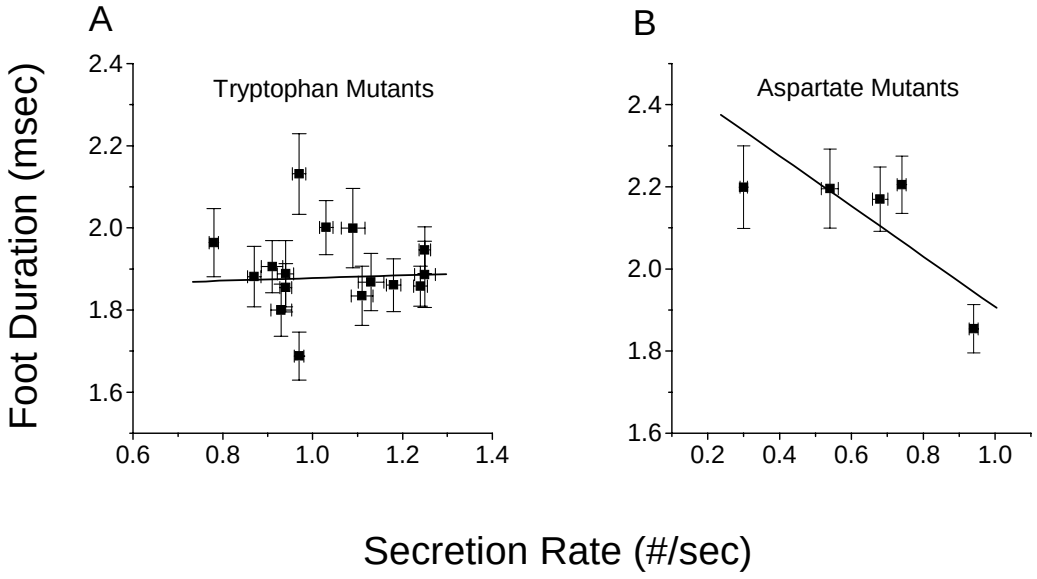

Figure 4-6. Fusion pore kinetics was not regulated by syx membrane anchor as a single unit. No correlation was observed between the foot duration (τ) and the secretion rate (*Fd*) for the tryptophan mutants (A) and the aspartate mutants (B). The line in each plot indicates the linear fit (P=0.63 in A and P=0.12 in B).

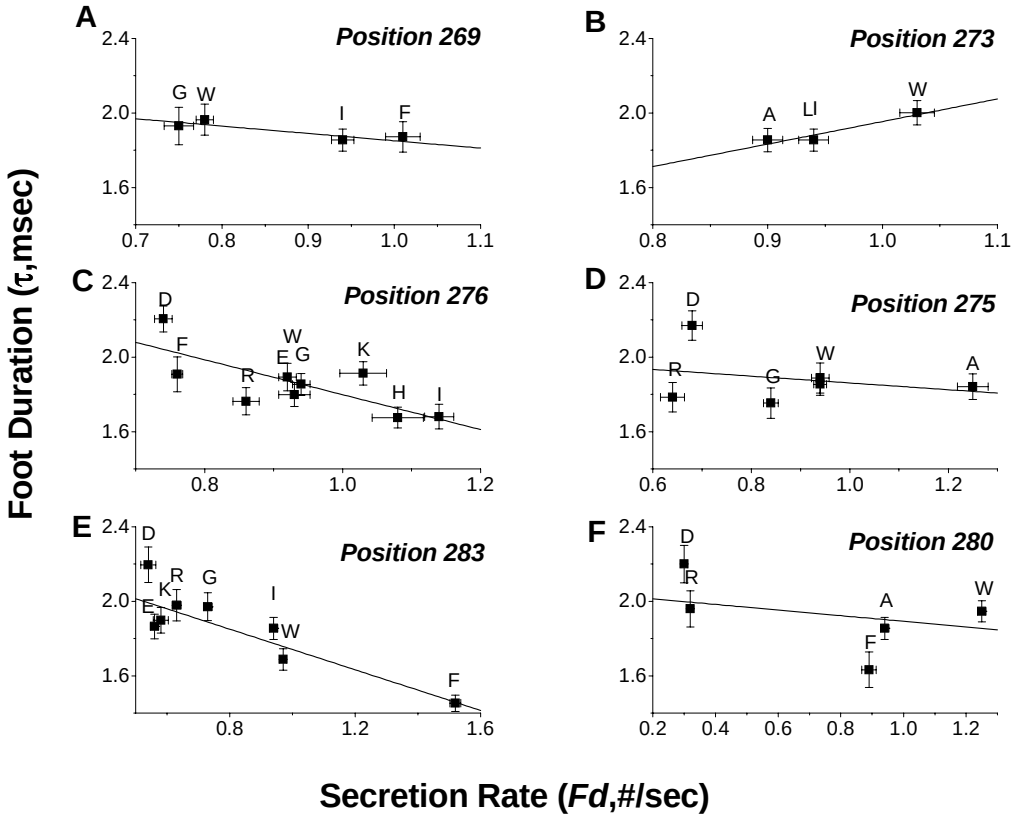

Figure 4-7. Relations between the foot duration (τ) and the secretion rate (*Fd*) for individual positions. An inverse correlation was observed for positions 276 (C) and 283 (E) (linear fit gave P=0.02 for position 276 and p<0.001 for position 283). No correlation was observed for positions 269 (A), 273 (B), 275 (D) and 280 (F) (P=0.14, 0.21, 0.57, and 0.54 for positions 269, 273, 275, and 280 respectively).

2.4. Fusion pore kinetics is independent of fusion pore permeability

In amperometry the foot duration and the secretion rate are two kinetic parameters, whereas the amplitude of the foot current represents the permeability of a fusion pore. When plotting the two kinetic parameters versus the permeability parameters, no correlations were observed (Figure 4-8). Thus, fusion pore kinetics is independent of the fusion pore permeability.

The fusion pore flux has been demonstrated to be sensitive to the size or charge of specific residues in the syx membrane anchor. However, neither the foot duration nor the secretion rate showed any correlation with the side chain volume at these positions (Figure 4-9). Residues that influenced the fusion pore flux reside on the same face of the syx membrane α-helix. By contrast, no α-helical periodicity was observed for residues that influenced the foot duration (Figure 4-2) or the secretion rate (Figure 4-5). Thence, the fusion pore permeability is further demonstrated as a structural parameter uniquely sensitive to the manipulation of the side chain size of the pore lining residues, like the conductance of ion channels.

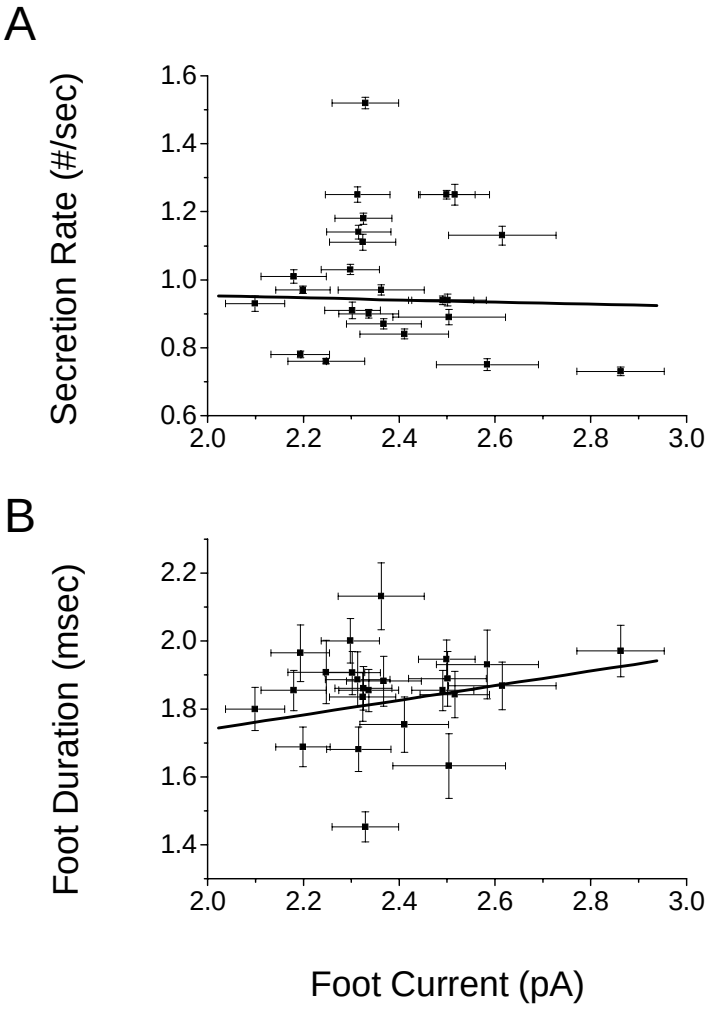

Figure 4-8. The fusion pore kinetic parameters are independent of the permeability parameter. Plots include all 24 syx membrane anchor mutants with different side chain sizes. No correlation was observed between the foot current and the secretion rate (A) or the foot duration (B). Linear regression gave P=0.9 and 0.3 for the secretion plot (A) and the foot duration plot (B) respectively.

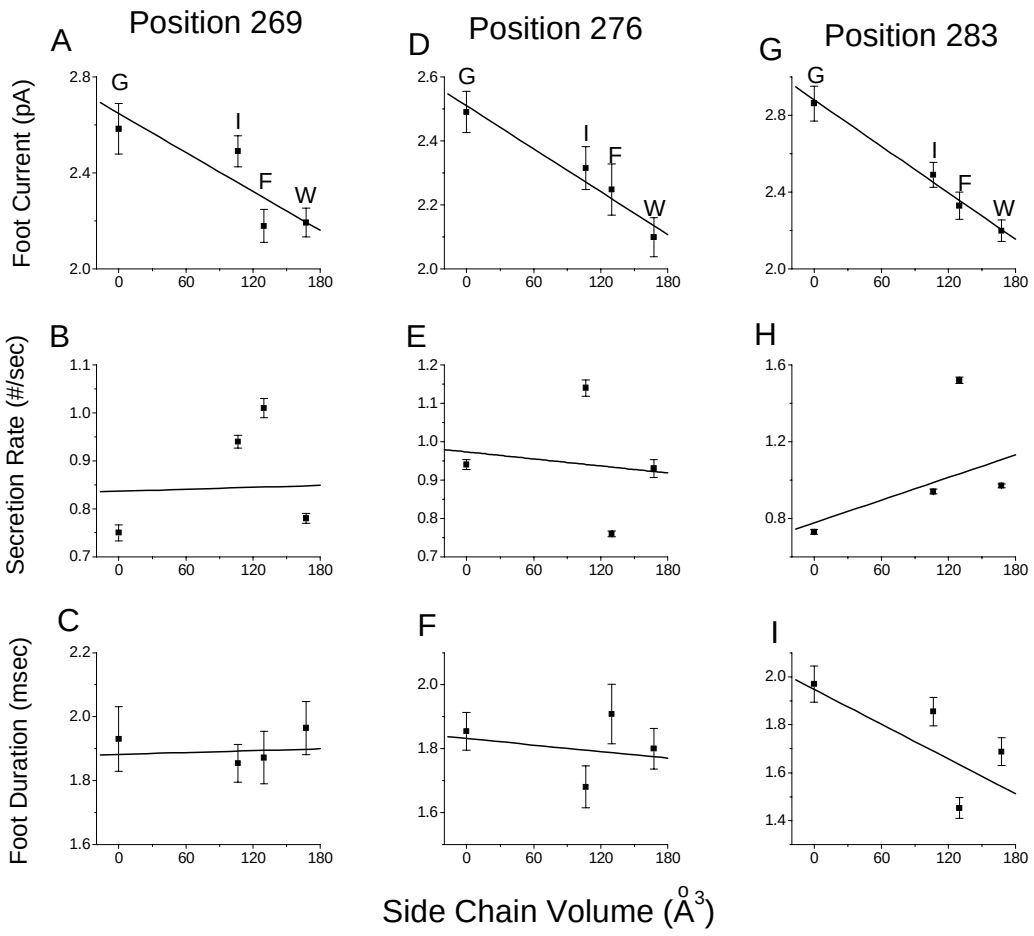

Figure 4-9. The fusion pore permeability is uniquely sensitive to the manipulation of the pore lining residues. Foot current is inversely correlated with the side chain volume. Linear regression for the foot current gave *P*=0.19, 0.03 and 0.007 for positions 269 (A), 276 (D) and 283 (G) respectively. The secretion rate and the foot duration showed no correlation with the side chain volume. *P* for no correlation between the secretion rate and side chain volume is *P*=0.98, 0.7, 0.4 for positions 269 (B), 276 (E) and 283 (H) respectively. *P* for no correlation between the foot duration and the side chain volume is *P*=0.89, 0.8, 0.5 for position 269 (C), 276 (F) and 283 (I) respectively. Data in panel A, D and G are from Figure 3-8.

CHAPTER 5. CONFORMATIONAL TRANSITIONS OF THE SNARE COMPLEX DURING FUSION PORE DILATION

1. Introduction

The SNARE proteins are essential components in membrane trafficking (Chen and others 2001; Jahn and Niemann 1994; Jahn and Sudhof 1999; Nickel and others 1999; Weber and others 1998). The way that the SNARE proteins mediate exocytosis is believed to be through the formation of the SNARE complex (Hayashi and others 1994; Sollner and others 1993b). The crystal structure of the SNARE complex revealed four parallel oriented α-helixes, one from syx, one from synaptobrevin and two from SNAP-25 (Sutton and others 1998). The α-helical domain of each SNARE protein is called the "SNARE motif". SNAP-25 has two SNARE motifs, with one close to the N-terminus called SNAP-25N, and the other one close to the C-terminus called SNAP-25C.

How the SNARE complex facilitates/mediates fusion is controversial. One hypothesis is the so called "zipper model" (Hanson and others 1997a; Otto and others 1997), which is primarily based on the topology of the SNARE complex in layers (Sutton and others 1998). In addition, syx and synaptobrevin are parallel in orientation with their C-terminal membrane anchors on the same side of the four-helix bundle. The parallel configuration was first predicted by fluorescence resonance energy transfer (FRET) between probes tagged to syx and synaptobrevin (Lin and Scheller 1997). This was subsequently confirmed by several structural studies using electron microscopy analysis (Hanson and others 1997b), site-directed electron spin resonance (Margittai and others 2001; Poirier

and others 1998b) and x-ray crystallography (Antonin and others 2002; Ernst and Brunger 2003; Sutton and others 1998).

The zipper model predicts that the SNARE complex forms by zipping from the membrane distal end to the membrane proximal end (Fasshauer 2003; Fiebig and others 1999; Hanson and others 1997a; Otto and others 1997). Intuitively, the zipper model provides an attractive explanation for the function of the SNARE complex in fusion. However, there is no direct experimental evidence for zipping. Recent studies showed that antibodies specific to the more C-terminal SNARE motif of SNAP-25N blocked the SNARE complex assembly and secretion to a greater degree compared to the antibody specific for the more N-terminal SNAP-25N SNARE motif (Xu and others 1999). Moreover, peptides corresponding to the C-terminal half of the synaptobrevin SNARE motif blocked secretion, whereas peptides corresponding to the N-terminal half did not (Melia and others 2002). These experiments indicated that the SNARE complex is likely polarized. However, they did not provide evidence for zipping. In contrast, one recent study suggested that four locations along the sequential layers assembled into the complex simultaneously, not like a zipper (Zhang and others 2004).

To address the function of the SNARE complex in exocytosis, we used mutants that affect its thermostability. By monitoring the kinetics of the fusion pore, the SNARE complex was shown to directly regulate fusion pore opening and dilation. SNARE complex formation throughout the entire four-helix bundle is important for exocytosis. However, only part of the SNARE complex is involved in dilating a fusion pore. These results demonstrated that the SNARE complex undergoes at least two conformational

transitions: one is essential for fusion pore initiation and the other one for fusion pore dilation.

2. Results and Discussion

2.1. The SNARE complex facilitates exocytosis

To test the function of the SNARE complex in exocytosis, a series of SNARE complex mutants were made and overexpressed in PC12 cells. Mutants contained single or double point substitutions in the hydrophobic layers. Substituted residues were generally hydrophobic with altered side chain size. A total of nine mutants were tested, including two syx mutants and seven SNAP-25C mutants (substitutions in the C-terminal SNARE motif of SNAP-25) (Summarized in Figure 5-1). Previous biochemical assays suggested that many mutations at the hydrophobic layers of the SNARE complex can be incorporated into the complex, but they altered the complex thermostability (Chen and others 1999; Fergestad and others 2001; Littleton and others 1998). Reduced thermostability of the SNARE complex was hypothesized to reduce the efficiency of fusion (Chen and others 1999; Fergestad and others 2001; Littleton and others 1998).

The two syx mutants tested were syx-V240A/A244V and syx-T251I. Syx-V240A/A244V contains double point substitutions at layers of +4 and +5, when mapped to the crystal structure of the SNARE complex (Sutton and others 1998). This syx mutant was shown to reduce the SNARE complex stability (Fergestad and others 2001; Kee and others 1995) and syx-Ca^{2+} channel interaction (Bezprozvanny and others 2000). The same mutation was also found in *Drosophila*, where it was designated as syx^{4} (Fergestad and

others 2001). The *syx*^{4} fly mutant was embryonic lethal with severely impaired neurosecretion. Syx-T251I contains a point mutation (threonine to isoleucine) at position 251 corresponding to layer +7. Syx-T251I was first identified as a paralytic fly mutant *syx*$^{3\text{-}69}$ (Littleton and others 1998). Mutant flies showed blocked synaptic transmission at an elevated temperature of 38ºC. In vitro syx-T251I was shown to reduce the thermostability of the SNARE complex and disrupt the interactions between syx and synaptobrevin.

We first examined the effect of these two syx mutants on secretion. Large dense core vesicle exocytosis in PC12 cells was detected by amperometry. A cumulative plot was made by counting the number of spikes with an amplitude greater than 2 pA (Figure 5-2, A). A linear fit to the rising phase of this plot was used to quantitatively evaluate the secretion rate (Figure 5-2, B). Overexpressing these mutants in PC12 cells reduced the secretion rate significantly (Figure 5-2, C). The reduced secretion rate is consistent with the observed defect in neurosecretion in mutant flies (Fergestad and others 2001; Littleton and others 1998).

Five SNAP-25C mutants tested (SNAP25C-L150/V153, I157/L160, M167/I171, I178/I181 and N188/I192) contain double point mutations to alanine (A) at adjacent hydrophobic layers. These mutants can form SNARE complexes, but with reduced thermostability (Chen and others 1999). In cracked PC12 cells, secretion can be blocked by applying BoNT/E (botulinum neurotoxin E), which cleaves 26 amino acids from the C-terminus of SNAP-25 (between R180 and I181). The mutant SNAP-25C peptide can

rescue secretion to a level below that obtained with the wild-type SNAP-25C peptide (Chen and others 1999).

We overexpressed the five SNAP-25C mutants with alanine double point substitutions in PC12 cells. KCl evoked secretion from PC12 cells was reduced to about 30% of that seen in cells overexpressing wild-type SNAP-25 (Figure 5-3, C). A reduction in the secretion rate in intact PC12 cells agrees with previous results in cracked PC12 cells (Chen and others 1999). The maximum amount of secretion at the end of a 20 second recording period was reduced by a factor of 3 for most of mutants. Interestingly, the mutant SNAP25C-I150/V153 reached a level of ~10 spikes/cell at the end of the recording period, about twice that of the other four mutants (Figure 5-3, A). The spike number reached 14 seconds after the end of 6 seconds of KCl stimulation is less indicative.

In order to cover the whole length of the SNARE motif of SNAP-25C, we designed two SNAP-25C mutants at position 199, with point substitutions to leucine (SNAP25C-A199L) and tryptophan (SNAP25C-A199W). SNAP25C-A199W reduced the secretion rate by a factor of ~2 (Figure 5-3), whereas SNAP25C-A199L did not alter the secretion rate. The reduced secretion rate with SNAP25-A199W could be through an alteration in the stability of the SNARE complex. Alternatively, this mutant could either prevent SNARE complex formation or form a non-functional complex. SNAP25C-A199L enhanced the secretion rate to about 1.6 spikes/sec compared to 1.2 spikes/sec seen in the control cells overexpressing GFP vector (table 4-1), which is undistinguishable from the wild-type SNAP-25. Based on this result, SNAP25C-A199L is likely incorporated into the SNARE complex properly.

Most of the mutants tested could reduce the thermostability of the SNARE complex in *vitro*. Based on the rationale that the thermostability of the complex would reflect the stability of the fusion-competent SNARE complex, our results further demonstrate that formation of a stable SNARE complex occurs during exocytosis. Moreover, since the SNAP-25C mutants tested covered the entire length of the SNARE complex, a complete assembly into the SNARE complex is important for exocytosis.

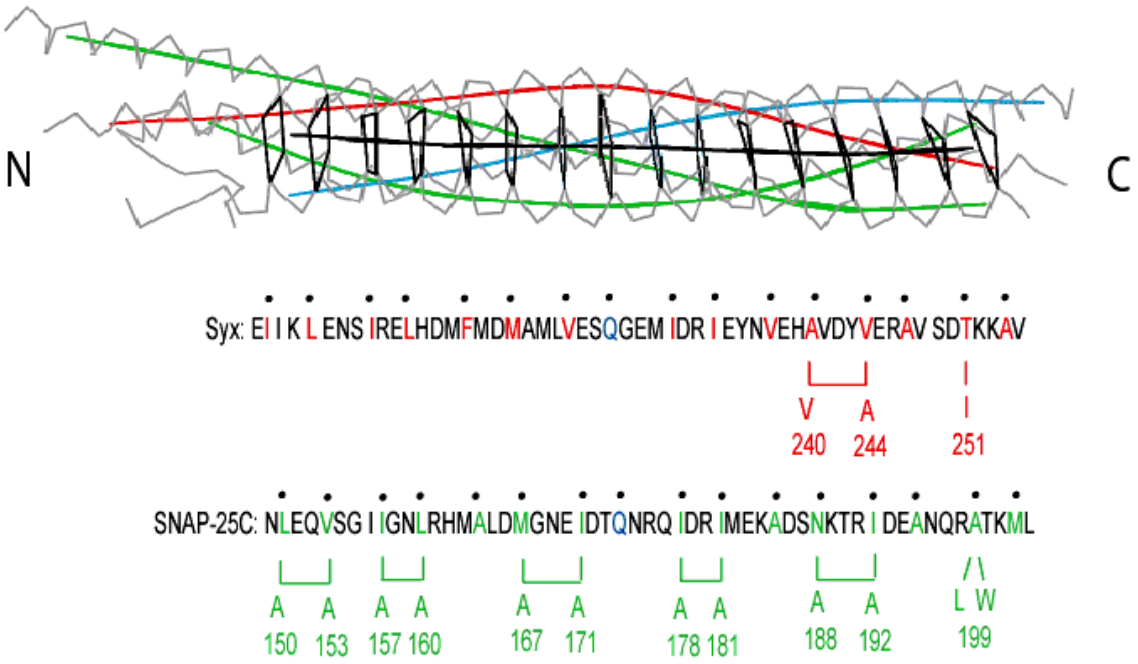

Figure 5-1. The SNARE complex mutants tested in the present study. The amino acid sequences of syx and SNAP-25 C-terminal SNARE motif (SNAP-25C) are shown. Residues residing at the hydrophobic layers are highlighted in red for syx and green for SNAP-25C. The ionic residue Q at the central layer is in blue. The point substitutions are indicated by residue position number.

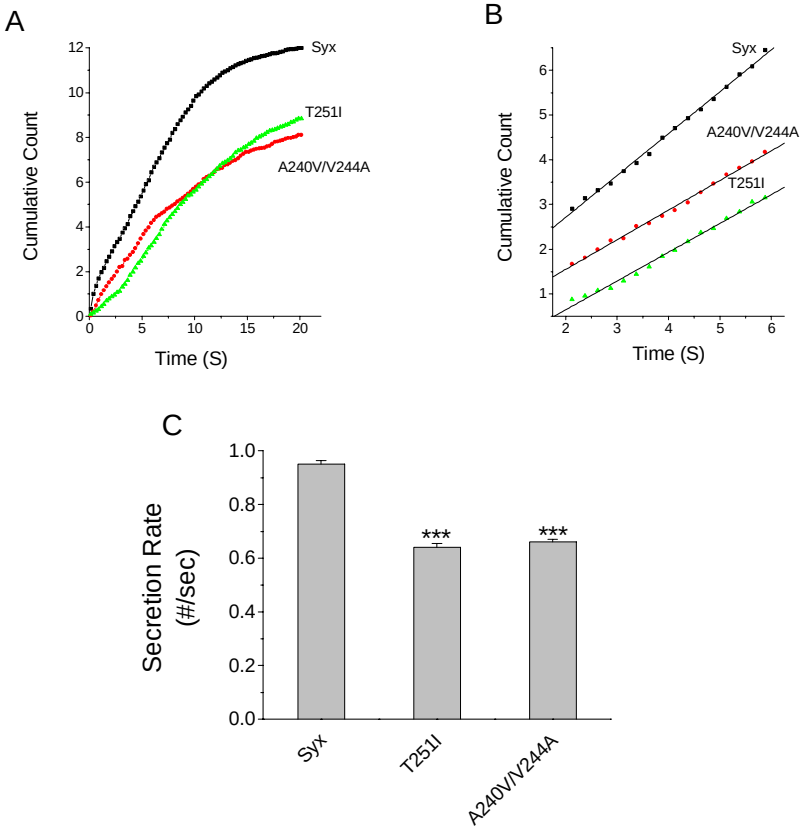

Figure 5-2. The secretion rate was reduced in PC12 cells overexpressing syx mutants. (A) Cumulative spike number is plotted. (B) The expanded trace during 2.0-6.0 seconds of KCl stimulation showed a roughly linear rising phase. A linear fit of this rising phase gave the secretion rate. (C) Syx mutants A240V/V244A and T251I reduced the secretion rate significantly (error bars are mean±SEM). ***, P<0.001 with a student's t-test.

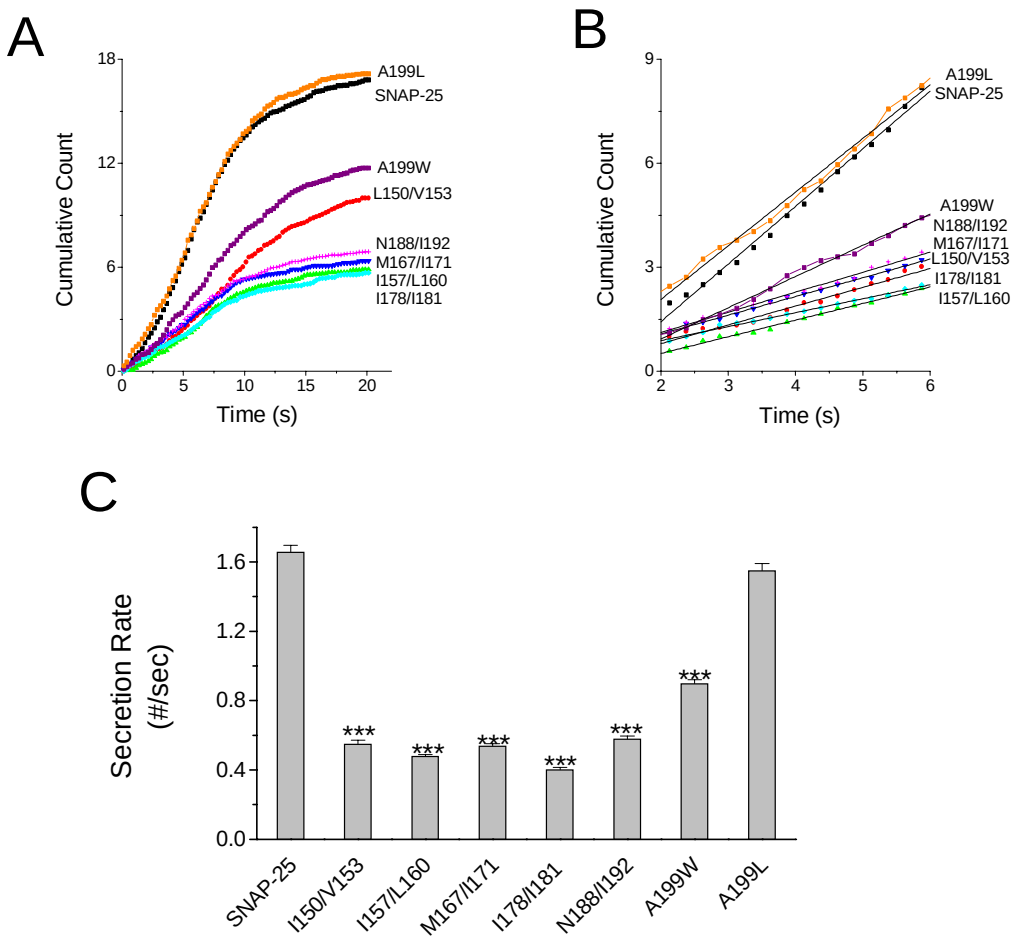

Figure 5-3. Overexpressing the SNAP-25 mutants in PC12 cells altered the secretion rate. Cumulative plots (A) and linear fit for the secretion rate (B) are indicated for various mutants. The mean secretion rates were compared to wild-type SNAP-25 (C). Most of SNAP-25C mutants reduced the secretion rate significantly. Only one mutant, SNAP25C-A199L, did not alter the secretion rate. ***, P<0.001 with a student t-test.

2.2. The SNARE complex undergoes a conformational transition during fusion pore dilation

Having established a role for the SNARE complex in the kinetics of exocytosis, we next focused on the fusion pore properties. None of the SNARE complex mutants altered the amplitude of the amperometric foot currents (Figure 5-4). This result underscores the uniqueness of the syx membrane anchor in fusion pore permeation. As discussed in CHAPTER 4, the stability of a fusion pore can be evaluated by measuring the fusion pore duration. The kinetic parameters of a fusion pore could be distinguished by plotting the fusion pore duration (τ) versus spike frequency (*Fd*). Following the kinetic analysis of the fusion pore in CHARPTER 4, in a scheme of

$$C \underset{Kc}{\overset{fo}{\rightleftarrows}} O \xrightarrow{Kd} D$$

we can estimate changes in the fusion pore kinetic parameters based on (Jackson 1992):

$$\tau = 1 / (Kc + Kd)$$

$$Fd \propto fo * Kd / (Kc + Kd)$$

The syx mutants A240V/V244A and T251I prolonged the mean amperometric foot duration (Figure 5-5). In addition, four out of seven SNAP-25C mutants L150/V153, I157/L160, M167/I171, I178/I181 also increased the mean fusion pore duration (Figure 5-6). An increase in the fusion pore duration together with a reduction in the secretion rate (Figure 5-2 and 5-3) indicates the fusion pore dilation rate *Kd* is reduced. Thus, these syx

and SNAP-25C mutants reduced the fusion pore dilation rate. However, an influence of these mutants on the opening speed factor cannot be ruled out.

Three SNAP-25 mutants (N188/I192, A199W and A199L) that did not alter the fusion pore duration reside on one end of the SNARE complex (Figure 5-6). The negative effect on the foot duration indicates that these residues were not involved in fusion pore dilation. Two SNAP25C mutants, N188/I192 and A199W, also reduced the secretion rate significantly (Figure 5-3), which indicates a reduction in the opening speed factor (*fo*). This result indicates that this part of the SNARE complex is involved in fusion pore opening, but not in fusion pore dilation.

Taking these results together, the entire SNARE complex is important in exocytosis, but only part of the SNARE complex engages with the fusion pore dilation. Thus, the SNARE complex may exist in two conformations, one correlated with the fusion pore opening and the other one with fusion pore dilation. A conformational transition of the SNARE complex between these two states mediates the fusion pore dilation.

How the conformational transition of the SNARE complex is regulated during fusion pore dilation is then an interesting question. One study indicates that three residues in SNAP-25C, D193, D186, and D179 were important for synaptotagmin-I binding (Zhang and others 2002b). Our study showed that the region where the SNARE complex experiences the transition starts around the residue I181. These parallels suggest a role of synaptotagmin-I in this transition step.

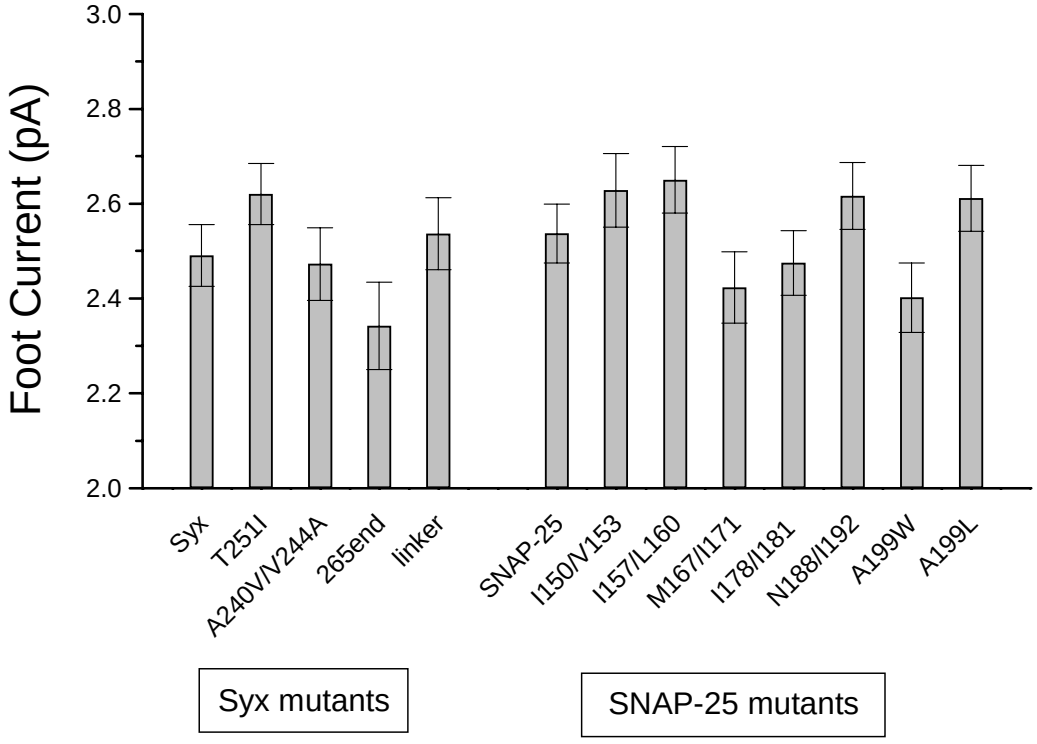

Figure 5-4. The SNARE complex mutants did not alter the amplitude of the amperometric foot current.

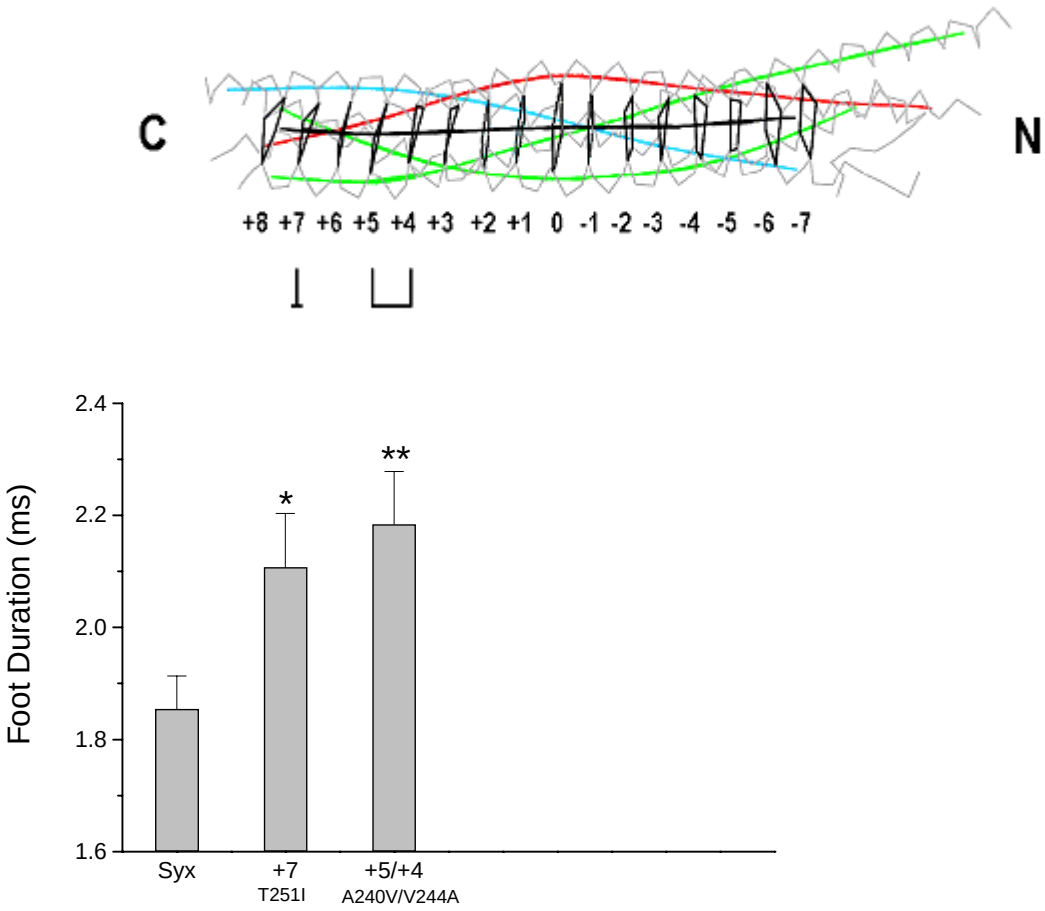

Figure 5-5. The mean foot duration was increased by syx mutants. Mutations at the corresponding hydrophobic layers are indicated on the helical layer model extracted from the crystal structure of the SNARE complex (Sutton and others 1998). T251I is at layer +7, and A240V/V244A is at layers +4/+5. T251I and A240V/V244A increased the foot duration significantly (*, P<0.05 and **, P<0.01 with a student t-test).

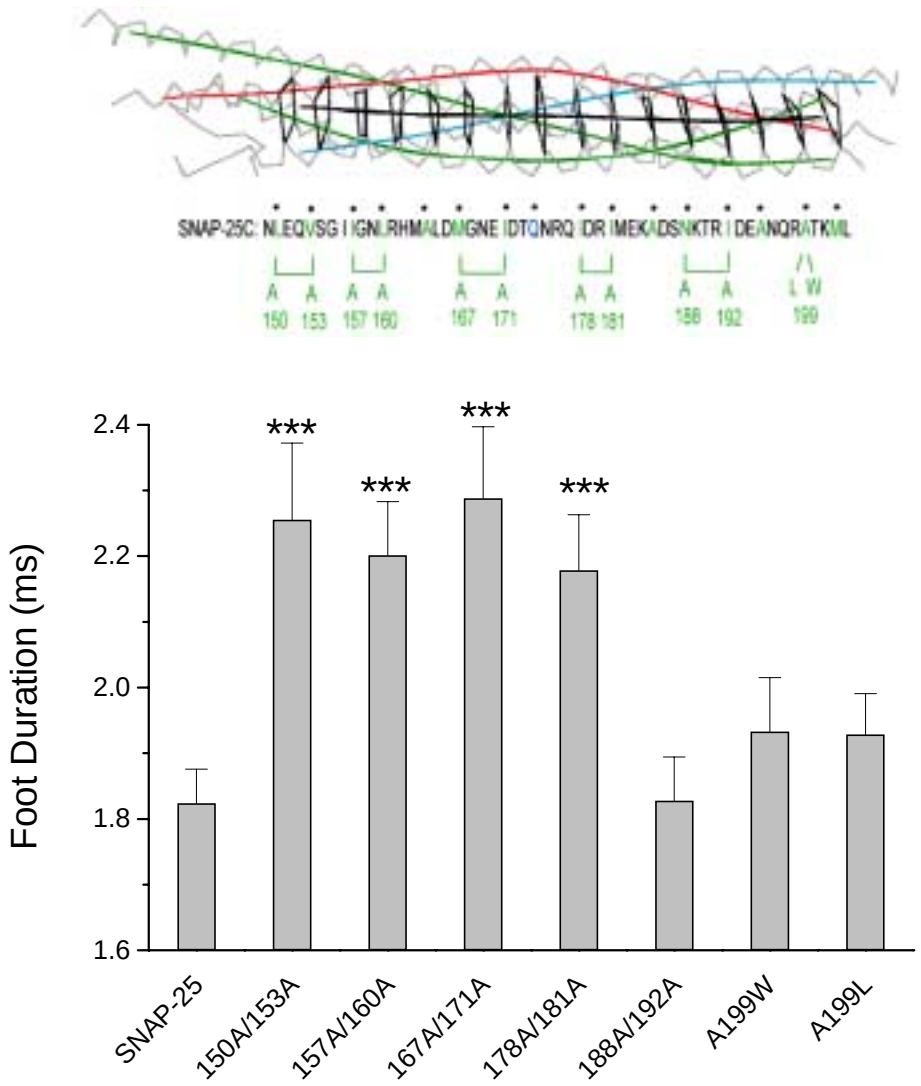

Figure 5-6. SNAP-25 mutants altered the mean foot duration. Four SNAP-25 mutants increased the foot duration with P<0.001 (***). SNAP-25 mutants were indicated on the helical layer model.

2.3. A possible anti-parallel configuration between syx and the SNAP-25 c-terminal α-helix

As the SNARE complex contributes to both the opening and dilation of a fusion pore, one would expect that manipulations of the same hydrophobic layer would produce similar effects on fusion pores. Two syx mutants are located at layer +7 and layer +4/+5 in the SNARE complex (Figure 5-5). If the SNARE motifs of syx and SNAP-25C are in parallel as indicated by the crystal structure (Sutton and others 1998), then the SNAP-25C mutants (SNAP25C-L150/V153, I157/L160, M167/I171, I178/I181, N188/I192 and A199W) that reduced the secretion rate would correspond to layers -7/-6, -5/-4, -2/-1, +1/+2, +4/+5 and +7 respectively (figure 5-7, A). Syx mutants at layer +4/+5 and +7 prolonged the foot durations. However, the corresponding mutations in SNAP-25C, 188A/192A and A199W, did not alter the foot duration (figure 5-6). But when we used a SNARE complex structure with syx and SNAP-25C in an anti-parallel configuration (Figure 5-7, B), the syx mutants A240V/V244A and T251I reside in the same layers with the SNAP-25 mutants I157/L160 and L150/V153. All four mutants increased the fusion pore duration. Based on this argument, we propose that in the SNARE complex formed during exocytosis, the α-helix of SNAP-25C has an orientation anti-parallel to the α-helix of syx.

A parallel configuration between syx and synaptobrevin in the SNARE complex would aid in pulling the plasma membrane and the vesicle membrane into close proximity. In contrast, intuitively, the relative configuration of syx and SNAP-25 in the SNARE complex can be either parallel or anti-parallel, because a proteinaceous fusion

pore would not require the lipidic membrane anchor of SNAP-25. In the crystal structure of the SNARE complex four SNARE motifs are in parallel (Antonin and others 2002; Ernst and Brunger 2003; Sutton and others 1998), which indicates that a parallel configuration of separated cytosolic α-helixes is the most chemically and energetically stable under the conditions of crystallization. However, in *vivo* syx and synaptobrevin are anchored to the membranes, and the two SNAP-25 α-helixes are linked together and anchored to the membrane through four palmitoylated cysteine residues. Thus, the physiologically fusion-competent SNARE complex might be very different from that observed in crystals.

An anti-parallel configuration between syx and SNAP-25C would put layers of residues that influenced the fusion pore dilation at the membrane proximal end, from layer -2 to layer +7. Mutations at the membrane distal end of the anti-parallel oriented SNAP-25C helix did not alter the fusion pore duration. This result suggests that the zipping is from the membrane distal end to the membrane proximal end leading to the dilation of the fusion pore.

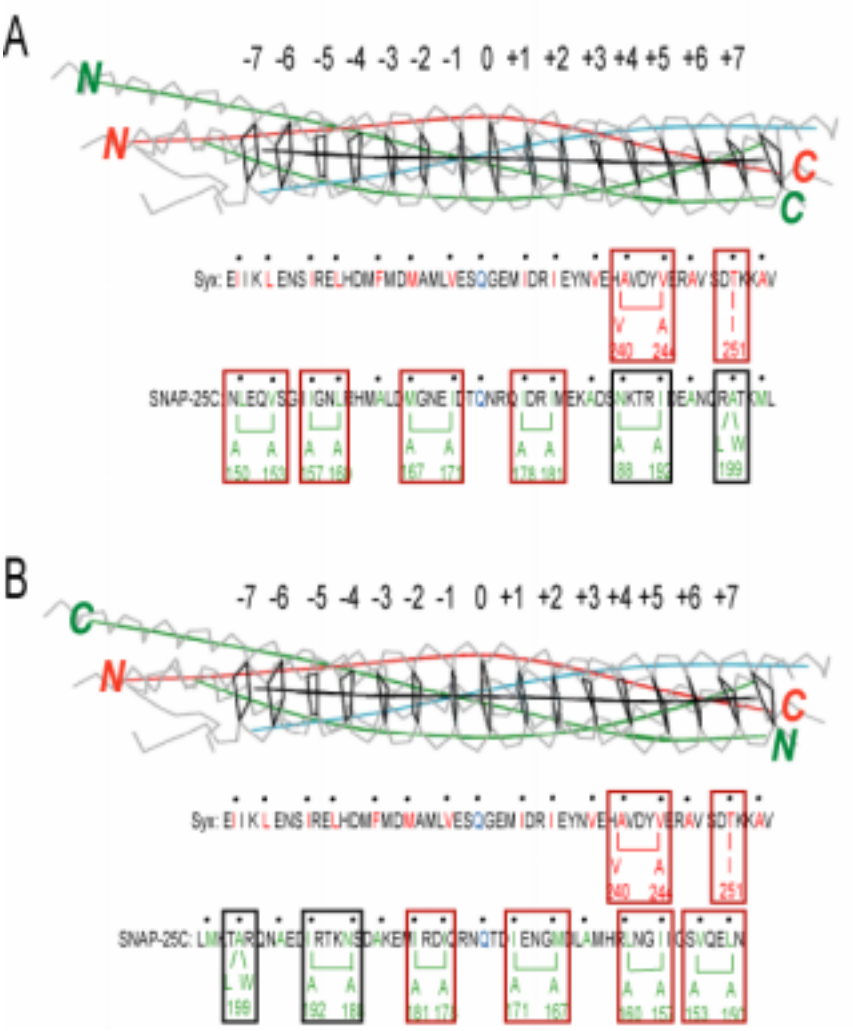

Figure 5-7. The relative configuration between syx and SNAP-25C. The helical layer model extracted from the crystal structure of the SNARE complex is shown (Sutton and others 1998). The N and C terminus of syx (the red helix) and SNAP-25C (one green helix) SNARE motifs are indicated. Red boxes indicate mutants that prolonged the foot durationt. Black boxes indicate mutants that failed to alter the foot duration. (A) A parallel configuration predicts that the syx mutants that prolonged the foot duration are in contact with layers where SNAP-25C mutations did not alter the foot duration. (B) An anti-parallel configuration matched the syx mutants that increased the foot duration to layers of SNAP-25C where mutations also increased the foot duration.

2.4. The SNARE complex regulates the fusion pore through a short syx linker

Syx contains a short linker region between the SNARE motif and the transmembrane domain. This region is enriched with basic amino acids (Weimbs and others 1998), which are likely unstructured and penetrate into the membrane (Kim and others 2002; Kweon and others 2002; Kweon and others 2003). Graded increases in the length of this linker region inhibited artificial liposome fusion progressively (McNew and others 1999; Wang and others 2001b). Based on the physical location, between the SNARE complex and syx transmembrane domain, this linker region was hypothesized to mechanically transduce the energy released from the SNARE complex formation to initiate fusion.

To investigate the coupling between the SNARE complex and the fusion pore, we first examined a truncated syx mutant without a transmembrane domain (syx-ΔTM). Syx-ΔTM contains the full length cytosolic domain and ends at position 265 (Figure 5-8). Overexpressing syx-ΔTM in PC12 cells inhibited secretion significantly (figure 5-9). But syx-ΔTM did not alter the PSF duration (figure 5-10) or amplitude (figure 5-5). The inhibitory effect of syx-ΔTM is likely to occur through incorporation into a SNARE complex, which cannot support fusion. The residual secretion could be due to endogenous syx.

We then increased the length of this linker region (syx-linker) by introducing 11 amino acids with glycine, glycine and serine (GGS) repeats, presumably forming a flexible structure (figure 5-8). The syx-linker mutant was previously shown to inhibit the reconstituted liposome fusion (McNew and others 1999). Overexpressing the syx-linker mutant in PC12 cells reduced the secretion rate significantly (figure 5-9). Moreover, the

syx-linker mutant also increased the foot duration (figure 5-10). Increased foot duration together with the reduced secretion rate indicates a reduction in the fusion pore dilation rate. The effect of the syx-linker mutant in slowing the rate of fusion pore dilation is similar to that observed with the SNARE complex mutants that have reduced thermostability.

The linker region in wild-type syx contains only about ten amino acids. With the juxtamembrane region of syx interacting with the plasma membrane (Kim, Kweon et al. 2002; Kweon, Kim et al. 2002), the SNARE complex would be positioned close to the plasma membrane, probably at an angle. The short linker would transmit the energy released from SNARE complex formation/zipping more efficiently to the fusion pore.

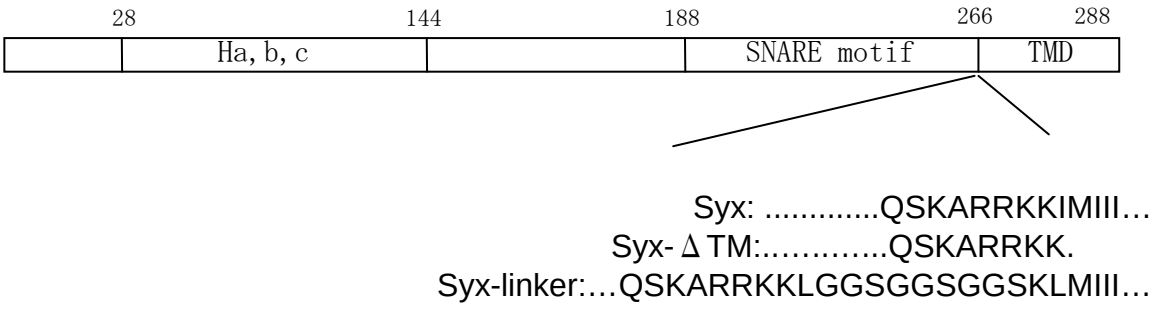

Figure 5-8. The syx mutants without a transmembrane domain or with a lengthened linker. The truncated form, syx-ΔTM, contains no transmembrane domain and ends at residue 265. The syx-linker mutant contains an extra 11 amino acid sequence between the SNARE motif and the transmembrane domain (TMD). The sequence of the introduced amino acids is indicated.

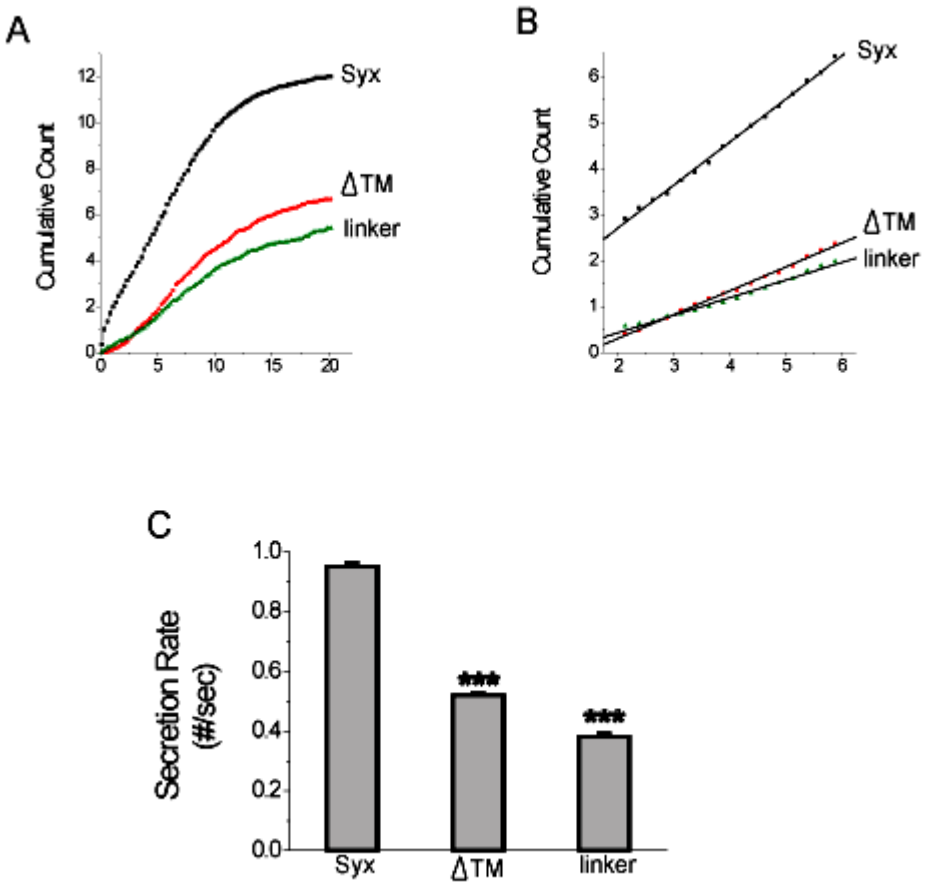

Figure 5-9. The secretion rates were reduced by syx mutants either without a transmembrane domain or with a lengthened linker. The cumulative spike count plots are shown in (A). The secretion rate is calculated by the linear fit (B) and compared to the wild-type syx (C). Both syx-ΔTM and syx-linker reduced secretion rates significantly (*, P<0.001).**

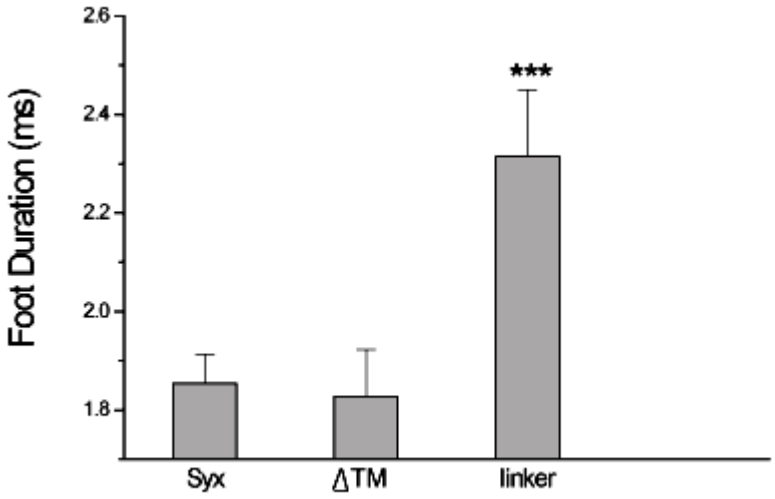

Figure 5-10. The syx-linker mutant significantly increased the mean foot duration (*, P<0.001 with a student t-test), but syx-ΔTM did not alter the mean foot duration.**

CONCLUSIONS AND PERSPECTIVES

Conclusions

In this study, the membrane anchor of syntaxin (syx) was demonstrated as a structural component of the fusion pore. Syx is a plasma membrane integral protein essential for Ca^{2+}-triggered exocytosis. Altering the size or charge of the pore lining residues influenced the neurotransmitter flux through the fusion pore, as well as the fusion pore conductance. Based on the conductance of the fusion pore, we proposed a fusion pore model formed by 5-8 copies of the syx membrane anchor in a circular arrangement.

Manipulations of the syx membrane anchor altered the kinetics of exocytosis. The pore lining residues had the greatest influence on the fusion pore dilation rate. During dilation, pore lining residues would experience a transition from a hydrophilic environment to a hydrophobic environment. This influence on the fusion pore dilation rate specifically by these residues provides further evidence for them to line the fusion pore. This result agrees with the fusion pore model formed by syx membrane anchor.

The SNARE complex was demonstrated to be involved in the final fusion step, based on the evidence that the SNARE complex influenced fusion pore stability. A fully assembled SNARE complex is important for exocytosis, but only part of the SNARE complex influenced the fusion pore dilation. Thus, the SNARE complex was predicted to exist in two conformations. One conformation regulates the opening of a fusion pore. The other conformation influenced the fusion pore dilation. The regions that influence the fusion pore dilation reside at one end of the SNARE complex. Moreover, the

conformational transition of the SNARE complex is coupled to the syx membrane anchor through a short linker region.

Taken together, SNARE complex mediated exocytosis includes a few physical elements: the syx membrane anchor a structural component of the fusion pore; the SNARE complex formation/conformational transition serves as the energy generator; the syx membrane anchor and the SNARE complex are tightly coupled through a short linker. Upon presentation of the Ca^{2+} trigger, the SNARE complex formation/conformational transition opens the fusion pore. Then the SNARE complex undergoes a transition to mediate fusion pore dilation. Based on this model, tight regulation of exocytosis was hypothesized to be achieved by regulating the fusion pore through the SNARE proteins or the SNARE complex.

Perspectives

The model of the fusion pore formed by syx in the plasma membrane implies a corresponding proteinaceous structure in the vesicle membrane. The present study has demonstrated an approach to characterize the fusion pore molecular structure. Similar studies on the membrane anchors of synaptobrevin and synaptotagmin may complete the proteinaceous fusion pore model.

With the syx membrane anchor forming the fusion pore and influencing the fusion pore dynamics, syx is further demonstrated as a central coordinator for exocytosis. Most in vitro biochemical studies were carried out with the cytosolic domain of syx. But little is known about the conformational changes of the full length syx upon interaction with other molecules. Biochemical studies with syx anchored to the membrane will provide more insight into the regulation of exocytosis.

Direct coupling of the SNARE complex to the fusion pore suggests that Ca^{2+} may exert an influence on the SNARE complex conformational transitions. But how the SNARE complex is regulated by Ca^{2+} is obscure. Synaptotagmin is the best candidate for the Ca^{2+} sensor, and it interacts with the SNARE proteins and the SNARE complex (Chapman 2002; Zhang and others 2002b). Regulation of the fusion pore by the SNARE complex could be triggered by synaptotagmin binding. In addition, synaptotagmins mediated different types of exocytosis, full fusion *vs*. kiss-and-run exocytosis (Wang and others 2003). These two exocytosis pathways could arise from different conformational states of the SNARE complex. Further studies on the interactions between synaptotagmins

and the SNARE complex/monomers should provide valuable information on the underlying mechanism of Ca^{2+} regulation.

A possible anti-parallel configuration between syx and the C-terminal SNAP-25 helix implies that the SNARE complex structure in *vivo* may be very different from that observed in solution and crystals. Similar examination (as described in CHAPTER 5) throughout the SNARE motifs of every SNARE protein would provide more information. Also, the relative configuration can be examined either by FRET with probes tagged to different locations of the monomeric SNARE proteins in *vivo* (Xia and others 2001), or by single molecule FRET with SNARE proteins anchored to the membrane in *vitro* (Bowen and others 2004; Weninger and others 2003).

Synaptic transmission operates on a sub-millisecond time scale (Augustine and others 1985; Katz and Miledi 1965). The fusion pore could remain open for a few milliseconds. From this point of view, regulation of the fusion pore may directly contribute to modifications of synaptic strength. Because of the technical limits, there is no direct measurement of the properties of fusion pores of synaptic vesicles. However, characterization of the fusion pore on the molecular level would allow further manipulations, such as reducing the fusion pore size or increasing the fusion pore duration. With these manipulations, one may be able to characterize the fusion pore in synapses. Such experiments raise the hope of revealing the coupling between the fusion pore and synaptic plasticity.

Overexpressing proteins of interest in PC12 cells was further demonstrated as a plausible way to study functions of specific molecules in exocytosis. The exact functions

of many fusion modulators (Jahn and Sudhof 1999; Lin and Scheller 2000), such as NSF (Weidman and others 1989), α/γ-SNAP (Hanson and others 1995; Sollner and others 1993b), munc-18 (Hata and others 1993), munc-13 (Betz and others 1997) are unclear. Potential functions of these molecules in regulating the fusion pore can be characterized in this system. With syx forming the fusion pore, molecules that interact with syx, such as complexin (McMahon and others 1995), cysteine string protein (Wu and others 1999), tomosyn (Fujita and others 1998), amisyn (Scales and others 2002), various channels and transporters, could also involve in exocytosis in some way.

Secretion from neuroendocrine PC12 cells upon KCl stimulation is slow with a latency of a few seconds after stimulation. This is even slower than chromaffin cells. The underlying mechanism for the delayed secretion in neuroendocrine cells is an important question in neuroscience. Various experiments have demonstrated that syx interacts with Ca^{2+}-channels (Bezprozvanny and others 1995; Bezprozvanny and others 2000; Sheng and others 1994) and this interaction might be important in docking vesicles around the Ca^{2+}-channel. A spatially uniform elevation of Ca^{2+} could trigger fastest secretion from chromaffin cells with a delay of a few milliseconds. However, the fastest secretion seen in the cracked PC12 cells has a latency of tens of milliseconds (Wang, CT personal communication). The longer latency observed in PC12 cells compared to chromaffin cells could be due to the lack of some molecules that can facilitate the coupling between syx and Ca^{2+}-channels. This possibility can be examined in PC12 cells. In addition, reconstitution of a tight excitation-secretion coupling in PC12 cells would advance our understanding of the tight stimulation-secretion coupling in neurons as well.

REFERENCES

Albillos A, Dernick G, Horstmann H, Almers W, Alvarez de Toledo G, Lindau M. 1997. The exocytotic event in chromaffin cells revealed by patch amperometry. Nature 389(6650):509-12.

Ales E, Tabares L, Poyato JM, Valero V, Lindau M, Alvarez de Toledo G. 1999. High calcium concentrations shift the mode of exocytosis to the kiss-and-run mechanism. Nat Cell Biol 1(1):40-4.

Almers W, Breckenridge LJ, Iwata A, Lee AK, Spruce AE, Tse FW. 1991. Millisecond studies of single membrane fusion events. Ann N Y Acad Sci 635:318-27.

Alvarez de Toledo G, Fernandez JM. 1988. The events leading to secretory granule fusion. Soc Gen Physiol Ser 43:333-44.

Alvarez de Toledo G, Fernandez-Chacon R, Fernandez JM. 1993. Release of secretory products during transient vesicle fusion. Nature 363(6429):554-8.

An SJ, Almers W. 2004. Tracking SNARE complex formation in live endocrine cells. Science 306(5698):1042-6.

Antonin W, Fasshauer D, Becker S, Jahn R, Schneider TR. 2002. Crystal structure of the endosomal SNARE complex reveals common structural principles of all SNAREs. Nat Struct Biol 9(2):107-11.

Aravamudan B, Fergestad T, Davis WS, Rodesch CK, Broadie K. 1999. Drosophila UNC-13 is essential for synaptic transmission. Nat Neurosci 2(11):965-71.

Aravanis AM, Pyle JL, Tsien RW. 2003. Single synaptic vesicles fusing transiently and successively without loss of identity. Nature 423(6940):643-7.

Augustin I, Rosenmund C, Sudhof TC, Brose N. 1999. Munc13-1 is essential for fusion competence of glutamatergic synaptic vesicles. Nature 400(6743):457-61.

Augustine GJ, Burns ME, DeBello WM, Hilfiker S, Morgan JR, Schweizer FE, Tokumaru H, Umayahara K. 1999. Proteins involved in synaptic vesicle trafficking. J Physiol 520(Pt 1):33-41.

Augustine GJ, Charlton MP, Smith SJ. 1985. Calcium entry and transmitter release at voltage-clamped nerve terminals of squid. J Physiol 367:163-81.

Augustine GJ, Neher E. 1992. Calcium requirements for secretion in bovine chromaffin cells. J Physiol 450:247-71.

Babcock M, Macleod GT, Leither J, Pallanck L. 2004. Genetic analysis of soluble N-ethylmaleimide-sensitive factor attachment protein function in Drosophila reveals positive and negative secretory roles. J Neurosci 24(16):3964-73.

Bai J, Tucker WC, Chapman ER. 2004a. PIP2 increases the speed of response of synaptotagmin and steers its membrane-penetration activity toward the plasma membrane. Nat Struct Mol Biol 11(1):36-44.

Bai J, Wang CT, Richards DA, Jackson MB, Chapman ER. 2004b. Fusion pore dynamics are regulated by synaptotagmin*t-SNARE interactions. Neuron 41(6):929-42.

Bai J, Wang P, Chapman ER. 2002. C2A activates a cryptic Ca(2+)-triggered membrane penetration activity within the C2B domain of synaptotagmin I. Proc Natl Acad Sci U S A 99(3):1665-70.

Balch WE, Dunphy WG, Braell WA, Rothman JE. 1984a. Reconstitution of the transport of protein between successive compartments of the Golgi measured by the coupled incorporation of N-acetylglucosamine. Cell 39(2 Pt 1):405-16.

Balch WE, Glick BS, Rothman JE. 1984b. Sequential intermediates in the pathway of intercompartmental transport in a cell-free system. Cell 39(3 Pt 2):525-36.

Barnstable CJ, Hofstein R, Akagawa K. 1985. A marker of early amacrine cell development in rat retina. Brain Res 352(2):286-90.

Baumert M, Maycox PR, Navone F, De Camilli P, Jahn R. 1989. Synaptobrevin: an integral membrane protein of 18,000 daltons present in small synaptic vesicles of rat brain. Embo J 8(2):379-84.

Bean BP. 1992. Whole-cell recording of calcium channel currents. Methods Enzymol 207:181-93.

Becherer U, Moser T, Stuhmer W, Oheim M. 2003. Calcium regulates exocytosis at the level of single vesicles. Nat Neurosci 6(8):846-53.

Beckers CJ, Block MR, Glick BS, Rothman JE, Balch WE. 1989. Vesicular transport between the endoplasmic reticulum and the Golgi stack requires the NEM-sensitive fusion protein. Nature 339(6223):397-8.

Bennett MK, Calakos N, Scheller RH. 1992. Syntaxin: a synaptic protein implicated in docking of synaptic vesicles at presynaptic active zones. Science 257(5067):255-9.

Bennett MK, Garcia-Arraras JE, Elferink LA, Peterson K, Fleming AM, Hazuka CD, Scheller RH. 1993. The syntaxin family of vesicular transport receptors. Cell 74(5):863-73.

Bennett MK, Scheller RH. 1993. The molecular machinery for secretion is conserved from yeast to neurons. Proc Natl Acad Sci U S A 90(7):2559-63.

Berdiev BK, Jovov B, Tucker WC, Naren AP, Fuller CM, Chapman ER, Benos DJ. 2004. ENaC subunit-subunit interactions and inhibition by syntaxin 1A. Am J Physiol Renal Physiol 2:2.

Bernstein AM, Whiteheart SW. 1999. Identification of a cellubrevin/vesicle associated membrane protein 3 homologue in human platelets. Blood 93(2):571-9.

Betz A, Okamoto M, Benseler F, Brose N. 1997. Direct interaction of the rat unc-13 homologue Munc13-1 with the N terminus of syntaxin. J Biol Chem 272(4):2520-6.

Betz WJ, Bewick GS. 1992. Optical analysis of synaptic vesicle recycling at the frog neuromuscular junction. Science 255(5041):200-3.

Betz WJ, Mao F, Bewick GS. 1992. Activity-dependent fluorescent staining and destaining of living vertebrate motor nerve terminals. J Neurosci 12(2):363-75.

Betz WJ, Mao F, Smith CB. 1996. Imaging exocytosis and endocytosis. Curr Opin Neurobiol 6(3):365-71.

Bezprozvanny I, Scheller RH, Tsien RW. 1995. Functional impact of syntaxin on gating of N-type and Q-type calcium channels. Nature 378(6557):623-6.

Bezprozvanny I, Zhong P, Scheller RH, Tsien RW. 2000. Molecular determinants of the functional interaction between syntaxin and N-type Ca2+ channel gating. PNAS 97(25):13943-13948.

Bhattacharya S, Stewart BA, Niemeyer BA, Burgess RW, McCabe BD, Lin P, Boulianne G, O'Kane CJ, Schwarz TL. 2002. Members of the synaptobrevin/vesicle-associated membrane protein (VAMP) family in Drosophila are functionally interchangeable in vivo for neurotransmitter release and cell viability. Proc Natl Acad Sci U S A 99(21):13867-72.

Blasi J, Chapman ER, Yamasaki S, Binz T, Niemann H, Jahn R. 1993. Botulinum neurotoxin C1 blocks neurotransmitter release by means of cleaving HPC-1/syntaxin. Embo J 12(12):4821-8.

Block MR, Glick BS, Wilcox CA, Wieland FT, Rothman JE. 1988. Purification of an N-ethylmaleimide-sensitive protein catalyzing vesicular transport. Proc Natl Acad Sci U S A 85(21):7852-6.

Blumenthal R, Sarkar DP, Durell S, Howard DE, Morris SJ. 1996. Dilation of the influenza hemagglutinin fusion pore revealed by the kinetics of individual cell-cell fusion events. J Cell Biol 135(1):63-71.

Bock JB, Matern HT, Peden AA, Scheller RH. 2001. A genomic perspective on membrane compartment organization. Nature 409(6822):839-41.

Bock JB, Scheller RH. 1997. Protein transport. A fusion of new ideas. Nature 387(6629):133-5.

Bowen ME, Weninger K, Brunger AT, Chu S. 2004. Single Molecule Observation of Liposome-Bilayer Fusion Thermally Induced by Soluble N-Ethyl Maleimide Sensitive-Factor Attachment Protein Receptors (SNAREs). Biophys J 87(5):3569-84.

Breckenridge LJ, Almers W. 1987. Currents through the fusion pore that forms during exocytosis of a secretory vesicle. Nature 328(6133):814-7.

Breckenridge LJ, Almers W. 1987b. Final steps in exocytosis observed in a cell with giant secretory granules. Proc Natl Acad Sci U S A 84(7):1945-9.

Brennwald P, Kearns B, Champion K, Keranen S, Bankaitis V, Novick P. 1994. Sec9 is a SNAP-25-like component of a yeast SNARE complex that may be the effector of Sec4 function in exocytosis. Cell 79(2):245-58.

Brose N, Petrenko AG, Sudhof TC, Jahn R. 1992. Synaptotagmin: a calcium sensor on the synaptic vesicle surface. Science 256(5059):1021-5.

Bruns D, Jahn R. 1995. Real-time measurement of transmitter release from single synaptic vesicles. Nature 377(6544):62-5.

Bruns D, Riedel D, Klingauf J, Jahn R. 2000. Quantal release of serotonin. Neuron 28(1):205-20.

Burgess TL, Kelly RB. 1987. Constitutive and regulated secretion of proteins. Annu Rev Cell Biol 3:243-93.

Carr CM, Novick PJ. 2000. Membrane fusion. Changing partners. Nature 404(6776):347-9.

Castillo PE, Schoch S, Schmitz F, Sudhof TC, Malenka RC. 2002. RIM1alpha is required for presynaptic long-term potentiation. Nature 415(6869):327-30.

Chandler D, Heuser J. 1980. Arrest of membrane fusion events in mast cells by quick-freezing. J. Cell Biol. 86(2):666-674.

Chandler DE, Bennett JP, Gomperts B. 1983. Freeze-fracture studies of chemotactic peptide-induced exocytosis in neutrophils: evidence for two patterns of secretory granule fusion. J Ultrastruct Res 82(2):221-32.

Chanturiya A, Chernomordik LV, Zimmerberg J. 1997. Flickering fusion pores comparable with initial exocytotic pores occur in protein-free phospholipid bilayers. PNAS 94(26):14423-14428.

Chapman ER. 2002. Synaptotagmin: a Ca(2+) sensor that triggers exocytosis? Nat Rev Mol Cell Biol 3(7):498-508.

Chapman ER, Davis AF. 1998. Direct interaction of a Ca2+-binding loop of synaptotagmin with lipid bilayers. J Biol Chem 273(22):13995-4001.

Chapman ER, Hanson PI, An S, Jahn R. 1995. Ca2+ regulates the interaction between synaptotagmin and syntaxin 1. J Biol Chem 270(40):23667-71.

Chapman ER, Jahn R. 1994. Calcium-dependent interaction of the cytoplasmic region of synaptotagmin with membranes. Autonomous function of a single C2-homologous domain. J Biol Chem 269(8):5735-41.

Chen YA, Scales SJ, Duvvuri V, Murthy M, Patel SM, Schulman H, Scheller RH. 2001. Calcium regulation of exocytosis in PC12 cells. Journal of Biological Chemistry 276(28):26680-26687.

Chen YA, Scales SJ, Patel SM, Doung YC, Scheller RH. 1999. SNARE complex formation is triggered by Ca2+ and drives membrane fusion. Cell 97(2):165-74.

Chernomordik LV, Frolov VA, Leikina E, Bronk P, Zimmerberg J. 1998. The pathway of membrane fusion catalyzed by influenza hemagglutinin: restriction of lipids, hemifusion, and lipidic fusion pore formation. J Cell Biol 140(6):1369-82.

Chernomordik LV, Leikina E, Frolov V, Bronk P, Zimmerberg J. 1997. An early stage of membrane fusion mediated by the low pH conformation of influenza hemagglutinin depends upon membrane lipids. J Cell Biol 136(1):81-93.

Chow RH, Klingauf J, Heinemann C, Zucker RS, Neher E. 1996. Mechanisms determining the time course of secretion in neuroendocrine cells. Neuron 16(2):369-76.

Chow RH, von Rüden L. 1995. Electrochemical detection of secretion from single cells. In: Sakmann B NE, editor. Single-Channel Recording. New York: Plenum Press. p 245-275.

Chow RH, von Ruden L, Neher E. 1992. Delay in vesicle fusion revealed by electrochemical monitoring of single secretory events in adrenal chromaffin cells. Nature 356(6364):60-3.

Clague MJ, Schoch C, Blumenthal R. 1991. Delay time for influenza virus hemagglutinin-induced membrane fusion depends on hemagglutinin surface density. J Virol 65(5):2402-7.

Clary DO, Griff IC, Rothman JE. 1990. SNAPs, a family of NSF attachment proteins involved in intracellular membrane fusion in animals and yeast. Cell 61(4):709-21.

Colliver TL, Hess EJ, Pothos EN, Sulzer D, Ewing AG. 2000a. Quantitative and statistical analysis of the shape of amperometric spikes recorded from two populations of cells. J Neurochem 74(3):1086-97.

Colliver TL, Pyott SJ, Achalabun M, Ewing AG. 2000b. VMAT-Mediated changes in quantal size and vesicular volume. J Neurosci 20(14):5276-82.

Colquhoun D, Sigworth FJ. 1995. Fitting and statistical analysis of single channel records. In: B S, E N, editors. Single-Channel Recording: Plenum, New York. p 483-587.

Condliffe SB, Zhang H, Frizzell RA. 2004. Syntaxin 1A regulates ENaC channel activity. J Biol Chem 279(11):10085-92. Epub 2003 Dec 31.

Cormack B. 1994. Introduction of a point mutation by sequential PCR steps. In: Ausubel FM BRea, editor. Current Protocols in Molecualr Biology. New York: John Wiley & Sons. p 397-482.

Cox HM, Rudolph A, Gschmeissner S. 1994. Ultrastructural co-localization of neuropeptide Y and vasoactive intestinal polypeptide in neurosecretory vesicles of submucous neurons in the rat jejunum. Neuroscience 59(2):469-76.

Craxton M. 2001. Genomic analysis of synaptotagmin genes. Genomics 77(1-2):43-9.

Danieli T, Pelletier SL, Henis YI, White JM. 1996. Membrane fusion mediated by the influenza virus hemagglutinin requires the concerted action of at least three hemagglutinin trimers. J Cell Biol 133(3):559-69.

De Camilli P, Jahn R. 1990. Pathways to regulated exocytosis in neurons. Annu Rev Physiol 52:625-45.

Debus K, Lindau M. 2000. Resolution of patch capacitance recordings and of fusion pore conductances in small vesicles. Biophys J 78(6):2983-97.

Deken SL, Beckman ML, Boos L, Quick MW. 2000. Transport rates of GABA transporters: regulation by the N-terminal domain and syntaxin 1A. Nat Neurosci 3(10):998-1003.

Dobrunz LE, Huang EP, Stevens CF. 1997. Very short-term plasticity in hippocampal synapses. Proc Natl Acad Sci U S A 94(26):14843-7.

Dong M, Richards DA, Goodnough MC, Tepp WH, Johnson EA, Chapman ER. 2003. Synaptotagmins I and II mediate entry of botulinum neurotoxin B into cells. J Cell Biol 162(7):1293-303.

Duncan RR, Greaves J, Wiegand UK, Matskevich I, Bodammer G, Apps DK, Shipston MJ, Chow RH. 2003. Functional and spatial segregation of secretory vesicle pools according to vesicle age. Nature 422(6928):176-80.

Earles CA, Bai J, Wang P, Chapman ER. 2001. The tandem C2 domains of synaptotagmin contain redundant Ca2+ binding sites that cooperate to engage t-SNAREs and trigger exocytosis. J Cell Biol 154(6):1117-23.

Eipper BA, Stoffers DA, Mains RE. 1992. The biosynthesis of neuropeptides: peptide alpha-amidation. Annu Rev Neurosci 15:57-85.

Elferink LA, Trimble WS, Scheller RH. 1989. Two vesicle-associated membrane protein genes are differentially expressed in the rat central nervous system. J Biol Chem 264(19):11061-4.

Erickson JD, Eiden LE. 1993. Functional identification and molecular cloning of a human brain vesicle monoamine transporter. J Neurochem 61(6):2314-7.

Ernst JA, Brunger AT. 2003. High resolution structure, stability, and synaptotagmin binding of a truncated neuronal SNARE complex. J Biol Chem 278(10):8630-6.

Etter EF, Kuhn MA, Fay FS. 1994. Detection of changes in near-membrane Ca2+ concentration using a novel membrane-associated Ca2+ indicator. J Biol Chem 269(13):10141-9.

Fasshauer D. 2003. Structural insights into the SNARE mechanism. Biochim Biophys Acta 1641(2-3):87-97.

Fasshauer D, Bruns D, Shen B, Jahn R, Brunger AT. 1997a. A structural change occurs upon binding of syntaxin to SNAP-25. J Biol Chem 272(7):4582-90.

Fasshauer D, Eliason WK, Brunger AT, Jahn R. 1998a. Identification of a minimal core of the synaptic SNARE complex sufficient for reversible assembly and disassembly. Biochemistry 37(29):10354-62.

Fasshauer D, Otto H, Eliason WK, Jahn R, Brunger AT. 1997b. Structural changes are associated with soluble N-ethylmaleimide-sensitive fusion protein attachment protein receptor complex formation. J Biol Chem 272(44):28036-41.

Fasshauer D, Sutton RB, Brunger AT, Jahn R. 1998b. Conserved structural features of the synaptic fusion complex: SNARE proteins reclassified as Q- and R-SNAREs. Proc Natl Acad Sci U S A 95(26):15781-6.

Fatt P, Katz B. 1952. Spontaneous subthreshold activity at motor nerve endings. J Physiol 117(1):109-28.

Fergestad T, Wu MN, Schulze KL, Lloyd TE, Bellen HJ, Broadie K. 2001. Targeted mutations in the syntaxin H3 domain specifically disrupt SNARE complex function in synaptic transmission. J Neurosci 21(23):9142-50.

Fernandez I, Arac D, Ubach J, Gerber SH, Shin O, Gao Y, Anderson RG, Sudhof TC, Rizo J. 2001. Three-dimensional structure of the synaptotagmin 1 C2B-domain: synaptotagmin 1 as a phospholipid binding machine. Neuron 32(6):1057-69.

Fernandez I, Ubach J, Dulubova I, Zhang X, Sudhof TC, Rizo J. 1998. Three-dimensional structure of an evolutionarily conserved N-terminal domain of syntaxin 1A. Cell 94(6):841-9.

Fernandez JM, Neher E, Gomperts BD. 1984. Capacitance measurements reveal stepwise fusion events in degranulating mast cells. Nature 312(5993):453-5.

Fernandez-Chacon R, Alvarez de Toledo G. 1995. Cytosolic calcium facilitates release of secretory products after exocytotic vesicle fusion. FEBS Lett 363(3):221-5.

Fernandez-Chacon R, Sudhof TC. 1999. Genetics of synaptic vesicle function: toward the complete functional anatomy of an organelle. Annu Rev Physiol 61:753-76.

Ferro-Novick S, Jahn R. 1994. Vesicle fusion from yeast to man. Nature 370(6486):191-3.

Fesce R, Grohovaz F, Valtorta F, Meldolesi J. 1994. Neurotransmitter release: fusion or 'kiss-and-run'? Trends Cell Biol 4(1):1-4.

Fiebig KM, Rice LM, Pollock E, Brunger AT. 1999. Folding intermediates of SNARE complex assembly. Nat Struct Biol 6(2):117-23.

Fili O, Michaelevski I, Bledi Y, Chikvashvili D, Singer-Lahat D, Boshwitz H, Linial M, Lotan I. 2001. Direct interaction of a brain voltage-gated K+ channel with syntaxin 1A: functional impact on channel gating. J Neurosci 21(6):1964-74.

Fujita Y, Shirataki H, Sakisaka T, Asakura T, Ohya T, Kotani H, Yokoyama S, Nishioka H, Matsuura Y, Mizoguchi A and others. 1998. Tomosyn: a syntaxin-1-binding protein that forms a novel complex in the neurotransmitter release process. Neuron 20(5):905-15.

Geerlings A, Lopez-Corcuera B, Aragon C. 2000. Characterization of the interactions between the glycine transporters GLYT1 and GLYT2 and the SNARE protein syntaxin 1A. FEBS Lett 470(1):51-4.

Gentet LJ, Stuart GJ, Clements JD. 2000. Direct measurement of specific membrane capacitance in neurons. Biophys J 79(1):314-20.

Geppert M, Goda Y, Hammer RE, Li C, Rosahl TW, Stevens CF, Sudhof TC. 1994. Synaptotagmin I: a major Ca2+ sensor for transmitter release at a central synapse. Cell 79(4):717-27.

Gerona RR, Larsen EC, Kowalchyk JA, Martin TF. 2000. The C terminus of SNAP25 is essential for Ca(2+)-dependent binding of synaptotagmin to SNARE complexes. J Biol Chem 275(9):6328-36.

Gillis KD, Mossner R, Neher E. 1996. Protein kinase C enhances exocytosis from chromaffin cells by increasing the size of the readily releasable pool of secretory granules. Neuron 16(6):1209-20.

Gong LW, Hafez I, Alvarez de Toledo G, Lindau M. 2003. Secretory vesicles membrane area is regulated in tandem with quantal size in chromaffin cells. J Neurosci 23(21):7917-21.

Graham ME, Sudlow AW, Burgoyne RD. 1997. Evidence against an acute inhibitory role of nSec-1 (munc-18) in late steps of regulated exocytosis in chromaffin and PC12 cells. J Neurochem 69(6):2369-77.

Grote E, Hao JC, Bennett MK, Kelly RB. 1995. A targeting signal in VAMP regulating transport to synaptic vesicles. Cell 81(4):581-9.

Hamill OP, Marty A, Neher E, Sakmann B, Sigworth FJ. 1981. Improved patch-clamp techniques for high-resolution current recording from cells and cell-free membrane patches. Pflugers Arch 391(2):85-100.

Han X, Jackson M. Submitted. Electrostatic Interactions Between the Syntaxin Membrane Anchor and Neurotransmitter Passing Through the Fusion Pore. Biophys J,.

Han X, Wang CT, Bai J, Chapman ER, Jackson MB. 2004. Transmembrane segments of syntaxin line the fusion pore of Ca2+-triggered exocytosis. Science 304(5668):289-92.

Hanson PI, Heuser JE, Jahn R. 1997a. Neurotransmitter release - four years of SNARE complexes. Curr Opin Neurobiol 7(3):310-5.

Hanson PI, Otto H, Barton N, Jahn R. 1995. The N-ethylmaleimide-sensitive fusion protein and alpha-SNAP induce a conformational change in syntaxin. J Biol Chem 270(28):16955-61.

Hanson PI, Roth R, Morisaki H, Jahn R, Heuser JE. 1997b. Structure and conformational changes in NSF and its membrane receptor complexes visualized by quick-freeze/deep-etch electron microscopy. Cell 90(3):523-35.

Hao JC, Salem N, Peng XR, Kelly RB, Bennett MK. 1997. Effect of mutations in vesicle-associated membrane protein (VAMP) on the assembly of multimeric protein complexes. J Neurosci 17(5):1596-603.

Hartmann J, Lindau M. 1995. A novel Ca(2+)-dependent step in exocytosis subsequent to vesicle fusion. FEBS Lett 363(3):217-20.

Hata Y, Slaughter CA, Sudhof TC. 1993. Synaptic vesicle fusion complex contains unc-18 homologue bound to syntaxin. Nature 366(6453):347-51.

Haucke V, De Camilli P. 1999. AP-2 recruitment to synaptotagmin stimulated by tyrosine-based endocytic motifs. Science 285(5431):1268-71.

Hay JC, Martin TF. 1992. Resolution of regulated secretion into sequential MgATP-dependent and calcium-dependent stages mediated by distinct cytosolic proteins. J Cell Biol 119(1):139-51.

Hayashi T, McMahon H, Yamasaki S, Binz T, Hata Y, Sudhof TC, Niemann H. 1994. Synaptic vesicle membrane fusion complex: action of clostridial neurotoxins on assembly. Embo J 13(21):5051-61.

Heidelberger R, Heinemann C, Neher E, Matthews G. 1994. Calcium dependence of the rate of exocytosis in a synaptic terminal. Nature 371(6497):513-5.

Heinemann C, Chow RH, Neher E, Zucker RS. 1994. Kinetics of the secretory response in bovine chromaffin cells following flash photolysis of caged Ca2+. Biophys J 67(6):2546-57.

Hess DT, Slater TM, Wilson MC, Skene JH. 1992. The 25 kDa synaptosomal-associated protein SNAP-25 is the major methionine-rich polypeptide in rapid axonal transport and a major substrate for palmitoylation in adult CNS. J Neurosci 12(12):4634-41.

Hessler NA, Shirke AM, Malinow R. 1993. The probability of transmitter release at a mammalian central synapse. Nature 366(6455):569-72.

Heuser JE, Reese TS, Dennis MJ, Jan Y, Jan L, Evans L. 1979. Synaptic vesicle exocytosis captured by quick freezing and correlated with quantal transmitter release. J Cell Biol 81(2):275-300.

Hille B. 1992. Ion Channels of Excitable Membrances. Sinauer: Sunderland.

Hokfelt T, Holets VR, Staines W, Meister B, Melander T, Schalling M, Schultzberg M, Freedman J, Bjorklund H, Olson L and others. 1986. Coexistence of neuronal messengers--an overview. Prog Brain Res 68:33-70.

Hsu SC, Ting AE, Hazuka CD, Davanger S, Kenny JW, Kee Y, Scheller RH. 1996. The mammalian brain rsec6/8 complex. Neuron 17(6):1209-19.

Hu K, Carroll J, Fedorovich S, Rickman C, Sukhodub A, Davletov B. 2002. Vesicular restriction of synaptobrevin suggests a role for calcium in membrane fusion. Nature 415(6872):646-50.

Hua Y, Scheller RH. 2001. Three SNARE complexes cooperate to mediate membrane fusion. Proc Natl Acad Sci U S A 98(14):8065-70.

Imoto K, Busch C, Sakmann B, Mishina M, Konno T, Nakai J, Bujo H, Mori Y, Fukuda K, Numa S. 1988. Rings of negatively charged amino acids determine the acetylcholine receptor channel conductance. Nature 335(6191):645-8.

Inoue A, Obata K, Akagawa K. 1992. Cloning and sequence analysis of cDNA for a neuronal cell membrane antigen, HPC-1. J Biol Chem 267(15):10613-9.

Jackson MB. 1992. Single channel analysis. Methods Enzymol. p 729-746.

Jahn R, Lang T, Sudhof TC. 2003. Membrane fusion. Cell 112(4):519-33.

Jahn R, Niemann H. 1994. Molecular mechanisms of clostridial neurotoxins. Ann N Y Acad Sci 733:245-55.

Jahn R, Sudhof TC. 1999. Membrane fusion and exocytosis. Annu Rev Biochem 68:863-911.

Karunanithi S, Marin L, Wong K, Atwood HL. 2002. Quantal size and variation determined by vesicle size in normal and mutant Drosophila glutamatergic synapses. J Neurosci 22(23):10267-76.

Katz B, Miledi R. 1965. The Measurement of Synaptic Delay, and the Time Course of Acetylcholine Release at the Neuromuscular Junction. Proc R Soc Lond B Biol Sci 161:483-95.

Katz L, Brennwald P. 2000. Testing the 3Q:1R "rule": mutational analysis of the ionic "zero" layer in the yeast exocytic SNARE complex reveals no requirement for arginine. Mol Biol Cell 11(11):3849-58.

Kee Y, Lin RC, Hsu SC, Scheller RH. 1995. Distinct domains of syntaxin are required for synaptic vesicle fusion complex formation and dissociation. Neuron 14(5):991-8.

Kim CS, Kweon DH, Shin YK. 2002. Membrane topologies of neuronal SNARE folding intermediates. Biochemistry 41(36):10928-33.

Kissinger PT, Hart JB, Adams RN. 1973. Voltammetry in brain tissue--a new neurophysiological measurement. Brain Res 55(1):209-13.

Klenchin VA, Martin TF. 2000. Priming in exocytosis: attaining fusion-competence after vesicle docking. Biochimie 82(5):399-407.

Klingauf J, Kavalali ET, Tsien RW. 1998. Kinetics and regulation of fast endocytosis at hippocampal synapses. Nature 394(6693):581-5.

Klyachko VA, Jackson MB. 2002. Capacitance steps and fusion pores of small and large-dense-core vesicles in nerve terminals. Nature 418(6893):89-92.

Koushika SP, Richmond JE, Hadwiger G, Weimer RM, Jorgensen EM, Nonet ML. 2001. A post-docking role for active zone protein Rim. Nat Neurosci 4(10):997-1005.

Krasnoperov VG, Bittner MA, Beavis R, Kuang Y, Salnikow KV, Chepurny OG, Little AR, Plotnikov AN, Wu D, Holz RW and others. 1997. alpha-Latrotoxin stimulates exocytosis by the interaction with a neuronal G-protein-coupled receptor. Neuron 18(6):925-37.

Kweon DH, Kim CS, Shin YK. 2002. The membrane-dipped neuronal SNARE complex: a site-directed spin labeling electron paramagnetic resonance study. Biochemistry 41(29):9264-8.

Kweon DH, Kim CS, Shin YK. 2003. Insertion of the membrane-proximal region of the neuronal SNARE coiled coil into the membrane. J Biol Chem 278(14):12367-73.

Laage R, Ungermann C. 2001. The N-terminal domain of the t-SNARE Vam3p coordinates priming and docking in yeast vacuole fusion. Mol Biol Cell 12(11):3375-85.

Langley K, Grant NJ. 1997. Are exocytosis mechanisms neurotransmitter specific? Neurochem Int 31(6):739-57.

Lester HA. 1992. The permeation pathway of neurotransmitter-gated ion channels. Annu Rev Biophys Biomol Struct 21:267-92.

Leszczyszyn DJ, Jankowski JA, Viveros OH, Diliberto EJ, Jr., Near JA, Wightman RM. 1990. Nicotinic receptor-mediated catecholamine secretion from individual chromaffin cells. Chemical evidence for exocytosis. J Biol Chem 265(25):14736-7.

Leszczyszyn DJ, Jankowski JA, Viveros OH, Diliberto EJ, Jr., Near JA, Wightman RM. 1991. Secretion of catecholamines from individual adrenal medullary chromaffin cells. J Neurochem 56(6):1855-63.

Lewis JL, Dong M, Earles CA, Chapman ER. 2001. The transmembrane domain of syntaxin 1A is critical for cytoplasmic domain protein-protein interactions. J Biol Chem 276(18):15458-65.

Li C, Ullrich B, Zhang JZ, Anderson RG, Brose N, Sudhof TC. 1995. Ca(2+)-dependent and -independent activities of neural and non-neural synaptotagmins. Nature 375(6532):594-9.

Lin RC, Scheller RH. 1997. Structural organization of the synaptic exocytosis core complex. Neuron 19(5):1087-94.

Lin RC, Scheller RH. 2000. Mechanisms of synaptic vesicle exocytosis. Annu Rev Cell Dev Biol 16:19-49.

Lindau M. 1991. Time-resolved capacitance measurements: monitoring exocytosis in single cells. Q Rev Biophys 24(1):75-101.

Lindau M, Almers W. 1995. Structure and function of fusion pores in exocytosis and ectoplasmic membrane fusion. Curr Opin Cell Biol 7(4):509-17.

Lindau M, Alvarez de Toledo G. 2003. The fusion pore. Biochim Biophys Acta 1641(2-3):167-73.

Lindau M, Nusse O, Bennett J, Cromwell O. 1993. The membrane fusion events in degranulating guinea pig eosinophils. J Cell Sci 104 (Pt 1):203-10.

Littleton JT, Chapman ER, Kreber R, Garment MB, Carlson SD, Ganetzky B. 1998. Temperature-sensitive paralytic mutations demonstrate that synaptic exocytosis requires SNARE complex assembly and disassembly. Neuron 21(2):401-13.

Liu Y, Peter D, Roghani A, Schuldiner S, Prive GG, Eisenberg D, Brecha N, Edwards RH. 1992. A cDNA that suppresses MPP+ toxicity encodes a vesicular amine transporter. Cell 70(4):539-51.

Llinas R, Steinberg IZ, Walton K. 1981. Relationship between presynaptic calcium current and postsynaptic potential in squid giant synapse. Biophys J 33(3):323-51.

Llinas R, Sugimori M, Silver RB. 1992. Microdomains of high calcium concentration in a presynaptic terminal. Science 256(5057):677-9.

Loewi O. 1921. Pfluger Arch. Ges. Physiol. 189:239.

Lollike K, Borregaard N, Lindau M. 1995. The exocytotic fusion pore of small granules has a conductance similar to an ion channel. J Cell Biol 129(1):99-104.

Lollike K, Lindau M. 1999. Membrane capacitance techniques to monitor granule exocytosis in neutrophils. J Immunol Methods 232(1-2):111-20.

Maler L, Mathieson WB. 1985. The effect of nerve activity on the distribution of synaptic vesicles. Cell Mol Neurobiol 5(4):373-87.

Malinski T, Taha Z. 1992. Nitric oxide release from a single cell measured in situ by a porphyrinic-based microsensor. Nature 358(6388):676-8.

Margittai M, Fasshauer D, Pabst S, Jahn R, Langen R. 2001. Homo- and heterooligomeric SNARE complexes studied by site-directed spin labeling. J Biol Chem 276(16):13169-77.

Matthew WD, Tsavaler L, Reichardt LF. 1981. Identification of a synaptic vesicle-specific membrane protein with a wide distribution in neuronal and neurosecretory tissue. J Cell Biol 91(1):257-69.

McMahon HT, Missler M, Li C, Sudhof TC. 1995. Complexins: cytosolic proteins that regulate SNAP receptor function. Cell 83(1):111-9.

McMahon HT, Ushkaryov YA, Edelmann L, Link E, Binz T, Niemann H, Jahn R, Sudhof TC. 1993. Cellubrevin is a ubiquitous tetanus-toxin substrate homologous to a putative synaptic vesicle fusion protein. Nature 364(6435):346-9.

McNew JA, Weber T, Engelman DM, Sollner TH, Rothman JE. 1999. The length of the flexible SNAREpin juxtamembrane region is a critical determinant of SNARE-dependent fusion. Mol Cell 4(3):415-21.

Melamed-Book N, Kachalsky SG, Kaiserman I, Rahamimoff R. 1999. Neuronal calcium sparks and intracellular calcium "noise". Proc Natl Acad Sci U S A 96(26):15217-21.

Melia TJ, Weber T, McNew JA, Fisher LE, Johnston RJ, Parlati F, Mahal LK, Sollner TH, Rothman JE. 2002. Regulation of membrane fusion by the membrane-proximal coil of the t-SNARE during zippering of SNAREpins. J Cell Biol 158(5):929-40.

Melikyan GB, Brener SA, Ok DC, Cohen FS. 1997. Inner but not outer membrane leaflets control the transition from glycosylphosphatidylinositol-anchored influenza hemagglutinin-induced hemifusion to full fusion. J Cell Biol 136(5):995-1005.

Melikyan GB, Niles WD, Cohen FS. 1993a. Influenza virus hemagglutinin-induced cell-planar bilayer fusion: quantitative dissection of fusion pore kinetics into stages. J Gen Physiol 102(6):1151-70.

Melikyan GB, Niles WD, Peeples ME, Cohen FS. 1993b. Influenza hemagglutinin-mediated fusion pores connecting cells to planar membranes: flickering to final expansion. J Gen Physiol 102(6):1131-49.

Melikyan GB, White JM, Cohen FS. 1995. GPI-anchored influenza hemagglutinin induces hemifusion to both red blood cell and planar bilayer membranes. J Cell Biol 131(3):679-91.

Merighi A, Polak JM, Theodosis DT. 1991. Ultrastructural visualization of glutamate and aspartate immunoreactivities in the rat dorsal horn, with special reference to the co-localization of glutamate, substance P and calcitonin-gene related peptide. Neuroscience 40(1):67-80.

Misura KM, Gonzalez LC, Jr., May AP, Scheller RH, Weis WI. 2001a. Crystal structure and biophysical properties of a complex between the N-terminal SNARE region of SNAP25 and syntaxin 1a. J Biol Chem 276(44):41301-9.

Misura KM, Scheller RH, Weis WI. 2000. Three-dimensional structure of the neuronal-Sec1-syntaxin 1a complex. Nature 404(6776):355-62.

Misura KM, Scheller RH, Weis WI. 2001b. Self-association of the H3 region of syntaxin 1A. Implications for intermediates in SNARE complex assembly. J Biol Chem 276(16):13273-82.

Morgan A, Dimaline R, Burgoyne RD. 1994. The ATPase activity of N-ethylmaleimide-sensitive fusion protein (NSF) is regulated by soluble NSF attachment proteins. J Biol Chem 269(47):29347-50.

Morris JF, Nordmann JJ, Dyball RE. 1978. Structure-function correlation in mammalian neurosecretion. Int Rev Exp Pathol 18:1-95.

Murthy VN, Sejnowski TJ, Stevens CF. 1997. Heterogeneous release properties of visualized individual hippocampal synapses. Neuron 18(4):599-612.

Nakata T, Sobue K, Hirokawa N. 1990. Conformational change and localization of calpactin I complex involved in exocytosis as revealed by quick-freeze, deep-etch electron microscopy and immunocytochemistry. J Cell Biol 110(1):13-25.

Nalefski EA, Falke JJ. 1996. The C2 domain calcium-binding motif: structural and functional diversity. Protein Sci 5(12):2375-90.

Neher E, Marty A. 1982. Discrete changes of cell membrane capacitance observed under conditions of enhanced secretion in bovine adrenal chromaffin cells. Proc Natl Acad Sci U S A 79(21):6712-6.

Neher E, Zucker RS. 1993. Multiple calcium-dependent processes related to secretion in bovine chromaffin cells. Neuron 10(1):21-30.

Nelson N. 1992. Evolution of organellar proton-ATPases. Biochim Biophys Acta 1100(2):109-24.

Nickel W, Weber T, McNew JA, Parlati F, Sollner TH, Rothman JE. 1999. Content mixing and membrane integrity during membrane fusion driven by pairing of isolated v-SNAREs and t-SNAREs. Proc Natl Acad Sci U S A 96(22):12571-6.

Nishiki T, Augustine GJ. 2004a. Synaptotagmin I synchronizes transmitter release in mouse hippocampal neurons. J Neurosci 24(27):6127-32.

Nishiki T, Augustine GJ. 2004b. Dual roles of the C2B domain of synaptotagmin I in synchronizing Ca2+-dependent neurotransmitter release. J Neurosci 24(39):8542-50.

Nishiki T, Kamata Y, Nemoto Y, Omori A, Ito T, Takahashi M, Kozaki S. 1994. Identification of protein receptor for Clostridium botulinum type B neurotoxin in rat brain synaptosomes. J Biol Chem 269(14):10498-503.

Nishiki T, Tokuyama Y, Kamata Y, Nemoto Y, Yoshida A, Sato K, Sekiguchi M, Takahashi M, Kozaki S. 1996a. The high-affinity binding of Clostridium botulinum type B neurotoxin to synaptotagmin II associated with gangliosides GT1b/GD1a. FEBS Lett 378(3):253-7.

Nishiki T, Tokuyama Y, Kamata Y, Nemoto Y, Yoshida A, Sekiguchi M, Takahashi M, Kozaki S. 1996b. Binding of botulinum type B neurotoxin to Chinese hamster ovary cells transfected with rat synaptotagmin II cDNA. Neurosci Lett 208(2):105-8.

Omann GM, Axelrod D. 1996. Membrane-proximal calcium transients in stimulated neutrophils detected by total internal reflection fluorescence. Biophys J 71(5):2885-91.

Ornberg R, Reese T. 1981. Beginning of exocytosis captured by rapid-freezing of Limulus amebocytes. J. Cell Biol. 90(1):40-54.

Ossig R, Dascher C, Trepte HH, Schmitt HD, Gallwitz D. 1991. The yeast SLY gene products, suppressors of defects in the essential GTP-binding Ypt1 protein, may act in endoplasmic reticulum-to-Golgi transport. Mol Cell Biol 11(6):2980-93.

Ossig R, Schmitt HD, de Groot B, Riedel D, Keranen S, Ronne H, Grubmuller H, Jahn R. 2000. Exocytosis requires asymmetry in the central layer of the SNARE complex. Embo J 19(22):6000-10.

Otto H, Hanson PI, Jahn R. 1997. Assembly and disassembly of a ternary complex of synaptobrevin, syntaxin, and SNAP-25 in the membrane of synaptic vesicles. Proc Natl Acad Sci U S A 94(12):6197-201.

Oyler GA, Higgins GA, Hart RA, Battenberg E, Billingsley M, Bloom FE, Wilson MC. 1989. The identification of a novel synaptosomal-associated protein, SNAP-25, differentially expressed by neuronal subpopulations. J Cell Biol 109(6 Pt 1):3039-52.

Parsons TD, Coorssen JR, Horstmann H, Almers W. 1995. Docked granules, the exocytic burst, and the need for ATP hydrolysis in endocrine cells. Neuron 15(5):1085-96.

Pasyk EA, Kang Y, Huang X, Cui N, Sheu L, Gaisano HY. 2004. Syntaxin-1A binds the nucleotide-binding folds of sulphonylurea receptor 1 to regulate the KATP channel. J Biol Chem 279(6):4234-40. Epub 2003 Nov 25.

Perin MS, Fried VA, Mignery GA, Jahn R, Sudhof TC. 1990. Phospholipid binding by a synaptic vesicle protein homologous to the regulatory region of protein kinase C. Nature 345(6272):260-3.

Perin MS, Fried VA, Slaughter CA, Sudhof TC. 1988. The structure of cytochrome b561, a secretory vesicle-specific electron transport protein. Embo J 7(9):2697-703.

Perin MS, Johnston PA, Ozcelik T, Jahn R, Francke U, Sudhof TC. 1991. Structural and functional conservation of synaptotagmin (p65) in Drosophila and humans. J Biol Chem 266(1):615-22.

Peters C, Bayer MJ, Buhler S, Andersen JS, Mann M, Mayer A. 2001. Trans-complex formation by proteolipid channels in the terminal phase of membrane fusion. Nature 409(6820):581-8.

Poirier MA, Hao JC, Malkus PN, Chan C, Moore MF, King DS, Bennett MK. 1998a. Protease resistance of syntaxin.SNAP-25.VAMP complexes. Implications for assembly and structure. J Biol Chem 273(18):11370-7.

Poirier MA, Xiao W, Macosko JC, Chan C, Shin YK, Bennett MK. 1998b. The synaptic SNARE complex is a parallel four-stranded helical bundle. Nat Struct Biol 5(9):765-9.

Pothos EN, Larsen KE, Krantz DE, Liu Y, Haycock JW, Setlik W, Gershon MD, Edwards RH, Sulzer D. 2000. Synaptic vesicle transporter expression regulates vesicle phenotype and quantal size. J Neurosci 20(19):7297-306.

Pyle JL, Kavalali ET, Piedras-Renteria ES, Tsien RW. 2000. Rapid reuse of readily releasable pool vesicles at hippocampal synapses. Neuron 28(1):221-31.

Quick MW. 2003. Regulating the conducting states of a mammalian serotonin transporter. Neuron 40(3):537-49.

Reist NE, Buchanan J, Li J, DiAntonio A, Buxton EM, Schwarz TL. 1998. Morphologically docked synaptic vesicles are reduced in synaptotagmin mutants of Drosophila. J Neurosci 18(19):7662-73.

Rickman C, Craxton M, Osborne S, Davletov B. 2004. Comparative analysis of tandem C2 domains from the mammalian synaptotagmin family. Biochem J 378(Pt 2):681-6.

Rindi G, Leiter AB, Kopin AS, Bordi C, Solcia E. 2004. The "normal" endocrine cell of the gut: changing concepts and new evidences. Ann N Y Acad Sci 1014:1-12.

Rizo J, Sudhof TC. 2002. Snares and Munc18 in synaptic vesicle fusion. Nat Rev Neurosci 3(8):641-53.

Rizzoli SO, Betz WJ. 2004. The structural organization of the readily releasable pool of synaptic vesicles. Science 303(5666):2037-9.

Rosenmund C, Clements JD, Westbrook GL. 1993. Nonuniform probability of glutamate release at a hippocampal synapse. Science 262(5134):754-7.

Rossi G, Salminen A, Rice LM, Brunger AT, Brennwald P. 1997. Analysis of a yeast SNARE complex reveals remarkable similarity to the neuronal SNARE complex and a novel function for the C terminus of the SNAP-25 homolog, Sec9. J Biol Chem 272(26):16610-7.

Rothman JE. 1996. The protein machinery of vesicle budding and fusion. Protein Sci 5(2):185-94.

Scales SJ, Hesser BA, Masuda ES, Scheller RH. 2002. Amisyn, a novel syntaxin-binding protein that may regulate SNARE complex assembly. J Biol Chem 277(31):28271-9.

Scales SJ, Yoo BY, Scheller RH. 2001. The ionic layer is required for efficient dissociation of the SNARE complex by alpha-SNAP and NSF. Proc Natl Acad Sci U S A 98(25):14262-7.

Scepek S, Coorssen JR, Lindau M. 1998. Fusion pore expansion in horse eosinophils is modulated by Ca2+ and protein kinase C via distinct mechanisms. Embo J 17(15):4340-5.

Schiavo G, Gu QM, Prestwich GD, Sollner TH, Rothman JE. 1996. Calcium-dependent switching of the specificity of phosphoinositide binding to synaptotagmin. Proc Natl Acad Sci U S A 93(23):13327-32.

Schiavo G, Stenbeck G, Rothman JE, Sollner TH. 1997. Binding of the synaptic vesicle v-SNARE, synaptotagmin, to the plasma membrane t-SNARE, SNAP-25, can explain docked vesicles at neurotoxin-treated synapses. Proc Natl Acad Sci U S A 94(3):997-1001.

Schikorski T, Stevens CF. 1997. Quantitative ultrastructural analysis of hippocampal excitatory synapses. J Neurosci 17(15):5858-67.

Schmidt W, Patzak A, Lingg G, Winkler H, Plattner H. 1983. Membrane events in adrenal chromaffin cells during exocytosis: a freeze-etching analysis after rapid cryofixation. Eur J Cell Biol 32(1):31-7.

Schoch S, Deak F, Konigstorfer A, Mozhayeva M, Sara Y, Sudhof TC, Kavalali ET. 2001. SNARE function analyzed in synaptobrevin/VAMP knockout mice. Science 294(5544):1117-22.

Schroeder TJ, Borges R, Finnegan JM, Pihel K, Amatore C, Wightman RM. 1996. Temporally resolved, independent stages of individual exocytotic secretion events. Biophys J 70(2):1061-8.

Schulze KL, Broadie K, Perin MS, Bellen HJ. 1995. Genetic and electrophysiological studies of Drosophila syntaxin-1A demonstrate its role in nonneuronal secretion and neurotransmission. Cell 80(2):311-20.

Sheng ZH, Rettig J, Takahashi M, Catterall WA. 1994. Identification of a syntaxin-binding site on N-type calcium channels. Neuron 13(6):1303-13.

Skehel JJ, Wiley DC. 2000. Receptor binding and membrane fusion in virus entry: the influenza hemagglutinin. Annu Rev Biochem 69:531-69.

Slepnev VI, De Camilli P. 2000. Accessory factors in clathrin-dependent synaptic vesicle endocytosis. Nat Rev Neurosci 1(3):161-72.

Sollner T, Bennett MK, Whiteheart SW, Scheller RH, Rothman JE. 1993a. A protein assembly-disassembly pathway in vitro that may correspond to sequential steps of synaptic vesicle docking, activation, and fusion. Cell 75(3):409-18.

Sollner T, Whiteheart SW, Brunner M, Erdjument-Bromage H, Geromanos S, Tempst P, Rothman JE. 1993b. SNAP receptors implicated in vesicle targeting and fusion. Nature 362(6418):318-24.

Sollner TH. 2003. Regulated exocytosis and SNARE function (Review). Mol Membr Biol 20(3):209-20.

Sorensen JB, Nagy G, Varoqueaux F, Nehring RB, Brose N, Wilson MC, Neher E. 2003. Differential control of the releasable vesicle pools by SNAP-25 splice variants and SNAP-23. Cell 114(1):75-86.

Spruce AE, Breckenridge LJ, Lee AK, Almers W. 1990. Properties of the fusion pore that forms during exocytosis of a mast cell secretory vesicle. Neuron 4(5):643-54.

Spruce AE, Iwata A, Almers W. 1991. The first milliseconds of the pore formed by a fusogenic viral envelope protein during membrane fusion. Proc Natl Acad Sci U S A 88(9):3623-7.

Spruce AE, Iwata A, White JM, Almers W. 1989. Patch clamp studies of single cell-fusion events mediated by a viral fusion protein. Nature 342(6249):555-8.

Srivastava M. 1995. Genomic structure and expression of the human gene encoding cytochrome b561, an integral protein of the chromaffin granule membrane. J Biol Chem 270(39):22714-20.

Stevens TH, Forgac M. 1997. Structure, function and regulation of the vacuolar (H+)-ATPase. Annu Rev Cell Dev Biol 13:779-808.

Stewart BA, Mohtashami M, Trimble WS, Boulianne GL. 2000. SNARE proteins contribute to calcium cooperativity of synaptic transmission. Proc Natl Acad Sci U S A 97(25):13955-60.

Sudhof TC, Baumert M, Perin MS, Jahn R. 1989. A synaptic vesicle membrane protein is conserved from mammals to Drosophila. Neuron 2(5):1475-81.

Suga K, Yamamori T, Akagawa K. 2003. Identification of the carboxyl-terminal membrane-anchoring region of HPC-1/syntaxin 1A with the substituted-cysteine-accessibility method and monoclonal antibodies. J Biochem (Tokyo) 133(3):325-34.

Sung U, Apparsundaram S, Galli A, Kahlig KM, Savchenko V, Schroeter S, Quick MW, Blakely RD. 2003. A regulated interaction of syntaxin 1A with the antidepressant-

sensitive norepinephrine transporter establishes catecholamine clearance capacity. J Neurosci 23(5):1697-709.

Supekova L, Sbia M, Supek F, Ma Y, Nelson N. 1996. A novel subunit of vacuolar H(+)-ATPase related to the b subunit of F-ATPases. J Exp Biol 199 (Pt 5):1147-56.

Sutton RB, Davletov BA, Berghuis AM, Sudhof TC, Sprang SR. 1995. Structure of the first C2 domain of synaptotagmin I: a novel Ca2+/phospholipid-binding fold. Cell 80(6):929-38.

Sutton RB, Fasshauer D, Jahn R, Brunger AT. 1998. Crystal structure of a SNARE complex involved in synaptic exocytosis at 2.4 angstrom resolution. Nature 395(6700):347-353.

Terskikh A, Fradkov A, Ermakova G, Zaraisky A, Tan P, Kajava AV, Zhao X, Lukyanov S, Matz M, Kim S and others. 2000. "Fluorescent timer": protein that changes color with time. Science 290(5496):1585-8.

Tolar LA, Pallanck L. 1998. NSF function in neurotransmitter release involves rearrangement of the SNARE complex downstream of synaptic vesicle docking. J Neurosci 18(24):10250-6.

Toonen RF, Verhage M. 2003. Vesicle trafficking: pleasure and pain from SM genes. Trends Cell Biol 13(4):177-86.

Trimble WS, Cowan DM, Scheller RH. 1988. VAMP-1: a synaptic vesicle-associated integral membrane protein. Proc Natl Acad Sci U S A 85(12):4538-42.

Trimble WS, Gray TS, Elferink LA, Wilson MC, Scheller RH. 1990. Distinct patterns of expression of two VAMP genes within the rat brain. J Neurosci 10(4):1380-7.

Trus M, Wiser O, Goodnough MC, Atlas D. 2001. The transmembrane domain of syntaxin 1A negatively regulates voltage-sensitive Ca2+ channels. Neuroscience 104(2):599-607.

Tse FW, Iwata A, Almers W. 1993. Membrane flux through the pore formed by a fusogenic viral envelope protein during cell fusion. J Cell Biol 121(3):543-52.

Tucker WC, Edwardson JM, Bai J, Kim HJ, Martin TF, Chapman ER. 2003. Identification of synaptotagmin effectors via acute inhibition of secretion from cracked PC12 cells. J Cell Biol 162(2):199-209.

Tucker WC, Weber T, Chapman ER. 2004. Reconstitution of Ca2+-regulated membrane fusion by synaptotagmin and SNAREs. Science 304(5669):435-8.

Ubach J, Zhang X, Shao X, Sudhof TC, Rizo J. 1998. Ca2+ binding to synaptotagmin: how many Ca2+ ions bind to the tip of a C2-domain? Embo J 17(14):3921-30.

Ungermann C, Sato K, Wickner W. 1998. Defining the functions of trans-SNARE pairs. Nature 396(6711):543-8.

Usdin TB, Eiden LE, Bonner TI, Erickson JD. 1995. Molecular biology of the vesicular ACh transporter. Trends Neurosci 18(5):218-24.

Veit M, Sollner TH, Rothman JE. 1996. Multiple palmitoylation of synaptotagmin and the t-SNARE SNAP-25. FEBS Lett 385(1-2):119-23.

Verhage M, Maia AS, Plomp JJ, Brussaard AB, Heeroma JH, Vermeer H, Toonen RF, Hammer RE, van den Berg TK, Missler M and others. 2000. Synaptic assembly of the brain in the absence of neurotransmitter secretion. Science 287(5454):864-9.

Vician L, Lim IK, Ferguson G, Tocco G, Baudry M, Herschman HR. 1995. Synaptotagmin IV is an immediate early gene induced by depolarization in PC12 cells and in brain. Proc Natl Acad Sci U S A 92(6):2164-8.

Voets T, Moser T, Lund PE, Chow RH, Geppert M, Sudhof TC, Neher E. 2001a. Intracellular calcium dependence of large dense-core vesicle exocytosis in the absence of synaptotagmin I. Proc Natl Acad Sci U S A 98(20):11680-5.

Voets T, Neher E, Moser T. 1999. Mechanisms underlying phasic and sustained secretion in chromaffin cells from mouse adrenal slices. Neuron 23(3):607-15.

Voets T, Toonen RF, Brian EC, de Wit H, Moser T, Rettig J, Sudhof TC, Neher E, Verhage M. 2001b. Munc18-1 promotes large dense-core vesicle docking. Neuron 31(4):581-91.

Vogel K, Roche PA. 1999. SNAP-23 and SNAP-25 are palmitoylated in vivo. Biochem Biophys Res Commun 258(2):407-10.

Walther K, Krauss M, Diril MK, Lemke S, Ricotta D, Honing S, Kaiser S, Haucke V. 2001. Human stoned B interacts with AP-2 and synaptotagmin and facilitates clathrin-coated vesicle uncoating. EMBO Rep 2(7):634-40.

Wang C-T, Grishanin R, Earles CA, Chang PY, Martin TFJ, Chapman ER, Jackson MB. 2001a. Synaptotagmin Modulation of Fusion Pore Kinetics in Regulated Exocytosis of Dense-Core Vesicles. Science 294(5544):1111-1115.

Wang CT, Lu JC, Bai J, Chang PY, Martin TF, Chapman ER, Jackson MB. 2003. Different domains of synaptotagmin control the choice between kiss-and-run and full fusion. Nature 424(6951):943-7.

Wang Y, Dulubova I, Rizo J, Sudhof TC. 2001b. Functional analysis of conserved structural elements in yeast syntaxin Vam3p. J Biol Chem 276(30):28598-605.

Washbourne P, Thompson PM, Carta M, Costa ET, Mathews JR, Lopez-Bendito G, Molnar Z, Becher MW, Valenzuela CF, Partridge LD and others. 2002. Genetic ablation of the t-SNARE SNAP-25 distinguishes mechanisms of neuroexocytosis. Nat Neurosci 5(1):19-26.

Weast RC, editor. 1977-1978. Handbook of chemistry and physics. 58th ed. Cleveland, OH: CRC Press, Inc.

Weber T, Zemelman BV, McNew JA, Westermann B, Gmachl M, Parlati F, Sollner TH, Rothman JE. 1998. SNAREpins: minimal machinery for membrane fusion. Cell 92(6):759-72.

Weidman PJ, Melancon P, Block MR, Rothman JE. 1989. Binding of an N-ethylmaleimide-sensitive fusion protein to Golgi membranes requires both a soluble protein(s) and an integral membrane receptor. J Cell Biol 108(5):1589-96.

Weimbs T, Mostov K, Low SH, Hofmann K. 1998. A model for structural similarity between different SNARE complexes based on sequence relationships. Trends Cell Biol 8(7):260-2.

Weninger K, Bowen ME, Chu S, Brunger AT. 2003. Single-molecule studies of SNARE complex assembly reveal parallel and antiparallel configurations. Proc Natl Acad Sci U S A 100(25):14800-5.

Whipps DE, Armston AE, Pryor HJ, Halestrap AP. 1987. Effects of glucagon and Ca2+ on the metabolism of phosphatidylinositol 4-phosphate and phosphatidylinositol 4,5-bisphosphate in isolated rat hepatocytes and plasma membranes. Biochem J 241(3):835-45.

Whiteheart SW, Griff IC, Brunner M, Clary DO, Mayer T, Buhrow SA, Rothman JE. 1993. SNAP family of NSF attachment proteins includes a brain-specific isoform. Nature 362(6418):353-5.

Whittaker VP. 1965. The application of subcellular fractionation techniques to the study of brain function. Prog Biophys Mol Biol 15:39-96.

Whittaker VP, Essman WB, Dowe GH. 1972. The isolation of pure cholinergic synaptic vesicles from the electric organs of elasmobranch fish of the family Torpedinidae. Biochem J 128(4):833-45.

Wickner W. 2002. Yeast vacuoles and membrane fusion pathways. Embo J 21(6):1241-7.

Wightman RM, Jankowski JA, Kennedy RT, Kawagoe KT, Schroeder TJ, Leszczyszyn DJ, Near JA, Diliberto EJ, Jr., Viveros OH. 1991. Temporally resolved catecholamine spikes correspond to single vesicle release from individual chromaffin cells. Proc Natl Acad Sci U S A 88(23):10754-8.

Wightman RM, Schroeder TJ, Finnegan JM, Ciolkowski EL, Pihel K. 1995. Time course of release of catecholamines from individual vesicles during exocytosis at adrenal medullary cells. Biophys J 68(1):383-90.

Wilson DW, Wilcox CA, Flynn GC, Chen E, Kuang WJ, Henzel WJ, Block MR, Ullrich A, Rothman JE. 1989. A fusion protein required for vesicle-mediated transport in both mammalian cells and yeast. Nature 339(6223):355-9.

Winkler H. 1997. Membrane composition of adrenergic large and small dense cored vesicles and of synaptic vesicles: consequences for their biogenesis. Neurochem Res 22(8):921-32.

Winkler H, Schmidle T, Fischer-Colbrie R, Kapelari S. 1991. Membrane antigens of endocrine, large dense-core and small synaptic vesicles. Biochem Soc Trans 19(1):79-83.

Wong SH, Zhang T, Xu Y, Subramaniam VN, Griffiths G, Hong W. 1998. Endobrevin, a novel synaptobrevin/VAMP-like protein preferentially associated with the early endosome. Mol Biol Cell 9(6):1549-63.

Wu MN, Fergestad T, Lloyd TE, He YC, Broadie K, Bellen HJ. 1999. Syntaxin 1A interacts with multiple exocytic proteins to regulate neurotransmitter release in vivo. Neuron 23(3):593-605.

Xia Z, Zhou Q, Lin J, Liu Y. 2001. Stable SNARE complex prior to evoked synaptic vesicle fusion revealed by fluorescence resonance energy transfer. J Biol Chem 276(3):1766-71.

Xiao W, Poirier MA, Bennett MK, Shin YK. 2001. The neuronal t-SNARE complex is a parallel four-helix bundle. Nat Struct Biol 8(4):308-11.

Xu T, Binz T, Niemann H, Neher E. 1998. Multiple kinetic components of exocytosis distinguished by neurotoxin sensitivity. Nat Neurosci 1(3):192-200.

Xu T, Rammner B, Margittai M, Artalejo AR, Neher E, Jahn R. 1999. Inhibition of SNARE complex assembly differentially affects kinetic components of exocytosis. Cell 99(7):713-22.

Yoshihara M, Littleton JT. 2002. Synaptotagmin I functions as a calcium sensor to synchronize neurotransmitter release. Neuron 36(5):897-908.

Zeng Q, Subramaniam VN, Wong SH, Tang BL, Parton RG, Rea S, James DE, Hong W. 1998. A novel synaptobrevin/VAMP homologous protein (VAMP5) is increased during in vitro myogenesis and present in the plasma membrane. Mol Biol Cell 9(9):2423-37.

Zenisek D, Steyer JA, Feldman ME, Almers W. 2002. A membrane marker leaves synaptic vesicles in milliseconds after exocytosis in retinal bipolar cells. Neuron 35(6):1085-97.

Zhang F, Chen Y, Kweon DH, Kim CS, Shin YK. 2002a. The four-helix bundle of the neuronal target membrane SNARE complex is neither disordered in the middle nor uncoiled at the C-terminal region. J Biol Chem 277(27):24294-8.

Zhang F, Chen Y, Su Z, Shin YK. 2004. SNARE assembly and membrane fusion: A kinetic analysis. J Biol Chem.

Zhang JZ, Davletov BA, Sudhof TC, Anderson RG. 1994. Synaptotagmin I is a high affinity receptor for clathrin AP-2: implications for membrane recycling. Cell 78(5):751-60.

Zhang X, Kim-Miller MJ, Fukuda M, Kowalchyk JA, Martin TF. 2002b. Ca2+-dependent synaptotagmin binding to SNAP-25 is essential for Ca2+-triggered exocytosis. Neuron 34(4):599-611.

Zimmerberg J, Blumenthal R, Sarkar DP, Curran M, Morris SJ. 1994. Restricted movement of lipid and aqueous dyes through pores formed by influenza hemagglutinin during cell fusion. J Cell Biol 127(6 Pt 2):1885-94.

Zimmerberg J, Curran M, Cohen FS, Brodwick M. 1987. Simultaneous electrical and optical measurements show that membrane fusion precedes secretory granule swelling during exocytosis of beige mouse mast cells. Proc Natl Acad Sci U S A 84(6):1585-9.